Author Responses:

Anonymous Referee #1

Received and published: 4 October 2017

General remarks:

The manuscripts provides a detailed analyses of two well established cloud retrieval methods using passive satellite measurements of solar radiation. Bispectral and polarimetric retrieval of cloud optical thickness, droplet effective radius, and effective variance are compared for cases of liquid maritime clouds. The study is not based on measurements of real clouds. To analyze the limits of the physics behind the retrieval approaches, cloud fields provided by LES model runs are used to generate synthetic radiation measurements by radiative transfer simulation. This approach has the advantage of being independent on different uncertainties introduced by real observations and that the retrieved quantities can be compared to the truth given by the LES model. It is concluded that the bispectral retrieval shows a higher uncertainty for the retrieval of cloud droplet size compared to polarimetric retrieval while cloud optical thickness agrees between both approaches.

The results presented by this study are of high value for current and future satellite remote sensing. Retrieval uncertainties, which originate from the general limitations of the retrieval algorithms are clearly quantified and may help to improve the interpretation of satellite cloud products. In this regard, the manuscript provides an important contribution to current and future research and is worth to be published.

However, in my opinion the manuscript lacks of some major issues which have to be reassessed in detail before publishing the manuscript. By neglecting measurement uncertainties, the retrieval comparison might be only of academic value because it does not reflect the real uncertainties of both retrieval approaches when real satellite observations are considered. Furthermore, new developments of the bispectral retrieval are not considered in the study and limit the conclusions for future satellite employments. The bias of the bispectral retrieval is surprisingly high considering the ideal setup of the study. A more accurate treatment of the vertical weighting function of the bispectral retrievals needs to be applied in order to guaranty the comparability with the LES and the polarimetric retrieval. Below, I compiled a list of comments which have to be considered in a revised version of the paper. There might be some contradictory statements resulting from my misinterpretation of the text when first reading. I am sure the authors will know how to weight in such cases and how to improve the text to avoid misinterpretations by other readers.

Major comments:

1. **Neglecting measurement uncertainties**
I understand the approach of the authors to use synthetic measurements generated from LES cloud fields and radiative transfer simulations. This approach leaves only a limited number of causes which can explain the difference between both retrieval approaches, such as the complexity of the cloud representation in the radiative transfer model (vertical profile). In this regard, the study provides good insight into the physics of the retrieval approaches. This is worth to be published but might be only of academic value. However, the conclusions on the performance of the retrieval approaches might change when measurement errors are considered. Uncertainties of the spectral radiance measured by the satellite sensors, e.g. radiometric calibration, might propagate differently in both retrieval approaches. An uncertainty of spectral radiance might have larger consequences on retrieved cloud properties compared to uncertainties in the polarimetric measurements. To judge, which retrieval algorithm provides the more accurate cloud properties when applied to real satellite measurements such a propagation of the measurement uncertainty has to be considered and analyzed. This should not replace the current results of the study. Please keep these results. I rather suggest to add an additional exercise with focus on the propagation of measurement uncertainties. On basis of the available data set, this should be easy to realize. The simulated radiances which are the exact synthetic measurement are available. By generating synthetic measurements including a measurement uncertainty and propagating through the retrieval algorithm should already give an estimate of these retrieval uncertainties. Your motivation to use a LES cloud field and IPA simulations would still hold for such a study, as 3D-radiative effect, etc. still can be ruled out. Only the propagation of pure sensor uncertainties will be analyzed.

    a. I have added a section discussing the impact of uncorrelated uncertainty on bispectral and polarimetric retrievals. While the discussion is admittedly limited because of the desire of not choosing a specific instrument uncertainty model, I feel like this current approach puts the rest of the biases discussed into context. It should be noted however that the behavior of uncertainty for these two retrievals is highly algorithm and instrument dependent.

2. **Vertical weighting functions**
As discussed by the authors, the vertical weighting function is essential to compare retrieved cloud properties with the LES model clouds. Therefore, I am wondering why a relative crude assumption for the weighting function of the bispectral retrieval is assumed. The two-way transmittance function is valid for single-scattering only which holds for the polarimetric retrieval where single scattering features are extracted from the measurements. But the bispectral retrieval certainly are effected by multiple scattering. Platnick (2000) clearly

shows that the vertical weighting functions significantly extend into the lower cloud layers. Even for 3.7 µm cloud layers at optical thickness larger than $\tau > 2$ contribute to the weighting function while the 2WT weighting already becomes zero for $\tau > 2$.

First, I was surprised by the relative large differences between bispectral retrieval and LES-truth because the setup of the study was chosen well and should not allow large differences. But the treatment of the vertical weighting functions may explain these differences. Considering the idealized setup using the LES clouds and the independent pixel approximation to generate the synthetic measurements, I do not see many sources of error than the vertical distribution of cloud particles and how these are represented in the radiative transfer model. I assume, that the calculation of the synthetic measurements and the calculation of the LUTs use the same radiative transfer code. For the synthetic measurements, the vertical cloud profile is considered, but not for the LUTs of the retrieval. So the radiative transfer code itself is no issue.

The inaccurate treatment of the vertical weighting fits also to the results shown in Figure 3a. The slight shift of the bispectral retrieval to smaller particle sizes compared to the 2WT weighing might result from different vertical weighting function. While the 2WT weighting only considered the larger particles at cloud top, the bi-spectral retrieval is also influenced by smaller particles at lower cloud levels. This could already lead to the observed differences. Therefore, I suggest to use a more realistic vertical weighting function for comparing the bispectral retrieval with the LES model. The weighting function considering multiple scattering can be easily calculated by the method presented by Platnick (2000). As an approximation the weighting functions can be calculated assuming vertically homogeneous clouds as for the retrieval LUTs. With this assumption they can be easily extracted from the LUTs as the slope of reflectance with increasing optical thickness. So all required simulations should be available.

a. I am not sure that a vertical weighting based on homogeneous vertical profile assumptions would be appropriate for this analysis. The LES clouds are not vertically homogeneous and there can be significant extinction cross-section variability within cloud vertical profiles. The intent of the applied vertical weighting techniques is to account for that vertical inhomogeneity directly.

b. The authors agree that the single scattering (2WT) vertical weighting may not sufficiently describe the behavior of scattering in the 2.13 µm spectral band. One of the reasons for implementing a single vertical weighting definition throughout this paper was to ensure that we were not comparing retrievals to a "moving target." Additionally, from our previous work in Miller et al. (2016) we knew that r_e(2WT) matched the r_e(3.75 µm) spectral retrieval reasonably well.

c. Despite the large variability in the comparison of vertical weighting and bispectral retrievals it is important to note that the mean biases are quite small. The logarithmic histogram in the joint PDF can possibly be emphasizing features that are occurring for clouds that have significant vertically inhomogeneous cloud tops.

d. To test the impact of using a more accurate vertical weighting function we implemented the approach described in equation 4 of Zhang et al. 2017, which includes an additional factor that accounts for multiple scattering contributions:

$$W(\tau) = c\tau^b \exp\left[-\tau\left(\frac{1}{\mu} + \frac{1}{\mu_0}\right)\right].$$

Where the τ^b factor is introduced to account for multiple scattering, and the rest is the same as previously defined in the paper. For b=0 we get back the original 2WT vertical weighting used previously. Below is a figure displaying the scene-averaged vertical weighting functions from the DYCOMS-II case, note that similar results (throughout this discussion) were found in other LES cases. Each of the curves corresponds to a different value of b and each is also color coded to indicate the resulting average vertically weighted cloud microphysical property r_e(VW) and v_e(VW). Increasing the value of b causes the weighting function to extend deeper into the cloud, changing the mean value of r_e(VW) and v_e(VW). The change in the mean value of r_e(vw) for these different weightings does not exceed 0.5 μm and the mean value of v_e(VW) changes less than 0.05. The small variability in r_e has a lot to do with the actual profile of $r_e(\tau)$, which has little variability near cloud top. In contrast the large variability in v_e is related to the rapid change in $v_e(\tau)$ just below cloud top. It should be noted that the b=0 vertical weighting has a similar r_e(VW) result as the b=9 case, which offers an explanation as to why r_e(2WT) just happened to be a decent point of comparison.

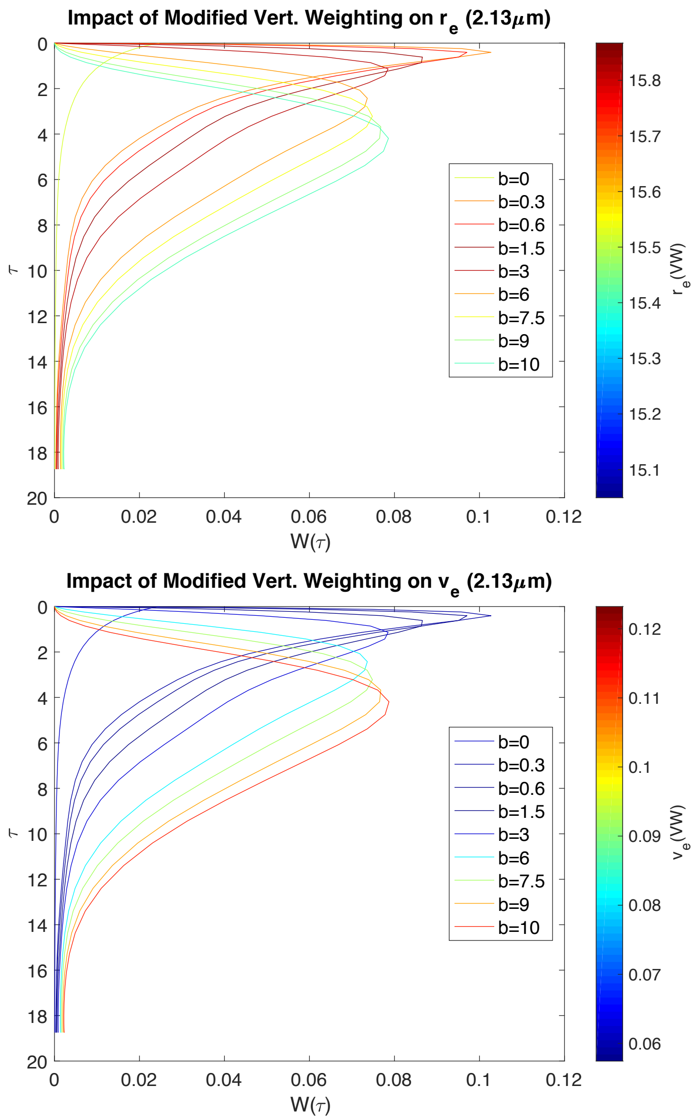

Figure 1: Scene average vertical weighting functions for the DYCOMS-II case with varying values of the parameter *b*. Lines are colored by the corresponding vertically weighted properties (r_e(VW,2.13) or v_e(VW,2.13))

Using this parameterization, we can tune the "quality of vertical weighting" by comparing the shape of the distribution of the bias between r_e(2.13) or r_e (3.75) with respect to their respective vertical weightings r_e(VW,2.13) and r_e(VW,3.75). By searching this histogram with different values of b we can find a parameterization that minimizes the mean bias, as well as the variability of the distribution – indicating a more appropriate vertical weighting definition for the bispectral retrieval in question. Several animated gif's of the behavior of this histogram as a function of b can be found here:

r_e(2.13)-r_e(VW,2.13) Histogram varying b
r_e(2.13)-r_e(VW,2.13) Histogram varying b (FOR τ>5 ONLY!)
r_e(3.75)-r_e(VW,3.75) histogram varying b

r_e(3.75,coupled to v_e(pol))-r_e(VW,3.75) Histogram varying b

Where for the 3.75μm spectral band we found that a b coefficient of 0.3 minimized mean bias and variability (when coupled with v_e information), whereas for 2.13μm a value of b=10 was found to be optimal. It is also important to note that the appropriate vertical weighting also depends on total optical thickness. As a consequence of the deep penetration of the 2.13 vertical weighting function some extremely high biased values of r_e(VW) exist for $\tau_{tot}<5$. This threshold was selected because $\tau=5$ is roughly the location of the peak of this vertical weighting function. For the ~5% of profiles with $\tau_{tot}<5$ we simply define b=0 in order to avoid applying an inaccurate multiple scattering vertical weighting.

The regression histograms of these new results are shown in Figure 2. The primary finding of this comparison is that the new flexible vertical weighting function produces results for the 2.13 μm band that have a far tighter regression. There is also a new bump in the comparison for 2.13 with $\tau_{tot}>3$ only, but this is associated with the population of high-biased r_e(VW) that remain below $\tau_{tot}<5$.

I also found a possible mistake in my plotting routines, I was only plotting nadir viewing r_e(2WT) and v_e(2WT) values for comparisons to the polarimetric retrieval. I have modified these results to include the other viewing geometries and those are shown in Figure 3.

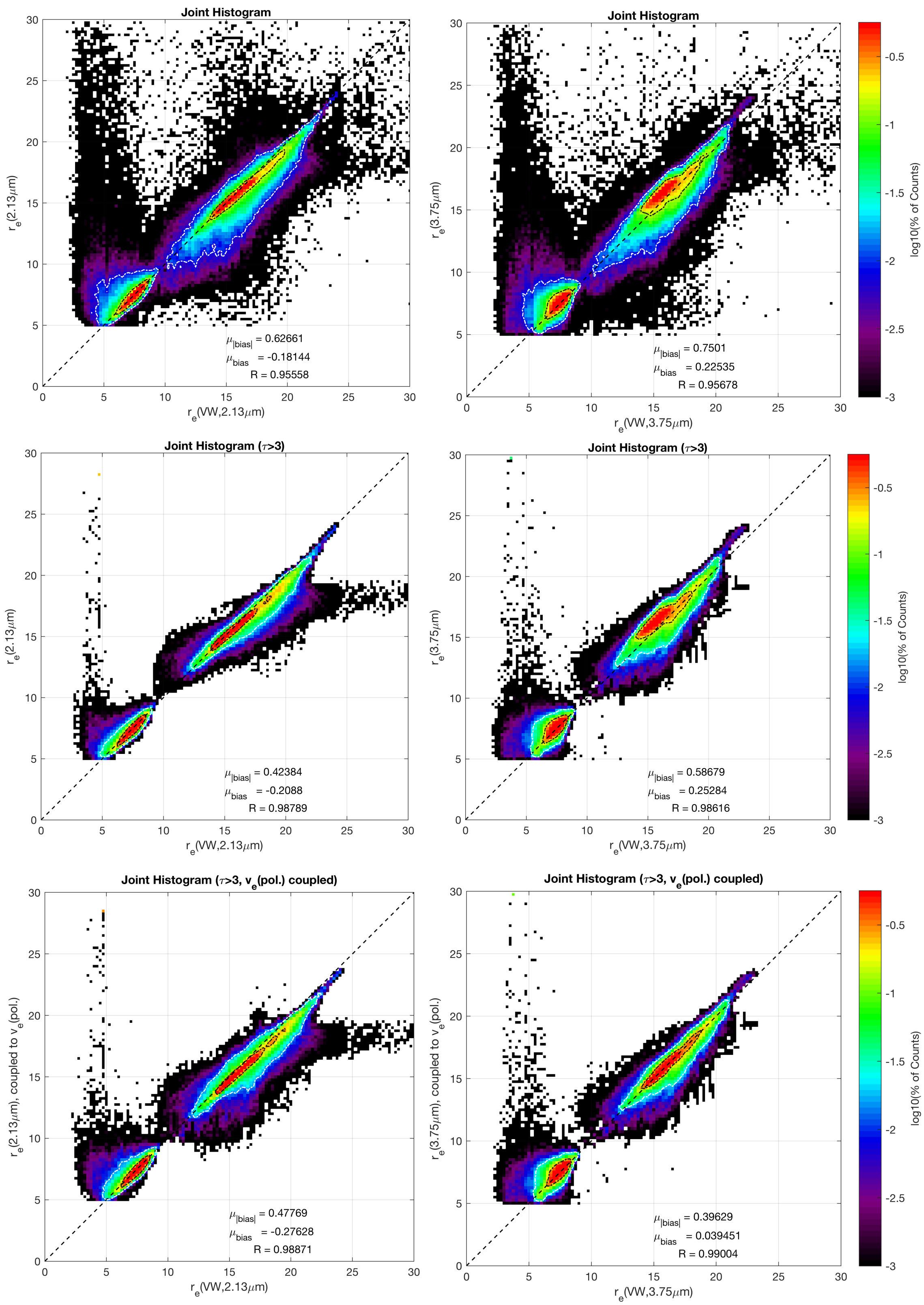

Figure 2: Refer to Figure 3 of the original manuscript for more figure information. This new version compares to a more flexible vertical weighting definition (denoted VW) than the single-scattering 2WT scheme.

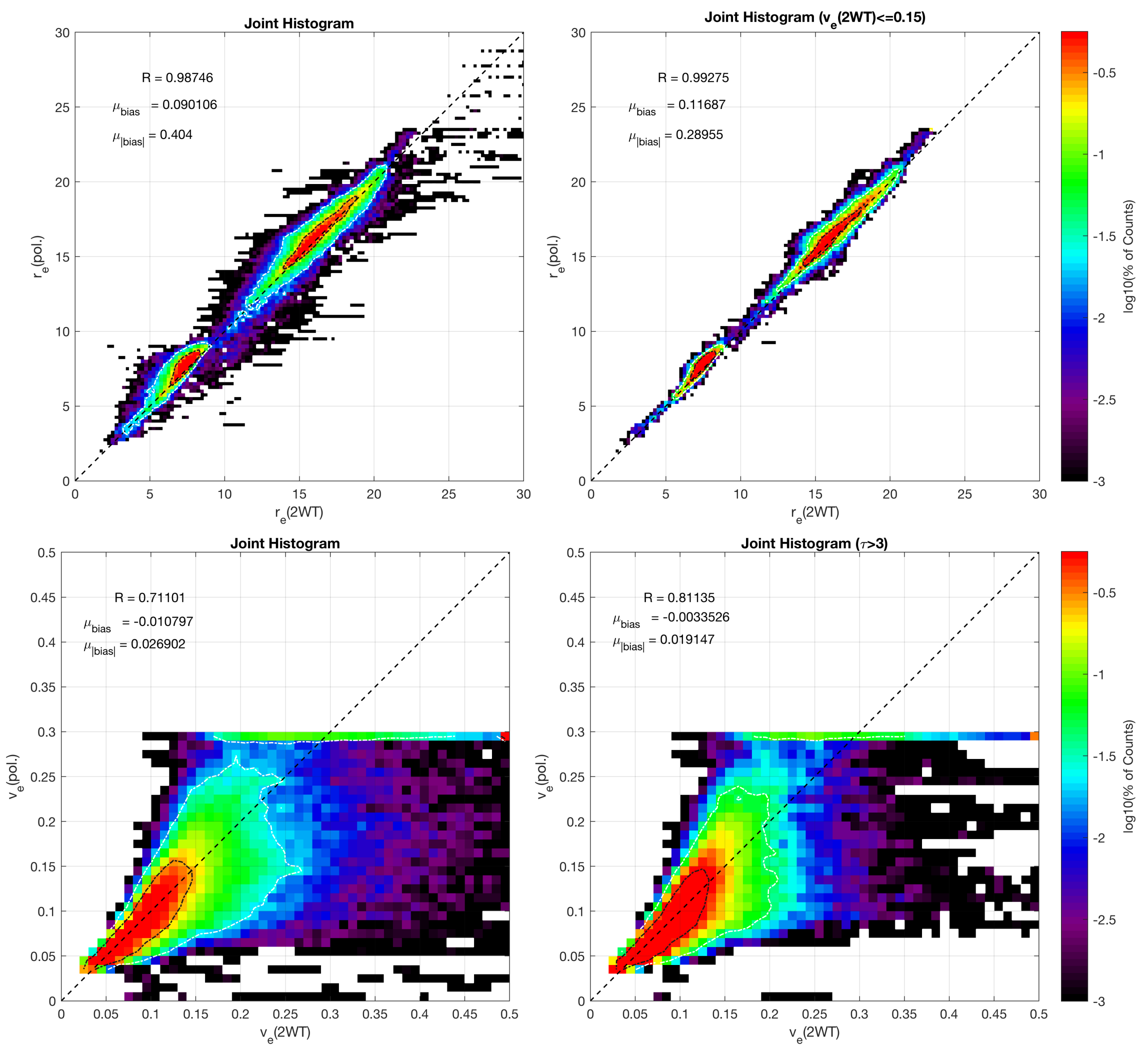

Figure 3: Refer to Figure 4 of the original manuscript for more figure information. These polarimetric retrieval comparison plots have been updated to include data from all the same viewing geometries used in the bispectral retrieval.

Zhang, Z., X. Dong, B. Xi, H. Song, P. L. Ma, S. J. Ghan, S. Platnick, and P. Minnis (2017), Intercomparisons of marine boundary layer cloud properties from the ARM CAP-MBL campaign and two MODIS cloud products, *J. Geophys. Res.*, *122*(4), 2351–2365, doi:10.1002/2016JD025763.

3. Radiance Ratio Retrieval

The manuscript motivates the study by future satellite missions providing multi-angular polarimetric observations. However, also the classic bispectral observation will profit from continuous improvement of the retrieval algorithms. In recent studies, the radiance ratio retrieval approach has been proposed (actually by one of the co-authors) to reduce some limitations of the bispectral retrieval (Werner el al. 2013, Ehrlich et al. 2017, LeBlanc et al. 2015, *Brückner et al. 2014). Using ratios of spectral radiance instead of absolute radiance improves the orthogonality of the LUTs and the impact of measurement uncertainties. Therefore, some limitations discussed for the bispectral retrieval might be improved. E.g. LUTs of radiance ratios are more spread for small cloud optical thickness, the PPH-bias is likely reduced having more orthogonal LUTs (similar to the differences between 2.1 µm and 3.7 µm). This improved retrieval approach should be considered in the manuscript as a third retrieval approach if it aims to be relevant for future satellite observations.*

Werner, F., Siebert, H., Pilewskie, P., Schmeissner, T., Shaw, R. A., and Wendisch, M.: New airborne retrieval approach for trade wind cumulus properties under overlying cirrus, J. Geophys. Res.-Atmos., 118, 3634–3649, https://doi.org/10.1002/jgrd.50334, 2013.

Ehrlich, A., Bierwirth, E., Istomina, L., and Wendisch, M.: Combined retrieval of Arctic C5 liquid water cloud and surface snow properties using airborne spectral solar remote sensing, Atmos. Meas. Tech., 10, 3215-3230, https://doi.org/10.5194/amt-10-3215- 2017, 2017.

LeBlanc, S. E., Pilewskie, P., Schmidt, K. S., and Coddington, O.: A spectral method for discriminating thermodynamic phase and retrieving cloud optical thickness and effective radius using transmitted solar radiance spectra, Atmos. Meas. Tech., 8, 1361– 1383, https://doi.org/10.5194/amt-8-1361-2015, 2015.

Brückner, M., Pospichal, B., Macke, A., and Wendisch, M.: A new multispectral cloud retrieval method for ship-based solar transmissivity measurements, J. Geophys. Res., 119, 11338–11354, https://doi.org/10.1002/2014JD021775, 2014.

a. We did a sensitivity study comparing the standard MODIS approach to a ratio retrieval built using the available bands in the MODIS LUT reflectance library. We found that for plane-parallel homogeneous clouds the ratio retrieval resulted in a reduction of uncertainty << 1%. Both retrieval approaches have significant issues for low optical thicknesses. The reflectance ratio method discussed in Werner et al. 2013 makes use of hyperspectral observations with 2 nm resolution. Our current thinking is that this approach becomes less fruitful with wider spectral bands. The MODIS spectral bands are significantly wider than this (on the order of 100nm), as are many imaging radiometers as a result of instrument design trade offs between spectral resolution and spatial coverage/resolution. Because the LUT used in this study is based on MODIS it is unfortunately not straightforward to reimplement a ratio retrieval for a hypothetical hyperspectral instrument using the same datasets.

b. One of the primary reasons for applying the ratio retrieval is to minimize the PPH bias associated with the impact of the curvature of the NJK LUT for broken/inhomogeneous clouds (at coarse resolutions). For the standard Nakajima-King approach, our group has been working on a technique that can provide a simple correction or estimate of this bias discussed in Zhang et al. (2016) and others. As a consequence, we believe that the PPH bias will be less severe with the development of this technique -- removing one of the motives for implementing a ratio retrieval.

Zhang, Z., F. Werner, H. M. Cho, and G. Wind (2016), A framework based on 2-D Taylor expansion for quantifying the impacts of subpixel reflectance variance and covariance on cloud optical thickness and effective radius retrievals based on the bispectral method, *Journal of Geophysical Research: Atmospheres*, doi:10.1063/1.4975502.

Werner, F., Siebert, H., Pilewskie, P., Schmeissner, T., Shaw, R. A., and Wendisch, M.: New airborne retrieval approach for trade wind cumulus properties under overlying cirrus, J. Geophys. Res.-Atmos., 118, 3634–3649, https://doi.org/10.1002/jgrd.50334, 2013.

4. **Polarimetric Retrieval**
How meaningful are the results of the study on effects of the horizontal resolution for the polarimetric retrieval? In the motivation it was mentioned, that for POLDER a footprint of 150 km has to be used to obtain measurements of the cloudbow? This is far from the scales analyzed here with the LES clouds. Is the spatial resolution of future spaceborne polarization sensors comparable to the scales analyzed in this study? The results presented in the manuscript suggest, that in the scales analyzed here, polarimetric measurements are not strongly effected by cloud inhomogeneities. Can this conclusion also be transferred to larger spatial scales? These issues should be discussed somehow in the manuscript.

a. You are correct to point out a "vastness of scale" problem between LES (50 m) and the POLDER satellite retrievals (~50-150 km depending on what paper you look at). The intent of this work is not to compare to the POLDER instrument, but to the newer actively developing spaceborne polarimeters that are expected to launch in the next decade. Perhaps we can make that argument more clearly in the introduction. The POLDER retrieval and its resolution are highlighted for historical context on spaceborne polarimetric retrievals because it's still the only spaceborne polarimeter that has looked at cloud microphysics.

b. The latest polarimetric instruments intended for spaceborne applications such as HARP (see link below) are currently aiming for a retrieval spatial resolution of ~2.5 km for cloud retrievals. That means that the LES retrievals shown here at up to 800 m resolutions are within an order of magnitude of the expected results. At 800 m we have 64 pixels of observations, and to avoid the poor statistics for coarse resolutions we stopped there. It should also be noted that the airborne versions of the polarimeters currently being developed often make observations at nadir resolutions within the ranges discussed here.
https://userpages.umbc.edu/~martins/laco/harp.htm

Minor comments

1. *P1 L1: Title:* *The study is limited to three very specific cases of liquid low level cloud over the ocean (trade wind cumulus, stratocumulus). At least "liquid clouds" has to be added in the title. "marine" or similar indicating, that only clouds over water have been analyzed should also be considered. Retrieval of ice clouds will certainly differ from the study presented here. Also results for clouds over land can differ due to surface albedo and the different cloud dynamics over land (vertical profile).*

    a. Response: This is a good point. The title will be amended as follows to indicate the focus on marine boundary layer clouds:
    "Comparisons of bispectral and polarimetric retrievals of marine boundary layer cloud microphysics: Case studies using a LES-satellite retrieval simulator"

2. *P5 L10:* *The reflectance at SWIR and VNIR bands both depend on optical thickness and effective radius. It is simply wrong to indicate that the sensitivities are decoupled. The lookup table shown in the manuscript clearly reveal the non-orthogonality especially for small optical thickness. This coupling has different implication on the bispectral retrieval (PPH-bias) which partly are already used to discus the retrieval biases.*

    a. This was not the intention, I will parse that sentence more carefully. Refer to amended statement on line 16 of page 5.

3. *P8 L12:* *The polarized phase function and the modeled polarized reflectance are two different quantities as far as I understood. How these can be fitted to each other? The degree of linear polarization calculated from polarized reflectance would be comparable to P12.*

a. All retrievals in this study are performed on polarized reflectance (Q) after transformation of the polarization state to the principal plane (so that the magnitude of U is approximately 0). The polarized phase function is equal to the polarized reflectance Q in the principal plane for single scattering. The degree of linear polarization is not used in this retrieval.

4. *P9 L27: Eq. 4: Wouldn't it be better to use/write the size of the coarser resolution pixel into brackets of the mean value. Instead R(0.865 µm, 50 m) better R(0.865 µm, 800 m)? The mean value is calculated for the coarse resolution pixel and independent on the fine resolution of 50 m.*
    a. No, the mean value at 800m is calculated using the 50m data. The values inside the brackets are simply the highest resolution data I have. For example, an 800m pixel has 16x16 pixels at 50m within it that are used in this calculation to get the mean and standard deviation. Hopefully this has been further clarified in the text.

5. *P10 L11: Is the comparison only done for a specific solar zenith angle or are all simulations mixed? In Sect. 4.2, Fig. 5 it was explicitly mentioned that all cases and geometries are included. Should be done here as well. P11 L3: Footnote: Why this was written as footnote? The explanation given in the footnote should be presented directly in the main text because it is needed to understand the systematic bias. Putting such parts into a footnote only disturbs the flow of reading.*
    a. All geometries and simulations are mixed; I will make an effort to highlight that in the text. And the footnote will be worked in to flow with the test.

6. *P14 L5: Figure 8: This comparison has to be done with respect to the LES-truth (see also comment to Figure 5). Only then you can judge which retrieval has a bias and which not. Comparing both retrieval to each other merges effects and does not tell which retrieval is closer to reality. In P14 L9 the differences between bispectral and polarimetric retrieval are rated by assuming the polarimetric retrieval to be the truth. This should be avoided as also the polarimetric retrieval may have caused these differences. You should always refer to the truth solution which is given by the LES cloud fields.*
    a. Refer to the response to the second reviewer regarding figure 8.

7. *P14 L10: typo: "less" and "lower"*

8. *Figure 1: Panel a): Something is wrong because the color codes do not fit to spectral bands! Likely the labeling of x-y axis is switched.*
    a. Indeed, this was an accidental figure editing error that got fixed already but didn't make it into the submitted copy. It is now updated correctly.

9. *Figure 2: Indicate horizontal scale!*
    a. I can include axes labels for these, but they would get even smaller… I have indicated resolution and scale in the figure as an alternative.

10. *Figure 3: Typo in caption: "or" should be "of"*

11. *Figure 5: I do not see a need for these plots. Comparing both approaches separately to the LES-truth already tells where the uncertainties of the individual approaches are. Comparing both to each other makes interpretation only very difficult but does not give any new conclusions. Both retrieval have to be compared to the LES-truth. The comparison in figure 5 also results in some incorrect conclusions (at least when these are only followed from Fig. 5 alone). The polarimetric retrieval has been found to be better compared to the bispectral retrieval. But this conclusion can not come from Fig. 5 because Fig 5 does not compare to the truth values. Therefore, I suggest to remove Fig. 5 or exchange by similar comparisons with the LES-truth. Also the corresponding discussion (P 12 L 20-30) should use the LES-truths as the reference.*
    a. These plots are necessary because, as indicated in the introduction, this is the sort of plot used in any instrument intercomparison. Put another way, for observational data sets, there is no such thing as an LES truth. Both retrieval approaches have already been compared to the LES truth in Figure 3 and 4. I added additional discussion at the opening of the intercomparison section to highlight the purpose of this approach.

12. *Figure 6: Some data does not fit into the LUT. Is this necessary? The range of optical thickness can be extended in your simulations? You should be able to calculate the maximum optical thickness from the LES field in advance. Or is there any other reason why these data does not fit?*
    a. The LUT has a maximum optical thickness below the maximum optical thickness of the LES. Unfortunately, I did not have this version of the LES when we first made the LUT several years ago and so here we are today. At this point it would be computationally expensive to extend the LUT for all geometries and combinations of r_e, v_e, τ – and it wouldn't alter any conclusions.

13. *Figure 6: What is the range of optical thickness? Can be labeled similar to the particle size.*
    a. The range of the optical thickness was stated in the background section (τ=[0.1:100] with 101 logarithmically spaced grid points). I would prefer not to further clutter the figure as optical thickness isn't the primary focus on the paper.

14. *Figure 7: This figure is also not needed. Both results have already been compared to the LES-truth. Figure 8: Very hard do distinguish the color code*

and circle size. Especially the size of the circles is not visible in the center of the data cloud. Only outliers are visible

a. As stated previously, the comparison figures are part of the primary objective of the paper. Folks comparing these two techniques to one another once they are in orbit don't have the advantage of comparison to LES, so this type of plot is useful in their context. This figure is intended to emphasize that the two retrievals of τ perform approximately the same when they are compared to one another.
b. Regarding figure 8 we have made substantial changes to the way we are attempting to visually display this conclusion. Refer to our response to the second reviewer for more information.

Anonymous Referee #2

Received and published: 27 November 2017

This is a review of the manuscript titled "Comparisons of bispectral and polarimetric cloud microphysical retrievals using LES-Satellite retrieval simulator" submitted to AMTD by Miller et al. The paper discusses the biases in retrieved drop effective radius and cloud optical thickness using two independent approaches, namely the bi-spectral approach and the polarimetric approach. Both methods are evaluated using simulated measurements based on large eddy simulations and 2D radiative transfer. Biases in retrieval products caused by vertical and horizontal inhomogeneity are evaluated. The work follows previous work by the same authors, especially that published in Miller et al. (2016) and Zhang et al. (2012). Those previous papers lacked the focus on polarimetric retrievals, so this paper is a useful addition to those studies. The polarimetric method is the more robust method, as also shown here, but requires multi-view polarization measurements at specific viewing geometries, which makes it not applicable everywhere. The polarimetric method is often seen as a means to validate the bi-spectral retrievals. Therefore, this comparison of the two methods is useful to better understand such comparisons. However, in my opinion, some of the means of presentation are difficult to interpret and not very effective. Also, while focus is on the effective radius retrievals, the optical thickness retrievals are also evaluated, but some rather surprising outliers in the optical thickness retrievals are not explained. Finally, the authors should provide more references in the results section to put their results in perspective to other relevant papers. Below I will provide more details to these major comments and will follow with some minor comments

Major comments:

1. The conclusions about polarimetric and bi-spectral retrievals are not new. As mentioned in the paper, the bispectral method is already well studied by several papers, including Miller et al. (2016) and Zhang et al. (2012). The polarimetric results are consistent with those by, for example, Alexandrov et al. (2012) and Shang et al. (2015). All of the papers mentioned above are referenced in the manuscript, but mostly in the introduction or conclusions. The authors should provide more references in the results section and put their results in perspective to the 4 papers mentioned above, and other relevant papers. For example, the reduced sensitivity of effective variance at high values, the effects of vertical variation and insensitivity of the approach to optical thickness are all discussed by Alexandrov et al. (2012). The sensitivity to sub-pixel inhomogeneity in the polarimetric approach is discussed by Shang et al. (2015). Retrieval biases in the bi-spectral approach is discussed by Miller et al. Specifically, Miller et al. conclude that biases are especially large in "transition zone" at the cloud edges. I find it surprising that this is not mentioned here at all. In summary, when discussing the results, please also discuss the appropriate references to set these results in context with these previous studies.

a. We have worked to integrate more citations and commentary on previous results into the data and analysis sections. Hopefully this more fully acknowledges that these uncited observations are not new, that was not our intention.
b. The importance of the cloud top transition zone discussed in Miller et al. 2016 is tied more directly to LWP retrievals than it is to the re retrieval directly. Getting a droplet size that is reduced from its maximum by entrainment processes can bias the LWP because of assumptions made about cloud vertical profile. However, in the context of retrieving the cloud top droplet size, the transition zone is a valid modification of the cloud top microphysics. It should be noted, that the transition zone would also modify the vertical weighting, so the both retrievals and the LES proxy should agree with one another in the presence of the transition zone.
c. In light of the previous point, some further commentary about the applications of cloud droplet size retrievals to different science questions was included at the end of the summary and discussion.

2. *The optical thickness retrievals are also evaluated in this study, but hardly discussed. I find it rather surprising that even at large optical depths, large biases occasionally occur. As mentioned, the optical depth retrievals are similarly biased using the polarimetry size retrievals. Looking at equation 4, I am curious what could cause these optical depth biases if not errors in assumed size distribution? It would be informative to further explore this bias in the paper.*
    a. The accuracy of all of these optical thickness retrievals depends on whether the VNIR band asymmetry parameters (phase functions) and extinction efficiencies associated with those distributions and their effective radii deviate significantly from values associated with the same effective radius in the LUTs (gamma dist., assumed variance). In this sense, the droplet size distributions (DSD) of the LES are not exactly gamma-distributed, and thus the combination of phase functions, effective radii, and variances, are not exactly connected directly with the assumption of the form assumed by the bispectral and polarimetric retrievals. For example, the LES distributions sometimes have multiple distribution modes. As a consequence, the size distribution differences reduce the cross section distribution (second moment of the DSD) that is used to define τ_{tot}. This difference in size distribution becomes even more severe for the distributions that are clearly non-gamma with ve>0.3. This is demonstrated by the figure below depicting the median DSD's and cross section distributions for each LES case. The results highlight that the cross section distribution has a reduced peak relative to the expected gamma-distribution. This largely stems from the increased number of droplets in small bins (relative to gamma) as well as an increased number of droplets in the larger bins. Surprisingly, the area and

volume distributions of these populations are similar in a relative sense, resulting in values of r_e that are consistent, but low biasing τ_{tot}.

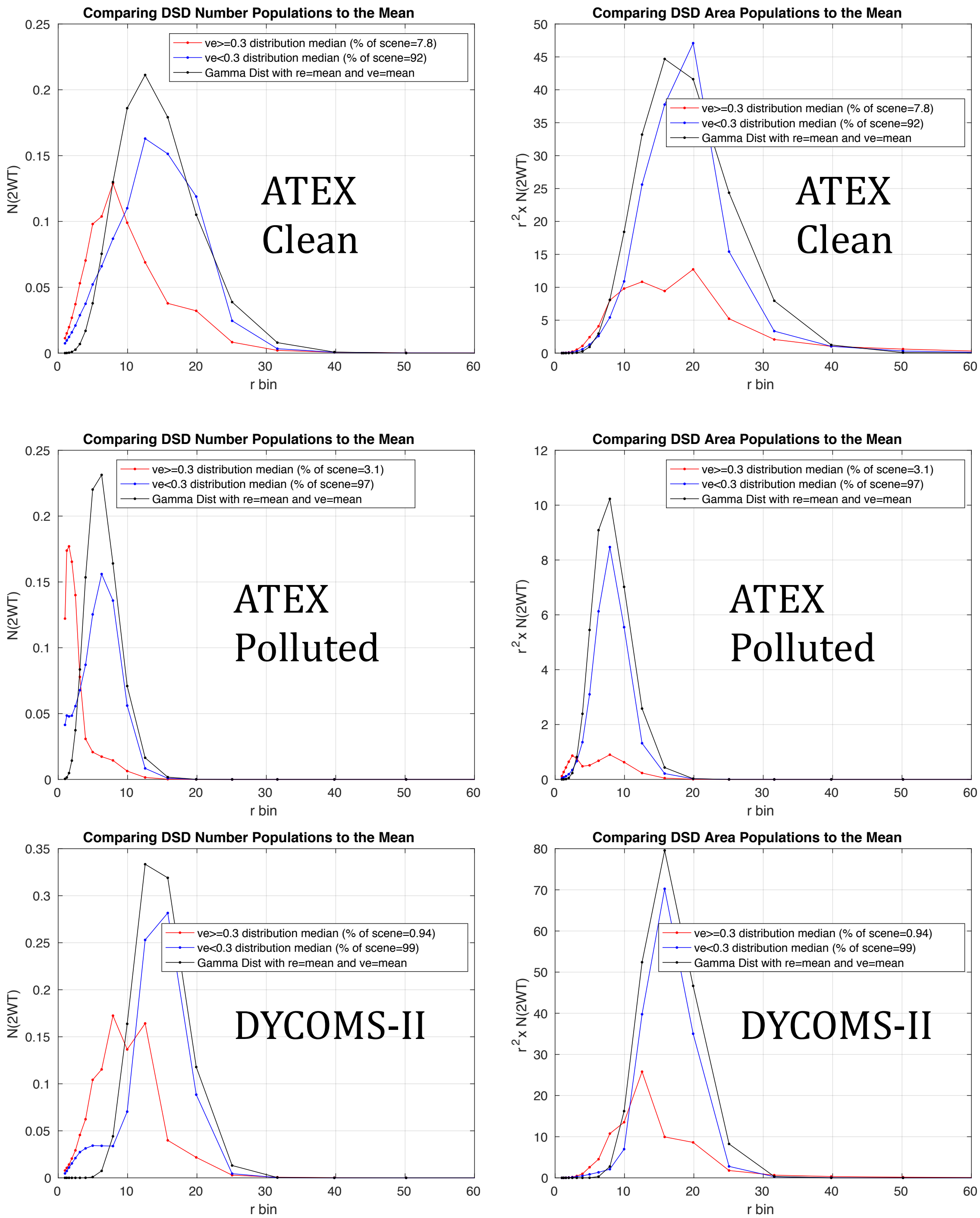

Figure 4: The panels on the left depict droplet size distributions for different populations of each LES case. The red curves denote distributions with non-gamma v_e>0.3, and the blue curves indicate the population with v_e<0.3. The black curves indicate the gamma distribution corresponding to the scene average r_e and v_e combination. The panels on the right are area distribution populations derived from the DSD's on the left.

b. Biases can also be associated with the vertical profile assumption in the LUT. The vertical distribution of the extinction coefficient is not homogeneous as conventionally assumed in the formulation of the bispectral LUT. In the adiabatic model the cloud top r_e is functionally defined with respect to τ_{tot}, indicating that it might be possible that biases in retrieval of one would impact the other.

c. I don't know if there is a lot that can be done regarding these limitations in the context of the two retrieval approaches discussed in this study. Creating retrieval LUT that assumes all clouds are vertically adiabatic is problematic. And the addition of more complicated size distribution assumptions isn't easily implemented in either of these techniques in a practical sense. However, for the droplet size distribution shape assumption, we can perhaps further highlight the Rainbow Fourier Transform method of Alexandrov et al. (2012). for evaluating the droplet size distribution shape and it's impact on retrieval techniques that assume gamma distributions.

3. *In figure 5, the effect of the fixed variance of 0.1 on the bispectral retrievals are evaluated. This is done by coupling the bispectral retrievals to the variance retrieved with the polarimetric approach. However, you showed that this retrieved variance often significantly differs from the true value. It performs best in the case around a value of 0.1, which is the value assumed for the bispectral method. So, in this test, often still a 'wrong' variance is used. It is difficult, if not impossible, to deduce solid conclusions from the present results. The authors should couple the bispectral retrievals to the true (2WT) value of variance for each gridbox for this evaluation.*

   a. While this could be changed, the results will be quite similar because the polarimetric retrieval of v_e behaves quite well below v_e=0.15, which is shown.
   b. One of the reasons why we coupled to the v_e(pol) retrieval was to highlight how the bispectral and polarimetric retrievals could compliment one another. We have added a brief statement of this purpose to the paper. It is also essentially a more formalized comparison of the argument first presented in figure 9 and 10 of Miller et al. (2016). Also as you already noted, this change has very little impact on the quality of the bispectral 2.13 μm retrieval, presumably because of the disconnection between the vertical weighting of the polarimetric retrieval and the 2.13 μm bispectral retrieval.

4. *Figure 8 convolves a lot of information and is therefore hard to interpret. The aim is to show the effect of pixel size and inhomogeneity on the bi-spectral and*

polarimetric technique. Here the two methods are compared, making it impossible to tell which technique is biased where and how. The authors concluded that "it is evident that as the spatial retrieval footprint reaches 800 m the sub-pixel inhomogeneity tends to increase and the re(2.13 μm) retrieval suffers from an increasingly high bias relative to the polarimetric retrieval." I do not get this from looking at this figure. Using the colors and open circles of different sizes produces a pretty colorful blob, but individual circles are impossible to spot mostly. I see some large circles with high biases, but have the impression that most are hiding in the colorful blob. The conclusions and abstract state that the methods compare well for high resolutions, but biases appear at coarser resolution. This conclusion appears to be based on this figure. Looking at figure 5, I see some very large differences between the methods for some cases, so the bispectral method also has issues at these fine resolutions, if not more. Also, the abstract and conclusion states "This bias largely stems from differences related to sensitivity of the two retrievals to unresolved inhomogeneities in effective variance and optical thickness." This suggests that the polarimetric retrievals also have sensitivity to the spatial resolution. They probably have somewhat (as concluded by Shang et al.), but this is not at all evident from this figure and analysis. Please produce figures that more clearly and systematically support these conclusions (or other conclusions). I suggest producing separate plots showing biases from true effective radius values in bi-spectral and polarimetric techniques as a function of H. Possibly the resolution can be on the y-axis and biases can be color coded?

a. One of the biggest problems with the original figure, as you point out, is that the spatial resolution information is hard to display simultaneously with the retrieval comparison. Also, because H_σ is the only variable that has a physical dependence on spatial resolution, showing their correlations separately actually makes more sense. We have attempted to deconvolve this plot further by breaking it into multiple parts. First of all, the following figures focus on the ATEX cases because there are more broken and inhomogeneous clouds in these two scenes than in DYCOMS-II.
b. The first part (in Figure 5) demonstrates the increasing population of inhomogeneous observations at coarser spatial resolutions by displaying the change in the histogram of H_σ as a function of resolution. This drives home the point that at coarse resolutions there is more inhomogeneity.
c. The second part (in Figure 6) displays joint histograms of retrieval bias (relative vertically weighted LES properties) and H_σ for the ATEX cloud cases. Note that these figures amass all of the data from the coarse resolution (100 to 800 m) ATEX cases because they have the most diversity in terms of H_σ.
d. I think that these figures provide a more detailed perspective than the previous versions so we will be modifying the manuscript to include them. Mixing all of the coarse spatial resolutions together for the joint

histograms is a valid exercise because the primary difference between a joint histogram of a single coarse resolution and all of them is largely just the sampling of the H_σ distribution.

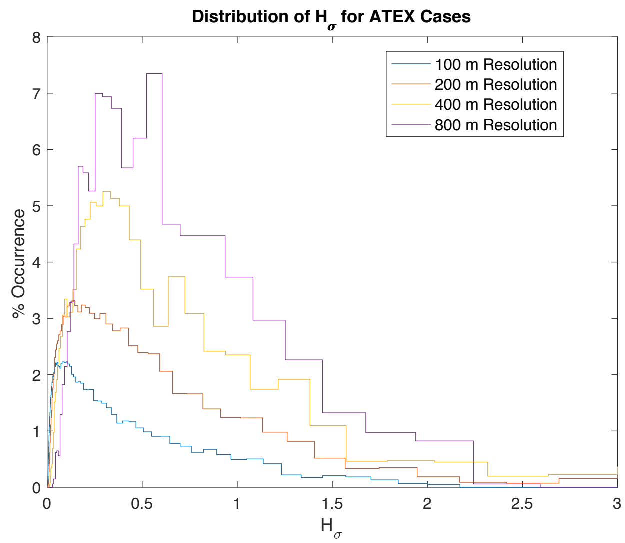

Figure 5: Distributions of H_σ for the ATEX polluted and clean cases at all coarsened spatial resolution (100, 200, 300, 400, 800 m).

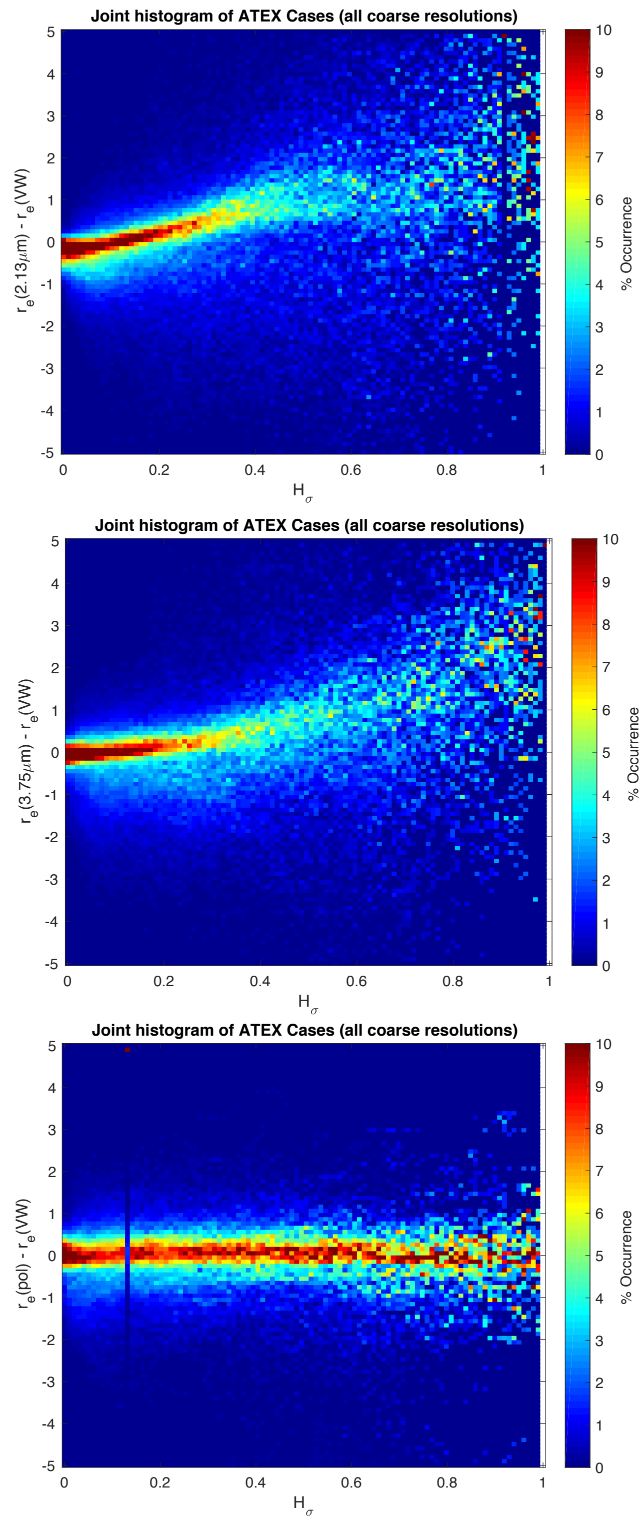

Figure 6: Joint histograms of retrieval biases (relative to VW) with respect to H_σ for the ATEX clean and polluted cases under all observation geometries at coarsened spatial resolution (100, 200, 300, 400, 800 m). The color bar indicates percent occurrence.

<u>Minor comments:</u>

1. *In figure 3, the cases with tau<3 are removed, revealing a better result. However, I am wondering how the 2D histogram for tau<3 looks like. Do the bulk of these retrievals still perform well, or are they all biased? That is not clear from these plots.*

2. *Figure 4 shows that the uncertainty in the retrievals of effective variance is rather high. Firstly, please relate your findings with those found by Alexandrov et al. (2012). Secondly, please discuss the appropriateness of the assumption of a gamma distribution for these LES fields. Is the model producing size distributions that can be well described by a gamma distribution? If not, this could explain part of the spread found in your results. Also, please discuss the possibility of non-parametric size distributions from polarimetry, as presented by Alexandrov et al. (2012; J. Quant. Spectrosc. Radiat. Transfer, 113, 2521-2535, doi:10.1016/j.jqsrt.2012.03.025.)*
    a. The paper now highlights the possibility of deviations from the gamma-distribution assumption. I also cited the rainbow fourier transform paper again during that discussion.

3. *Figure 9 shows the variation in polarization measurements for sub-pixels in a 800m pixel. For the case including the thin cloud parts, there appears to be a substantial spread, but this is mostly in absolute magnitude. Please note in the text that the polarimetry technique is not sensitive to the absolute magnitude of the measurements, and these variations are therefore not an issue for this technique.*
    a. This has been noted in the text.

<u>Minor text edits:</u>

1. *Page 2, line 9: add “which” before “simultaneously”*
2. *Page 2, line 13: Add “Suomi” in front of “National” (and NPP)*

Page 9: [1] Deleted **Daniel Miller** **2/8/18 2:20 PM**
corresponds

Page 9: [1] Deleted **Daniel Miller** **2/8/18 2:20 PM**
corresponds

Page 9: [2] Deleted **Daniel Miller** **2/13/18 10:50 AM**
2WT

Page 9: [2] Deleted **Daniel Miller** **2/13/18 10:50 AM**
2WT

Page 9: [2] Deleted **Daniel Miller** **2/13/18 10:50 AM**
2WT

Page 9: [2] Deleted **Daniel Miller** **2/13/18 10:50 AM**
2WT

Page 9: [2] Deleted **Daniel Miller** **2/13/18 10:50 AM**
2WT

Page 9: [2] Deleted **Daniel Miller** **2/13/18 10:50 AM**
2WT

Page 9: [2] Deleted **Daniel Miller** **2/13/18 10:50 AM**
2WT

Page 9: [3] Deleted **Daniel Miller** **3/4/18 12:49 PM**
directly

Page 9: [3] Deleted **Daniel Miller** **3/4/18 12:49 PM**
directly

Page 9: [3] Deleted **Daniel Miller** **3/4/18 12:49 PM**
directly

Page 9: [3] Deleted **Daniel Miller** **3/4/18 12:49 PM**
directly

Page 9: [3] Deleted **Daniel Miller** **3/4/18 12:49 PM**
directly

Page 9: [4] Moved to page 9 (Move #2) **Daniel Miller** **2/13/18 10:53 AM**
section 2 of (Miller et al., 2016).

Page 9: [4] Moved to page 9 (Move #2) **Daniel Miller** **2/13/18 10:53 AM**
section 2 of (Miller et al., 2016).

Page 9: [5] Deleted **Daniel Miller** **2/13/18 1:11 PM**

. We note that the 2WT vertical weighting function provides a reasonable approximation when the signal is contributed mainly by single scattering (i.e., 3.7 µm or polarimetric reflectances) but becomes less accurate for spectral bands with more multiple scattering (Platnick, 2000).

Page 9: [5] Deleted **Daniel Miller** **2/13/18 1:11 PM**

. We note that the 2WT vertical weighting function provides a reasonable approximation when the signal is contributed mainly by single scattering (i.e., 3.7 µm or polarimetric reflectances) but becomes less accurate for spectral bands with more multiple scattering (Platnick, 2000).

Page 9: [5] Deleted **Daniel Miller** **2/13/18 1:11 PM**

. We note that the 2WT vertical weighting function provides a reasonable approximation when the signal is contributed mainly by single scattering (i.e., 3.7 µm or polarimetric reflectances) but becomes less accurate for spectral bands with more multiple scattering (Platnick, 2000).

Page 9: [5] Deleted **Daniel Miller** **2/13/18 1:11 PM**

. We note that the 2WT vertical weighting function provides a reasonable approximation when the signal is contributed mainly by single scattering (i.e., 3.7 µm or polarimetric reflectances) but becomes less accurate for spectral bands with more multiple scattering (Platnick, 2000).

Page 9: [5] Deleted **Daniel Miller** **2/13/18 1:11 PM**

. We note that the 2WT vertical weighting function provides a reasonable approximation when the signal is contributed mainly by single scattering (i.e., 3.7 µm or polarimetric reflectances) but becomes less accurate for spectral bands with more multiple scattering (Platnick, 2000).

Page 9: [5] Deleted **Daniel Miller** **2/13/18 1:11 PM**

. We note that the 2WT vertical weighting function provides a reasonable approximation when the signal is contributed mainly by single scattering (i.e., 3.7 µm or polarimetric reflectances) but becomes less accurate for spectral bands with more multiple scattering (Platnick, 2000).

Page 9: [5] Deleted **Daniel Miller** **2/13/18 1:11 PM**

. We note that the 2WT vertical weighting function provides a reasonable approximation when the signal is contributed mainly by single scattering (i.e., 3.7 µm or polarimetric reflectances) but becomes less accurate for spectral bands with more multiple scattering (Platnick, 2000).

Page 9: [5] Deleted **Daniel Miller** **2/13/18 1:11 PM**

. We note that the 2WT vertical weighting function provides a reasonable approximation when the signal is contributed mainly by single scattering (i.e., 3.7 µm or polarimetric reflectances) but becomes less accurate for spectral bands with more multiple scattering (Platnick, 2000).

Page 9: [5] Deleted **Daniel Miller** **2/13/18 1:11 PM**

. We note that the 2WT vertical weighting function provides a reasonable approximation when the signal is contributed mainly by single scattering (i.e., 3.7 μm or polarimetric reflectances) but becomes less accurate for spectral bands with more multiple scattering (Platnick, 2000).

Page 9: [5] Deleted **Daniel Miller** **2/13/18 1:11 PM**

. We note that the 2WT vertical weighting function provides a reasonable approximation when the signal is contributed mainly by single scattering (i.e., 3.7 μm or polarimetric reflectances) but becomes less accurate for spectral bands with more multiple scattering (Platnick, 2000).

Page 9: [5] Deleted **Daniel Miller** **2/13/18 1:11 PM**

. We note that the 2WT vertical weighting function provides a reasonable approximation when the signal is contributed mainly by single scattering (i.e., 3.7 μm or polarimetric reflectances) but becomes less accurate for spectral bands with more multiple scattering (Platnick, 2000).

Page 9: [5] Deleted **Daniel Miller** **2/13/18 1:11 PM**

. We note that the 2WT vertical weighting function provides a reasonable approximation when the signal is contributed mainly by single scattering (i.e., 3.7 μm or polarimetric reflectances) but becomes less accurate for spectral bands with more multiple scattering (Platnick, 2000).

Page 9: [5] Deleted **Daniel Miller** **2/13/18 1:11 PM**

. We note that the 2WT vertical weighting function provides a reasonable approximation when the signal is contributed mainly by single scattering (i.e., 3.7 μm or polarimetric reflectances) but becomes less accurate for spectral bands with more multiple scattering (Platnick, 2000).

Page 9: [5] Deleted **Daniel Miller** **2/13/18 1:11 PM**

. We note that the 2WT vertical weighting function provides a reasonable approximation when the signal is contributed mainly by single scattering (i.e., 3.7 μm or polarimetric reflectances) but becomes less accurate for spectral bands with more multiple scattering (Platnick, 2000).

Page 9: [5] Deleted **Daniel Miller** **2/13/18 1:11 PM**

. We note that the 2WT vertical weighting function provides a reasonable approximation when the signal is contributed mainly by single scattering (i.e., 3.7 μm or polarimetric reflectances) but becomes less accurate for spectral bands with more multiple scattering (Platnick, 2000).

Page 11: [6] Deleted **Daniel Miller** **2/13/18 2:22 PM**

in this section

Page 11: [6] Deleted **Daniel Miller** **2/13/18 2:22 PM**

in this section

Page 11: [7] Deleted **Daniel Miller** **3/4/18 4:44 PM**

SWIR

Page 11: [7] Deleted **Daniel Miller** **3/4/18 4:44 PM**

SWIR

Page 11: [7] Deleted **Daniel Miller** **3/4/18 4:44 PM**

SWIR

Page 11: [7] Deleted **Daniel Miller** **3/4/18 4:44 PM**

SWIR

Page 11: [7] Deleted **Daniel Miller** **3/4/18 4:44 PM**

SWIR

Page 11: [7] Deleted **Daniel Miller** **3/4/18 4:44 PM**

SWIR

Page 11: [7] Deleted **Daniel Miller** **3/4/18 4:44 PM**

SWIR

Page 11: [7] Deleted **Daniel Miller** **3/4/18 4:44 PM**

SWIR

Page 11: [7] Deleted **Daniel Miller** **3/4/18 4:44 PM**

SWIR

Page 11: [7] Deleted **Daniel Miller** **3/4/18 4:44 PM**

SWIR

Page 11: [7] Deleted **Daniel Miller** **3/4/18 4:44 PM**

SWIR

Page 11: [7] Deleted **Daniel Miller** **3/4/18 4:44 PM**

SWIR

Page 11: [7] Deleted **Daniel Miller** **3/4/18 4:44 PM**

SWIR

Page 11: [7] Deleted **Daniel Miller** **3/4/18 4:44 PM**

SWIR

Page 11: [7] Deleted **Daniel Miller** **3/4/18 4:44 PM**

SWIR

Page 11: [7] Deleted **Daniel Miller** **3/4/18 4:44 PM**

SWIR

Page 11: [7] Deleted **Daniel Miller** **3/4/18 4:44 PM**

SWIR

Page 11: [7] Deleted **Daniel Miller** **3/4/18 4:44 PM**

SWIR

Page 11: [7] Deleted	Daniel Miller	3/4/18 4:44 PM

SWIR

Page 11: [7] Deleted	Daniel Miller	3/4/18 4:44 PM

SWIR

Page 11: [7] Deleted	Daniel Miller	3/4/18 4:44 PM

SWIR

Page 11: [7] Deleted	Daniel Miller	3/4/18 4:44 PM

SWIR

Page 11: [7] Deleted	Daniel Miller	3/4/18 4:44 PM

SWIR

Page 11: [7] Deleted	Daniel Miller	3/4/18 4:44 PM

SWIR

Page 11: [8] Deleted	Daniel Miller	2/26/18 10:09 AM

The joint histograms

Page 11: [8] Deleted	Daniel Miller	2/26/18 10:09 AM

The joint histograms

Page 11: [8] Deleted	Daniel Miller	2/26/18 10:09 AM

The joint histograms

Page 11: [8] Deleted	Daniel Miller	2/26/18 10:09 AM

The joint histograms

Page 11: [8] Deleted	Daniel Miller	2/26/18 10:09 AM

The joint histograms

Page 11: [8] Deleted	Daniel Miller	2/26/18 10:09 AM

The joint histograms

Page 11: [8] Deleted	Daniel Miller	2/26/18 10:09 AM

The joint histograms

Page 16: [9] Deleted	Daniel Miller	2/14/18 3:39 PM

panels (a) and (b) of Figure 8 compare r_e(pol) to the r_e(2.13 µm) and r_e(3.75 µm) respectively at increasingly coarsened spatial resolutions (as indicated by the size of the circles). In addition to the spatial resolution, these plots also indicate the magnitude the of sub-pixel inhomogeneity index (H_σ) (as indicated by the color of the circles). It is evident that as the spatial retrieval footprint reaches 800 m the sub-pixel inhomogeneity tends to increase and the r_e(2.13 µm) retrieval suffers from an increasingly high bias relative to the polarimetric retrieval. The presence of this behavior is less pronounced for in the r_e(3.7 μm) comparison is lower, although the trend is still clearly present.

Page 28: [10] Deleted	Daniel Miller	2/26/18 1:23 PM

Ackerman, A. S., Kirkpatrick, M. P., Stevens, D. E. and Toon, O. B.: The impact of humidity above stratiform clouds on indirect aerosol climate forcing, Nature, 432(7020), 1014–1017, 2004.

Ackerman, A. S., vanZanten, M. C., Stevens, B., Savic-Jovcic, V., Bretherton, C. S., Chlond, A., Golaz, J.-C., Jiang, H., Khairoutdinov, M., Krueger, S. K., Lewellen, D. C., Lock, A., Moeng, C.-H., Nakamura, K., Petters, M. D., Snider, J. R., Weinbrecht, S. and Zulauf, M.: Large-Eddy Simulations of a Drizzling, Stratocumulus-Topped Marine Boundary Layer, Mon. Wea. Rev., 137(3), 1083–1110, doi:10.1175/2008MWR2582.1, 2009.

Alexandrov, M. D., Cairns, B. and Mishchenko, M. I.: Rainbow Fourier transform, Journal of Quantitative Spectroscopy and Radiative Transfer, 113(18), 2521–2535, doi:10.1016/j.jqsrt.2012.03.025, 2012a.

Alexandrov, M. D., Cairns, B., Emde, C., Ackerman, A. S. and van Diedenhoven, B.: Accuracy assessments of cloud droplet size retrievals from polarized reflectance measurements by the research scanning polarimeter

, Remote Sensing of Environment, 125, 92–111, doi:10.1016/j.rse.2012.07.012, 2012b.

Alexandrov, M. D., Cairns, B., Wasilewski, A. P., Ackerman, A. S., McGill, M. J., Yorks, J. E., Hlavka, D. L., Platnick, S. E., Thomas Arnold, G., van Diedenhoven, B., Chowdhary, J., Ottaviani, M. and Knobelspiesse, K. D.: Liquid water cloud properties during the Polarimeter Definition Experiment (PODEX), Remote Sensing of Environment, 169, 20–36, doi:10.1016/j.rse.2015.07.029, 2015.

Bréon, F. M. and Doutriaux-Boucher, M.: A comparison of cloud droplet radii measured from space, IEEE Trans. Geosci. Remote Sensing, 43(8), 1796–1805, doi:10.1109/TGRS.2005.852838, 2005.

Bréon, F. M. and Goloub, P.: Cloud droplet effective radius from spaceborne polarization measurements, Geophys. Res. Lett., 25(11), 1879–1882, 1998.

Cairns, B., Russell, E. E. and Travis, L. D.: Research Scanning Polarimeter: calibration and ground-based measurements, SPIE's Conference on Polarization: Measurement, Analysis, and Remote Sensing II, 186–196, doi:10.1117/12.366329, 1999.

Cho, H. M., Zhang, Z., Meyer, K., Lebsock, M., Platnick, S., Ackerman, A. S., Di Girolamo, L., C Labonnote, L., Cornet, C., Riedi, J. and Holz, R. E.: Frequency and causes of failed MODIS cloud property retrievals for liquid phase clouds over global oceans, J. Geophys. Res., 120(9), 4132–4154, doi:10.1002/2015JD023161, 2015.

De Haan, J. F., Bosma, P. B. and Hovenier, J. W.: The adding method for multiple scattering calculations of polarized light, Astronomy and Astrophysics, 183, 371–391, 1987.

Deirmendjian, D.: Scattering and polarization properties of water clouds and hazes in the visible and infrared, Appl. Opt., 3(2), 187–196, 1964.

Deschamps, P. Y., Breon, F. M., Leroy, M., Podaire, A., Bricaud, A., Buriez, J. C. and Seze, G.: The POLDER mission: instrument characteristics and scientific objectives, IEEE Trans. Geosci. Remote Sensing, 32(3), 598–615, doi:10.1109/36.297978, 1994.

Diner, D. J., Xu, F., Garay, M. J., Martonchik, J. V., Rheingans, B. E., Geier, S., Davis, A., Hancock, B. R., Jovanovic, V. M., Bull, M. A., Capraro, K., Chipman, R. A. and McClain, S. C.: The Airborne Multiangle

SpectroPolarimetric Imager (AirMSPI): a new tool for aerosol and cloud remote sensing, Atmos. Meas. Tech., 6(8), 2007–2025, doi:10.5194/amt-6-2007-2013, 2013.

Fridlind, A. M. and Ackerman, A. S.: Estimating the Sensitivity of Radiative Impacts of Shallow, Broken Marine Clouds to Boundary Layer Aerosol Size Distribution Parameter Uncertainties for Evaluation of Satellite Retrieval Requirements, J. Atmos. Oceanic Technol., 28(4), 530–538, doi:10.1175/2010JTECHA1520.1, 2011.

Hansen, J. E.: Circular Polarization of Sunlight Reflected by Clouds, http://dx.doi.org/10.1175/1520-0469(1971)028<1515:CPOSRB>2.0.CO;2, doi:10.1175/1520-0469(1971)028<1515:CPOSRB>2.0.CO;2, 2010.

Hansen, J. E. and Travis, L. D.: Light scattering in planetary atmospheres, Space Sci Rev, 16(4), 527–610, 1974.

King, M. D., Menzel, W. P., Kaufman, Y. J., Tanré, D., Bo-Cai Gao, Platnick, S., Ackerman, S. A., Remer, L. A., Pincus, R. and Hubanks, P. A.: Cloud and aerosol properties, precipitable water, and profiles of temperature and water vapor from MODIS, IEEE Trans. Geosci. Remote Sensing, 41(2), 442–458, doi:10.1109/TGRS.2002.808226, 2003.

Knobelspiesse, K., Segal-Rosenhaimer, M., Redemann, J., Cairns, B. and Alexandrov, M. D.: Multi-angle, polarimetric cloud observations using a radiative transfer model trained neural network, College Park, MD. 2017.

Liu, Y. and Diner, D. J.: Multi-Angle Imager for Aerosols, Public Health Reports, 132(1), 14–17, doi:10.1177/0033354916679983, 2017.

Lohmann, U., Stier, P., Hoose, C., Ferrachat, S., Kloster, S., Roeckner, E. and Zhang, J.: Cloud microphysics and aerosol indirect effects in the global climate model ECHAM5-HAM, Atmos. Chem. Phys., 7(13), 3425–3446, doi:10.5194/acp-7-3425-2007, 2007.

Marbach, T., Phillips, P., Lacan, A. and Schlussel, P.: The 3MI Mission: Multi-Viewing -Channel - Polarisation Imager of the EUMETSAT Polar System - Second Generation (EPS-SG) dedicated to aerosol and cloud monitoring, in Sensors, Systems, and Next-Generation Satellites XVII, vol. 8889, p. 88890I, International Society for Optics and Photonics. 2013.

Martin, G. M., Johnson, D. W. and Spice, A.: The measurement and parameterization of effective radius of droplets in warm stratocumulus clouds, J. Atmos. Sci., 51(13), 1823–1842, 1994.

Martins, J. V., Fernandez-Borda, R., McBride, B., Espinosa, R. and Remer, L.: Combination between in-situ and remote sensing of tropospheric aerosols, College Park, MD. 2017.

Miles, N. L., Verlinde, J. and Clothiaux, E. E.: Cloud Droplet Size Distributions in Low-Level Stratiform Clouds, J. Atmos. Sci., 57(2), 295–311, doi:10.1175/1520-0469(2000)057<0295:CDSDIL>2.0.CO;2, 2000.

Miller, D. J., Zhang, Z., Ackerman, A. S., Platnick, S. and Baum, B. A.: The impact of cloud vertical profile on liquid water path retrieval based on the bispectral method: A theoretical study based on large-eddy simulations of shallow marine boundary layer clouds, J. Geophys. Res., 121(8), 4122–4141, doi:10.1002/2015JD024322, 2016.

Mishchenko, M. I., Cairns, B., Travis, L. D., Kopp, G., Schueler, C. F., Fafaul, B. A., Hooker, R. J., Maring, H. B., Itchkawich, T., Hansen, J. E., Kopp, G., Schueler, C. F., Fafaul, B. A., Hooker, R. J., Maring, H. B. and Itchkawich, T.: Accurate Monitoring of Terrestrial Aerosols and Total Solar Irradiance: Introducing the Glory Mission, http://dx.doi.org/10.1175/BAMS-88-5-677, 88(5), 677–691, doi:10.1175/BAMS-88-5-677, 2007.

Nakajima, T. and King, M. D.: Determination of the Optical Thickness and Effective Particle Radius of Clouds from Reflected Solar Radiation Measurements. Part I: Theory, J. Atmos. Sci., 47(15), 1878–1893, doi:10.1175/1520-0469(1990)047<1878:dotota>2.0.co;2, 1990a.

Nakajima, T. and King, M. D.: Determination of the optical thickness and effective particle radius of clouds from reflected solar radiation measurements. Part I: Theory, J. Atmos. Sci., 47(15), 1878–1893, 1990b.

Planck, M.: The theory of heat radiation, 2nd ed., P. Blakiston's Son & Co., Philadelphia, PA. [online] Available from: http://gutenberg.org/ebooks/40030, 1914.

Platnick, S.: Vertical photon transport in cloud remote sensing problems, J. Geophys. Res., 105(D18), 22919–22935, 2000.

Platnick, S., King, M. D., Ackerman, S. A., Menzel, W. P., Baum, B. A., Riedi, J. C. and Frey, R. A.: The MODIS cloud products: algorithms and examples from terra, IEEE Trans. Geosci. Remote Sensing, 41(2), 459–473, doi:10.1109/TGRS.2002.808301, 2003.

Platnick, S., Meyer, K. G., King, M. D., Wind, G., Amarasinghe, N., Marchant, B., Arnold, G. T., Zhang, Z., Hubanks, P. A., Holz, R. E., Yang, P., Ridgway, W. L. and Riedi, J.: The MODIS Cloud Optical and Microphysical Products: Collection 6 Updates and Examples From Terra and Aqua, IEEE Trans. Geosci. Remote Sensing, 55(1), 502–525, doi:10.1109/TGRS.2016.2610522, 2016.

Pruppacher, H. R. and Klett, J. D.: Diffusion Growth and Evaporation of Water Drops and Ice Crystals, in Microphysics of Clouds and Precipitation, pp. 412–463, Springer Netherlands, Dordrecht. 1978.

Roebeling, R. A., Feijt, A. J. and Stammes, P.: Cloud property retrievals for climate monitoring: Implications of differences between Spinning Enhanced Visible and Infrared Imager (SEVIRI) on METEOSAT-8 and Advanced Very High Resolution Radiometer (AVHRR) on NOAA-17, J. Geophys. Res., 111(D20), D20210, doi:10.1029/2005JD006990, 2006.

Rosenfeld, D., Liu, G., Yu, X., Zhu, Y., Dai, J., Xu, X. and Yue, Z.: High-resolution (375 m) cloud microstructure as seen from the NPP/VIIRS satellite imager, Atmos. Chem. Phys., 14(5), 2479–2496, doi:10.5194/acp-14-2479-2014, 2014.

Shang, H., Chen, L., Breon, F. M., Letu, H., Li, S., Wang, Z. and Su, L.: A better understanding of POLDER's cloud droplet size retrieval: impact of cloud horizontal inhomogeneity and directional sampling, Atmos. Meas. Tech. Discuss., 8(7), 6559–6597, doi:10.5194/amtd-8-6559-2015, 2015.

Stevens, B., Ackerman, A. S. and Albrecht, B. A.: Simulations of trade wind cumuli under a strong inversion, J. Atmos. Sci., 58(14), 1870–1891, doi:10.1175/1520-0469(2001)058<1870:sotwcu>2.0.co;2, 2001.

Stevens, B., Lenschow, D. H., Vali, G., Gerber, H., Bandy, A., Blomquist, B., Brenguier, J. L., Bretherton, C. S., Burnet, F., Campos, T., Chai, S., Faloona, I., Friesen, D., Haimov, S., Laursen, K., Lilly, D. K., Loehrer, S. M., Malinowski, S. P., Morley, B., Petters, M. D., Rogers, D. C., Russell, L., Savic-Jovcic, V., Snider, J. R., Straub, D., Szumowski, M. J., Takagi, H., Thornton, D. C., Tschudi, M., Twohy, C., Wetzel, M. and van Zanten, M. C.: Dynamics and chemistry of marine stratocumulus–DYCOMS-II, Bull. Amer. Meteor. Soc., 84(5), 579–593, doi:10.1175/BAMS-84-5-579, 2003.

Stevens, B., Moeng, C.-H., Ackerman, A. S., Bretherton, C. S., Chlond, A., de Roode, S., Edwards, J., Golaz, J.-C., Jiang, H., Khairoutdinov, M., Kirkpatrick, M. P., Lewellen, D. C., Lock, A., Müller, F., Stevens, D. E., Whelan, E. and Zhu, P.: Evaluation of Large-Eddy Simulations via Observations of Nocturnal Marine Stratocumulus, Mon. Wea. Rev., 133(6), 1443–, doi:10.1175/MWR2930.1, 2005.

Tampieri, F. and Tomasi, C.: Size distribution models of fog and cloud droplets in terms of the modified gamma function, Tellus, 28(4), 333–347, doi:10.1111/j.2153-3490.1976.tb00682.x, 1976.

Twomey, S.: The Influence of Pollution on the Shortwave Albedo of Clouds, J. Atmos. Sci., 34(7), 1149–1152, doi:10.1175/1520-0469(1977)034<1149:TIOPOT>2.0.CO;2, 1977.

Werner, F., Siebert, H., Pilewskie, P., Schmeissner, T., Shaw, R. A. and Wendisch, M.: New airborne retrieval approach for trade wind cumulus properties under overlying cirrus, J. Geophys. Res., 118(9), 3634–3649, doi:10.1002/jgrd.50334, 2013.

Wiscombe, W. J.: Mie scattering calculations: Advances in technique and fast, vector-speed computer codes, NCAR Tech, National Center for Atmospheric Research, Boulder, Colorado. 1979.

Zhang, Z. and Platnick, S.: An assessment of differences between cloud effective particle radius retrievals for marine water clouds from three MODIS spectral bands, J. Geophys. Res., 116(D20), D20215, doi:10.1029/2011JD016216, 2011.

Zhang, Z., Ackerman, A. S., Feingold, G., Platnick, S., Pincus, R. and Xue, H.: Effects of cloud horizontal inhomogeneity and drizzle on remote sensing of cloud droplet effective radius: Case studies based on large-eddy simulations, J. Geophys. Res., 117(D19), n/a–n/a, doi:10.1029/2012JD017655, 2012.

Zhang, Z., Platnick, S., Yang, P., Heidinger, A. K. and Comstock, J. M.: Effects of ice particle size vertical inhomogeneity on the passive remote sensing of ice clouds, J. Geophys. Res., 115(D17), doi:10.1029/2010JD013835, 2010.

Zhang, Z., Werner, F., Cho, H. M. and Wind, G.: A framework based on 2-D Taylor expansion for quantifying the impacts of subpixel reflectance variance and covariance on cloud optical thickness and effective …, Journal of …, doi:10.1063/1.4975502, 2016.

Zinner, T., Wind, G., Platnick, S. and Ackerman, A. S.: Testing remote sensing on artificial observations: impact of drizzle and 3-D cloud structure on effective radius retrievals, Atmos. Chem. Phys., 10(19), 9535–9549, doi:10.5194/acp-10-9535-2010, 2010.

Comparisons of bispectral and polarimetric retrievals of marine boundary layer cloud microphysics: Case studies using a LES-satellite retrieval simulator

Daniel J. Miller[1,3], Zhibo Zhang[1,2], Steven Platnick[3], Andrew S. Ackerman[4], Frank Werner[2], Celine Cornet[5], Kirk Knobelspiesse[3]

[1]Physics, UMBC, Baltimore, 21250, USA
[2]Joint Center for Earth Systems Technology, UMBC, Baltimore, MD, USA
[3]NASA Goddard Space Flight Center, Greenbelt, MD, USA
[4]NASA Goddard Institute for Space Studies, New York, NY, USA
[5]Laboratoire d'Optique Atmosphérique, Université des Sciences et Technologies de Lille, Villeneuve d'Ascq, France

Correspondence to: Daniel J. Miller (Daniel.J.Miller@nasa.gov)

Abstract. Many passive remote sensing techniques have been developed to retrieve cloud microphysical properties from satellite-based sensors, with the most common approaches being the bispectral and polarimetric techniques. These two vastly different retrieval techniques have been implemented for a variety of polar-orbiting and geostationary satellite platforms, providing global climatological datasets. Prior instrument comparison studies have shown that there are systematic differences between the droplet size retrieval products (effective radius) of bispectral (e.g. MODIS, Moderate Resolution Imaging Spectroradiometer) and polarimetric (e.g. POLDER, Polarization and Directionality of Earth's Reflectances) instruments. However, intercomparisons of airborne bispectral and polarimetric instruments have yielded results that do not appear to be systematically biased relative to one another. Diagnosing this discrepancy is complicated, because it is often difficult for instrument intercomparison studies to isolate differences between retrieval technique sensitivities and specific instrumental differences such as calibration, atmospheric correction, etc. In addition to these technical differences the polarimetric retrieval is also sensitive to the dispersion of the droplet size distribution (effective variance), which could influence the interpretation of the droplet size retrieval. To avoid these instrument-dependent complications, this study makes use of a cloud remote sensing retrieval simulator. Created by coupling a large eddy simulation (LES) cloud model with a 1-D radiative transfer model, the simulator serves as a test bed for understanding differences between bispectral and polarimetric retrievals. With the help of this simulator we can not only compare the two techniques to one another (retrieval intercomparison), but also validate retrievals directly against the LES cloud properties. Using the satellite retrieval simulator we are able to verify that at high spatial resolution (50 m) the bispectral and polarimetric retrievals are highly correlated with one another within expected observational uncertainties. The relatively small systematic biases at high spatial resolution can be attributed to different sensitivity limitations of the two retrievals. In contrast, a systematic difference between the two retrievals emerges at coarser resolution. This bias largely stems from differences related to sensitivity of the two retrievals to

Daniel Miller 1/29/2018 10:43 AM
Deleted: al
Daniel Miller 1/29/2018 10:43 AM
Deleted: retrievals
Daniel Miller 1/29/2018 10:44 AM
Deleted: S
Daniel Miller 3/4/2018 5:04 PM
Deleted: DJ-Miller@umbc.edu
Daniel Miller 3/4/2018 5:05 PM
Deleted: s
Daniel Miller 3/4/2018 4:34 PM
Deleted: indeed h
Daniel Miller 3/4/2018 9:20 PM
Deleted: differences

unresolved inhomogeneities in effective variance and optical thickness. The influence of coarse angular resolution is found to increase uncertainty in the polarimetric retrieval, but generally maintains a constant mean value.

1 Introduction

The cloud droplet size distribution (DSD) is an important microphysical property of liquid-phase clouds. Given the cloud water content, it largely determines the shortwave radiative effects of clouds (Twomey, 1977). It also plays a critical role in cloud-precipitation processes (Pruppacher and Klett, 1978). As a result, anthropogenic perturbation to the DSD could lead to a variety of cloud property changes with significant climate implications (Lohmann et al., 2007).

Many satellite-based techniques have been developed to retrieve cloud DSD properties from regional to global scales. These techniques typically infer DSD properties based on an assumed size distribution shape, characterized by an effective radius (r_e), and an effective variance (v_e). One such retrieval method is called the bispectral total reflectance technique, hereafter referred to as the "bispectral technique," which simultaneously retrieves cloud optical thickness (τ) and r_e from a pair of cloud reflectances, typically one in the visible to near infrared (VNIR) and the other in the shortwave infrared (SWIR) or midwave infared (MWIR) spectral range (Nakajima and King, 1990b). This retrieval technique has been implemented for numerous satellite and airborne instruments, such as the Moderate Resolution Imaging Spectro-radiometer (MODIS, (King et al., 2003; Platnick et al., 2003; 2017)), the Spinning Enhanced Visible and Infrared Imager (SEVIRI, (Roebeling et al., 2006)), and the Suomi National Polar-orbiting Partnership Visible Infrared Imaging Radiometer Suite (Suomi NPP VIIRS, (Rosenfeld et al., 2014)).

A second, fundamentally different, retrieval technique is the multi-angular polarimetric reflectance technique, hereafter referred to as the "polarimetric technique". This retrieval requires multi-angular observations of the polarized reflectance in the cloudbow scattering region. In addition to r_e, the polarimetric technique can also retrieve v_e (Bréon and Goloub, 1998). Global retrievals using the polarimetric technique were first demonstrated by the Polarization and Directionality of Earth Reflectance (POLDER, (Deschamps et al., 1994)) instruments operating from 1996 to 2013 on three different satellite platforms. The Aerosol Polarimetry Sensor (APS, (Mishchenko et al., 2007)) would have been the first space-borne multi-angular polarimeter from U.S. to provide global aerosol and cloud property retrievals. Unfortunately, it was lost as a result of the satellite launch failure in 2011, which suddenly interrupted development of polarimetric-based remote sensing in the U.S. Recognizing the great potential of polarimetric techniques for aerosol and cloud remote sensing, NASA has invested heavily in recent years on the development of airborne polarimeters, such as the Research Scanning Polarimeter (RSP, (Cairns et al., 1999)), the Airborne Multi-angle Spectro-Polarimetric Imager (AirMSPI, (Diner et al., 2013)) and the Airborne Hyper-Angular Rainbow Polarimeter (Air-HARP, (Martins et al., 2017)). Moreover, several space-borne missions are in development, such as the Multi-Angle Imager for Aerosols (MAIA, (Liu and Diner, 2017)), HARP, the Plankton, Aerosols, Cloud, ocean Ecosystem mission (PACE) and the Multi-viewing, Multi-channel, Multi-polarization imaging mission (3MI, (Marbach et al., 2013)). Each of these missions will have a multi-angular polarimeter on-board. In

Daniel Miller 3/2/2018 3:04 PM
Deleted: 2016

Steven Platnick 2/28/2018 4:26 PM
Deleted: vastly

the foreseeable future, we may expect to have operational global retrievals of cloud droplet size distributions from both bispectral and polarimetric methods.

The bispectral and polarimetric remote sensing techniques are the primary tools we have to obtain DSD observations on a global scale. It is therefore essential to identify and explain differences between the two techniques so we can better understand their respective advantages and limitations. A satellite retrieval intercomparison of POLDER and MODIS r_e retrievals by Bréon and Doutriaux-Boucher (2005) represented one of the first attempts to identify and understand the differences between the two techniques. The main finding from this study is that the bispectral-based MODIS retrieval of r_e(2.13µm) (using the 2.13 µm SWIR band) is persistently 2 µm larger than the 150 km scale polarimetric-based POLDER retrieval over ocean, despite a close correlation between the two. A variety of factors, from differences in sensitivity to cloud vertical profile to influence of cloud horizontal inhomogeneity, have been suggested to explain this difference. However, as pointed out by the authors, all these factors might contribute to the difference. It is difficult, if not impossible, to untangle them in observations and determine their relative importance. In addition, POLDER observations in this study were aggregated from the nominal 6 km spatial resolution to a much coarser 150 km resolution to achieve the angular resolution needed to resolve the cloud bow. The vast difference in spatial resolution (i.e., 150 km for POLDER and 1 km for MODIS) makes the interpretation of the 2 µm r_e difference between the two retrievals even more difficult.

A more recent study by Alexandrov et al. (2015) is based on observations from the recent sub-orbital Polarimeter Definition Experiment (PODEX) in 2013. In that study, the polarimetric r_e retrievals for marine stratocumulus decks off the California coast from the airborne RSP instrument are compared to collocated bispectral retrievals from the Autonomous Modular Sensor (AMS). Interestingly, the two retrievals are found to be in close agreement, with a correlation of 0.928 and negligible bias of less than a micron. Beyond the clear instrument differences of the Alexandrov et al. (2015) and Bréon and Doutriaux-Boucher (2005) studies, it is still unclear how well the bispectral and polarimetric retrievals should compare to one another and what situations might cause them to differ, raising numerous questions and motivating this study.

A great challenge facing these observational studies is the intertwining of various instrument and scene dependent factors that lead to retrieval differences. For example, the polarimetric and bispectral methods have different sensitivity to the cloud vertical profile, and at the same time they are also both affected by cloud horizontal inhomogeneity (Zinner et al., 2010; Zhang et al., 2012; 2016; Miller et al., 2016). It is difficult, if not impossible, to disentangle these factors based on observations alone. This study approaches the intercomparison of bispectral and polarimetric retrievals through a different route: rather than use observational remote sensing data, synthetic retrievals are generated from large-eddy simulations (LES) of clouds. Modeling radiative transfer in an LES scene to obtain total and polarized reflectances opens up the possibility of using the LES to perform synthetic bispectral and polarimetric retrievals. This retrieval simulator framework has proven to be a useful tool in other cloud remote sensing studies (Miller et al., 2016; Zhang et al., 2012). Using this idealized simulation at high spatial resolution, we can attempt to parse the effects of unresolved sub-pixel inhomogeneity, spatial resolution, and angular resolution on the intercomparison of polarimetric and bispectral retrievals. The scale of the LES simulations (~10 km) in this study prevents us from examining resolutions as large as the standard POLDER retrieval

Daniel Miller 1/23/2018 4:17 PM
Deleted: Because

Daniel Miller 3/4/2018 11:41 AM
Deleted: ,

Daniel Miller 1/23/2018 4:18 PM
Deleted: it is important

Daniel Miller 1/23/2018 4:18 PM
Deleted: the

Daniel Miller 1/23/2018 4:18 PM
Deleted: between them

Daniel Miller 1/23/2018 4:21 PM
Deleted: the

Daniel Miller 1/23/2018 4:21 PM
Deleted: of each technique

Daniel Miller 2/26/2018 1:23 PM
Deleted: Bréon and Doutriaux-Boucher (2005)

Steven Platnick 2/28/2018 4:36 PM
Deleted: by about 2 µm

Daniel Miller 2/26/2018 1:23 PM
Deleted: Bréon and Doutriaux-Boucher (2005)

Daniel Miller 2/25/2018 10:10 PM
Deleted: whether

Daniel Miller 2/25/2018 10:10 PM
Deleted: well

Daniel Miller 2/25/2018 10:10 PM
Deleted: or not

Daniel Miller 2/25/2018 10:11 PM
Deleted: that

Daniel Miller 2/25/2018 10:11 PM
Deleted: e

Daniel Miller 3/2/2018 3:55 PM
Deleted: Miller et al., 2016

Daniel Miller 3/2/2018 3:55 PM
Deleted: ; Zinner et al., 2010

(~150 km), but we are able to advance understanding how spatial resolutions from 50 m to 1 km. These scales are suitable for airborne instrument comparisons, which certainly fall somewhere in this range. The use of a satellite retrieval simulator opens up two unique opportunities for developing and studying cloud microphysical retrievals: First, it provides the means to compare retrievals directly to LES cloud microphysics. Second, it allows us to perform a retrieval technique intercomparison that is independent of instrument characteristics and other differences that complicate observational studies. This study focuses on three particular questions:

- How well do the bispectral and polarimetric retrievals perform relative to the LES fields used as input to the retrievals?
- How do the bispectral and polarimetric retrieval techniques compare to one another at high spatial resolution?
- How are the bispectral and polarimetric retrieval techniques sensitive to specific observational conditions (i.e., the influence of spatial and angular resolution)?

The rest of the paper is organized as follows: Section 2 provides a brief introduction to the theoretical basis of the two retrieval techniques; Section 3 describes the LES-based satellite retrieval simulations used in this study; the comparisons between the two techniques based on the LES cases are presented in Section 4; followed by summary and discussion in Section 5.

2 Background

2. Cloud microphysical and optical properties

In satellite remote sensing DSDs are often described using theoretical distributions that fit well with in situ observations, in addition to being mathematically convenient (Deirmendjian, 1964; Tampieri and Tomasi, 1976; Martin et al., 1994; Miles et al., 2000). A popular theoretical DSD is the gamma distribution proposed by Hansen and Travis (1974):

Daniel Miller 3/2/2018 4:06 PM
Deleted: ; Tampieri and Tomasi, 1976

$$N\left(r\,;r_e,v_e\right)\equiv N_0 C\, r^{(1-3v_e)/v_e}\exp\left[-r/\left(r_e v_e\right)\right], \quad (1)$$

where the independent variable r is the cloud droplet radius, $N(r)$ is the droplet size distribution, N_0 is the droplet number concentration, and C is a normalization constant. The two distribution parameters are the effective radius (r_e) and the effective variance (v_e) of the DSD:

$$r_e\equiv\frac{\int_0^\infty Q_e(r)r^3N(r)dr}{\int_0^\infty Q_e(r)r^2N(r)dr}\approx\frac{\int_0^\infty r^3N\left(r\,;r_e,v_e\right)dr}{\int_0^\infty r^2N\left(r\,;r_e,v_e\right)dr}=\frac{\left\langle r^3\right\rangle}{\left\langle r^2\right\rangle}, \quad (2)$$

$$v_e\equiv\frac{1}{r_e^2}\frac{\int_0^\infty Q_e(r)(r-r_e)^2r^2N(r)dr}{\int_0^\infty Q_e(r)r^2N(r)dr}\approx\frac{1}{r_e^2}\frac{\int_0^\infty (r-r_e)^2r^2N\left(r\,;r_e,v_e\right)dr}{\int_0^\infty r^2N\left(r\,;r_e,v_e\right)dr}=\frac{\left\langle r^4\right\rangle\left\langle r^2\right\rangle}{\left\langle r^3\right\rangle^2}-1. \quad (3)$$

where $\langle r^n \rangle = \int_0^\infty r^n N(r)dr$ is the n^{th} moment of the DSD. For the spectral bands relevant to this study, the extinction efficiency (Q_e) is approximately constant (i.e., Q_e(r)~const.=2). Thus, the relationships between r_e and v_e can be conveniently reduced to relations between arithmetic moments of the DSD. The DSD plays an important role in defining the bulk optical properties of a cloud. The optical property libraries used in this study are based on single-scattering Mie calculations of monodisperse droplet optical properties that are averaged with respect to size, according to the gamma DSD (Wiscombe, 1979). In addition, these single-scattering optical properties are averaged with respect to wavelength over an instrument-specific spectral response function (based on MODIS bands in this study) and solar source functions (Planck blackbody function (Planck, 1914)). The single-scattering bulk cloud optical properties are subsequently used to run radiative transfer calculations for the creation of the so-called bispectral reflectance look-up-table (LUT). This LUT is made up of pre-calculated reflectances of plane-parallel and homogeneous (PPH) clouds over a high-resolution grid of combinations of τ, r_e, and v_e. Here, τ is defined in terms of the DSD:

$$\tau_{tot,\lambda} \equiv \int_{\text{TOA}}^{0} \left[\int_0^\infty Q_{e,\lambda}(r) \pi r^2 N_0 n(r) dr \right] dz \quad (4)$$

2.2 Bispectral and Polarimetric Retrieval Methods

The bispectral method retrieves τ and r_e simultaneously from a pair of observed cloud reflectances, typically using a combination of VNIR and SWIR/MWIR bands. The VNIR band, with relatively negligible liquid water droplet absorption, and the SWIR/MWIR band, where droplets are moderately absorptive, can be used to remotely infer τ and r_e because of this difference in sensitivity to multiple scattering (thickness) and absorption (droplet size). This method is usually implemented using a LUT, shown graphically in Figure 1(a), which has a fixed v_e. Cloud reflectance in the VNIR band (centered around 0.865 µm) increases with τ (gray) for a fixed r_e, while the reflectance in the MWIR band (centered around 3.75 µm) decreases with r_e (colored) when τ is fixed. The retrieved properties are obtained by performing a two-dimensional inverse interpolation between observed reflectance and the τ-r_e grid. A notable characteristic of the bispectral LUT is that when the optical thickness is low (τ<3), the isolines of the LUT are more densely packed and less orthogonal, which results in reduced sensitivity and increased retrieval uncertainty (Werner et al., 2013). The bispectral technique is not particularly sensitive to v_e, so typically a fixed value is assumed (e.g., v_e=0.1 in the operational MODIS retrieval, though it is kept as an error source in calculating pixel-level uncertainties). While different combinations of bands are used to perform the bispectral retrieval, in this study we focus on VNIR reflectances centered on 0.865 µm with the second band is selected from either a 2.13 µm centered SWIR band, or a 3.75 µm centered MWIR band There are consequences for the r_e retrieval depending on the particular set of bands selected. For example, a strongly absorbing SWIR/MWIR band limits penetration into the cloud and

Daniel Miller 2/14/2018 10:20 AM
Deleted:

Steven Platnick 2/28/2018 10:13 AM
Deleted: observed in

Steven Platnick 2/28/2018 10:13 AM
Deleted: , respectively

Steven Platnick 2/28/2018 10:14 AM
Deleted: dominated by multiple scattering

Steven Platnick 2/28/2018 10:15 AM
Deleted: liquid water

Daniel Miller 1/29/2018 10:45 AM
Deleted: The VNIR band, dominated by multiple scattering, provides sensitivity to τ; the selected SWIR band, where liquid water droplets are moderately absorptive, provides sensitivity to r_e.

Steven Platnick 2/28/2018 10:16 AM
Deleted: like the one

Daniel Miller 3/4/2018 4:40 PM
Deleted: SWIR

Daniel Miller 3/4/2018 4:50 PM
Deleted: a priori

Daniel Miller 3/4/2018 4:42 PM
Deleted: VNIR and SWIR

Daniel Miller 3/4/2018 4:43 PM
Deleted: and

Daniel Miller 3/4/2018 4:41 PM
Deleted: reflectances centered on both

Daniel Miller 3/4/2018 4:41 PM
Deleted: 2.13 and

Daniel Miller 3/4/2018 4:42 PM
Deleted: .

Daniel Miller 3/4/2018 4:43 PM
Deleted: SWIR

as a result the retrieved r_e is vertically weighted toward the microphysics prevalent in the uppermost part of the cloud (Platnick, 2000).

For the polarimetric retrieval, the angular pattern of the linearly polarized reflectance[1] is the source of sensitivity to cloud microphysical properties. Polarized reflectances are dominated by single scattering because multiple scattering induces depolarization. As a result, the single-scattering polarized phase functions ($-P_{12}$) shown in Figure 1 (b) and (c) are good approximations to the observed angular pattern of polarized cloud reflectances (Bréon and Goloub, 1998). These phase functions demonstrate the sensitivity of the polarimetric retrieval to both r_e and v_e. As r_e increases in Figure 1(b) the supernumerary bow peaks (around a scattering angle of 142°) become narrower and shift toward smaller scattering angles. In contrast, as v_e increases in Figure 1(c) the supernumerary bow peaks erode in magnitude, eventually smoothing out for broad DSDs (v_e>0.15). A consequence of this erosion of the supernumerary peaks is that the polarimetric retrieval has less sensitivity to both r_e and v_e for very broad DSDs. The polarimetric retrieval does not significantly rely on multispectral information, although observations in several bands may help provide stronger observational constraints due to the shift in the supernumerary bows with changing wavelength (refer to figure 3 of Bréon and Goloub (1998). The dominance of the single scattering contributions to the polarized reflectance leads to cloud retrievals that represent microphysical properties with a mean penetration depth of $\langle\tau_{SS}\rangle \leq 0.5$ and sensitivity that saturates for optical depths greater than ~3 from the cloud top. The polarimetric retrieval is often based on a parametric curve fitting retrieval algorithm like the one presented in Alexandrov et al. (2012b), although there are other techniques (e.g., the Rainbow Fourier Transform technique of Alexandrov et al. (2012a), which can retrieve DSD's with arbitrary mathematical form.) The parametric technique relies on a library of $-P_{12}$ curves with varying r_e and v_e that are parametrically scaled and adjusted to fit the observed reflectance via a nonlinear least squares optimization procedure. This process yields the phase function that best matches the angular pattern of the observation, thus determining the r_e(pol) and v_e(pol) retrieval. The polarimetric method described above does not result in a retrieval of τ; however, it can still be obtained by implementing a simplified variant of the bispectral τ retrieval. With simultaneous measurements of the total reflectance in a VNIR band and the r_e(pol) retrieval, a VNIR-only LUT curve can be used to perform a 1-D interpolation of the corresponding bispectral LUT curve for $R_{VNIR}(r_e(\text{pol}), \tau)$.

Both bispectral and polarimetric techniques are susceptible to a variety of retrieval uncertainties. The main objective of this study is to understand how the retrieval uncertainties influence each technique and whether they can lead to deviation between the two techniques in terms of retrieval results. In this study, we focus on three major sources of retrieval uncertainty for both techniques:

1) Cloud vertical profile: In the operational retrievals, both bispectral and polarimetric techniques assume vertically homogenous clouds. However, clouds in reality often have significant vertical variability resulting from various processes (e.g., condensational growth, coalescence, sedimentation, entrainment). Deviations from the assumed profile gives rise to many questions. For example, how do we interpret the r_e and v_e retrievals based on the homogenous cloud assumption? To

1 Note that throughout this paper, we will refer to "linearly polarized reflectances" simply as "polarized reflectances" in recognition of the negligible contribution of circularly polarized light in the atmosphere (Hansen, 2010).

Daniel Miller 2/14/2018 10:21 AM
Deleted:

Daniel Miller 2/14/2018 10:21 AM
Deleted:

Daniel Miller 3/4/2018 4:53 PM
Deleted: within the top

Daniel Miller 3/4/2018 4:56 PM
Deleted:

Daniel Miller 3/4/2018 4:57 PM
Deleted: optical depths

Daniel Miller 3/4/2018 4:53 PM
Deleted: in

Daniel Miller 2/26/2018 1:23 PM
Deleted: Alexandrov et al. (2012b)

Daniel Miller 2/26/2018 1:23 PM
Deleted: Alexandrov et al. (2012a)

Daniel Miller 3/5/2018 10:18 AM
Deleted: multi-modal

what extent does cloud vertical profile influence the bispectral and polarimetric techniques? Note that Platnick (2000) developed a method utilizing the so-called "vertical weighting function" to interpret the r_e retrieval from the bispectral method for clouds with vertically varying r_e profile. Recently, Alexandrov et al., (2012b) took an approach that focused on the vertical weighting of the droplet size distribution to interpret the r_e and v_e retrievals from the polarimetric technique. Miller et al. (2016) demonstrated the usefulness of this vertical weighting approach for understanding both bispectral and polarimetric r_e retrievals. In Section 4.1, we will apply the vertical weighting function method to both techniques on the basis of the LES cloud fields, to help understand if cloud vertical structure could lead to significant differences between the two techniques.

2) Sensitivity to observational uncertainty: The uncertainties associated with observations of total and polarized reflectances can differ, indicating that uncertainty may also impact bispectral and polarimetric retrievals differently. Additionally, the two retrievals rely on different number of uncertain observations; a pair of uncertain total reflectances (bispectral) as compared to numerous uncertain polarized reflectances (polarimetric). Furthermore the different algorithmic approaches, two-dimensional interpolation vs. nonlinear optimal curve fitting introduce additional layers of complexity in terms of the impact of uncertainty. The impact of uncertainty on retrieval results for each method are highlighted and explored in section 4.2.

3) Reduced sensitivity: It can be clearly seen from Figure 1 (a) that when clouds are optically thin (τ<3), the LUT for the bispectral retrieval becomes less orthogonal and the isolines of r_e become more densely packed. This reduction in sensitivity can lead to significant retrieval uncertainties in bispectral techniques for optically thin clouds (τ<3). Similarly, the sensitivity of the polarimetric technique to r_e and v_e is reduced when DSD becomes very broad (i.e., v_e>0.15), in which case the supernumerary bow features are barely distinguishable (Figure 1 (c)). In Section 4.3 we will investigate the impacts of the reduction of sensitivity on retrieval consistency between the two techniques.

4) Sub-pixel inhomogeneity: The impact of spatial resolution and unresolved sub-pixel cloud inhomogeneity on bispectral retrievals has been well studied (Zhang and Platnick, 2011; Zhang et al., 2012; 2016). An important conclusion from these studies is that the so-called plane-parallel homogenous bias (PPHB) can cause the bispectral technique to significantly overestimate r_e. In contrast, the sensitivity of the polarimetric retrieval to unresolved sub-pixel inhomogeneity and resolution has not been thoroughly studied. In Section 4.4, we will compare the impacts of sub-pixel inhomogeneity on bispectral and polarimetric techniques, and investigate whether it can cause deviation between the two techniques.

5) Angular resolution and sampling for polarimetric technique: In addition to spatial resolution, angular resolution and sampling is also important for the polarimetric technique. A coarse angular resolution may not be able to resolve the feature of the supernumerary bows. Similarly, if the scattering angles corresponding to the supernumerary bows are not or only partly sampled, then the polarimetric technique may not have enough information content for retrieval. This issue will be discussed in Section 4.5.

Daniel Miller 2/26/2018 1:23 PM
Deleted: Alexandrov et al. (2012b)

Daniel Miller 3/4/2018 4:58 PM
Deleted: modified this method slightly and applied it

Daniel Miller 2/13/2018 10:40 AM
Deleted: 2

Daniel Miller 2/13/2018 10:17 AM
Deleted: 2

Daniel Miller 2/13/2018 10:40 AM
Deleted: 4

Daniel Miller 2/13/2018 10:17 AM
Deleted: 3

Daniel Miller 2/13/2018 10:18 AM
Deleted: 4

Daniel Miller 2/13/2018 10:31 AM
Deleted:

Daniel Miller 2/13/2018 10:17 AM
Deleted: 4

3 Model and Methodology

The satellite retrieval simulator implemented in this study is built around an LES model (DHARMA) with bin microphysics (Ackerman et al., 2004; Zhang et al., 2012; Miller et al., 2016). The LES provides freely evolving 3-D cloud microphysical properties, which are used as reference when comparing to numerically simulated retrievals. The LES in this study adopts 25 droplet size bins to represent droplet size distributions (Ackerman et al., 1995). The optical properties of each size bin are computed by bulk averaging Mie scattering properties over a highly resolved flat sub-bin droplet size distribution. The optical properties of each bin are provided as input to radiative transfer simulations based on the size distributions of the LES cloud fields. Vector radiative transfer calculations are performed using a polarized doubling-adding technique (PDA) to produce 1-D total and polarized reflectances at the horizontal resolution of the LES grid (described below) (De Haan et al., 1987). The sole consideration of 1-D retrievals avoids 3-D radiative effects and focuses this study on retrieval technique differences rather than on radiative processes. A future study will focus on the comparison of 3-D retrievals to these 1-D bispectral and polarimetric retrievals. The radiative transfer modeling in this work is performed for numerous solar zenith angles (SZA=[20, 40, 60]˚), viewing zenith angles (VZA=[−70 : +70]˚), and a constant relative azimuthal angle (ΔΦ = 30°). The VZA resolution results in a scattering angle (Θ) resolution on the order of 0.5°. Reflectances in spectral bands (based on MODIS spectral response functions) are centered on 0.865, 2.13, and 3.75 µm wavelengths. Total reflectances in all bands are used to produce bispectral retrievals, whereas linearly polarized reflectances in the 0.865 µm band are used to produce polarimetric retrievals. Subsequently, bispectral and polarimetric retrievals are performed on the simulated reflectances to obtain r_e, v_e, and τ retrievals. Bispectral and polarimetric retrievals are performed over a subset of observation geometries, with bispectral retrievals performed for VZA=[50, 40, 30, 20, 10, 0, −10]° and all SZA. Meanwhile, the polarimetric retrievals are performed for a SZA=20° and a range of VZA=[0:27]° that result in reflectances spanning scattering angles required to observe the primary and supernumerary bow features (i.e., Θ=[135:160]°). Reflectances are also aggregated from the 50 m native LES resolution up to coarser 100, 200, 400, and 800 m horizontal resolutions to reflect the influence of different remote sensing footprints. The retrievals in this study are also performed at all of the footprint resolutions. The bispectral LUT implemented in this study spans microphysical properties r_e=[2:30] µm in steps of 0.5 µm and v_e=[0.01:0.11] in steps of 0.01. The τ retrieval in this study is anchored to the 0.865 band optical properties and spans τ=[0.1:100] with 101 logarithmically spaced grid points. Including v_e variability in the bispectral LUT allows for the comparison of standard MODIS-like retrievals (the v_e=0.1 LUT) to retrievals with other v_e assumptions. The bispectral retrieval is then accomplished by performing a 2-D linear interpolation of the observed reflectances and inverting between the reflectance and retrieval space. For the polarimetric retrieval, the polarimetric phase function library spans r_e=[2:40] µm in steps of 0.25 µm and v_e=[0.01:0.3] in steps of 0.01. The polarimetric retrieval implemented in this study is based on the approach of Alexandrov et al. (2012a), fitting the polarized phase functions in their eq. (3) to the modeled polarized reflectances of the LES scene. The optimal parametric fit in the $-P_{12}$ library is determined by using a Levenberg-Marquardt nonlinear least squares algorithm. This optimal phase function is then used to identify the

Daniel Miller 3/4/2018 4:26 PM
Deleted: ; Miller et al., 2016

Daniel Miller 2/8/2018 2:19 PM
Deleted: the

Daniel Miller 2/8/2018 2:20 PM
Deleted: ly fitting

corresponding r_e(pol) and v_e(pol) retrieval. As previously stated in section 2.2 the polarimetric retrieval of τ is accomplished by using a constrained 1-D version of the bispectral LUT.

The LES cloud fields are used not only to drive the radiative transfer simulations, but also to help interpret and understand the retrieval results. As mentioned in Section 2.2, it is not trivial to interpret the r_e and v_e retrievals based on the homogenous cloud assumption when the cloud has significant vertical structure. To address this issue, for each LES column with detailed vertical profiles of DSD, we derive two reference variables r_e(VW) and v_e(VW) from the vertical weighted (VW) integration of the DSD profile. The vertical integration is weighted by a function to account for the penetration depth and multiple scattering of radiation in the corresponding wavelength of the retrieval. Thus, r_e(VW) and v_e(VW) should be comparable to the retrieved r_e and v_e from the simulated reflectance (Alexandrov et al., 2012b; Miller et al., 2016; Zhang et al., 2017). The method of vertical weighting in this study is described in detail in section 2 of Miller et al. (2016), however in this study we will modify the vertical weighting function to account for multiple scattering. Following the parametric approach suggested in eq. 4 of Zhang et al. (2017) the new vertical weighting function is,

$$W(\tau) = a\tau^{b} \exp\left[-\tau\left(\frac{1}{\mu}+\frac{1}{\mu_0}\right)\right], \tag{4}$$

where the τ^b factor is introduced to account for multiple scattering, and a is the normalization factor. For b=0 we get back the original single scattering vertical weighting used in Miller et al. 2016. For larger values of b, the droplet size distribution properties deeper in the cloud begin to contribute more to the vertically weighted value. A single value of b is selected for each retrieval approach such that it minimizes the mean and standard deviation of retrieval biases over all of the LES retrieval data. For the polarimetric retrieval, b=0 was found to be optimal, likely due to the dominance of single scattering in polarized reflectances. In contrast, multiple scattering can significantly impact total reflectances. We found that for the 3.75 µm bispectral retrieval a vertical weighting function using a value of b=0.3 was optimal, because the 3.75 µm band is strongly absorbing and therefore less multiple scattering occurs. The weaker absorption in the 2.13 µm band leads to deeper penetration into the cloud and so a vertical weighting function using a value of b=10 was found to be optimal. In addition to r_e(VW) and v_e(VW), we also derive τ_{LES} for each LES column simply by integrating the extinction coefficient (for λ=0.865 µm) from cloud bottom to cloud top. The r_e(VW), v_e(VW) and τ_{LES} are used as references in the retrieval and LES property comparison in section 4.1 to understand the differences between the retrievals and the original LES fields. After obtaining the r_e(VW), v_e(VW) and τ_{LES} at the 50 m native LES resolution, they are aggregated to 100, 200, 400, and 800 m to help interpret the retrievals at these coarser resolutions. It is important to note that there is a subtle difference between directly aggregating r_e(VW) or v_e(VW), and aggregating the DSD (i.e., $N(r)$) first and then deriving the corresponding r_e(VW) and v_e(VW). The differences between the two methods are discussed in the Appendix. The main conclusion is that, although the two aggregation methods could be different in some hypothetical cases with unrealistically large variability in the unresolved

Daniel Miller 2/8/2018 2:20 PM
Deleted: corresponds …orrespondingto the ... [1]

Daniel Miller 2/13/2018 10:50 AM
Deleted: 2WT…W) and v_e(2WT…W) fron ... [2]

Daniel Miller 2/13/2018 10:52 AM
Moved (insertion) [1]

Daniel Miller 3/4/2018 12:49 PM
Deleted: directly …omparable to the nume ... [3]

Daniel Miller 2/13/2018 10:53 AM
Moved (insertion) [2]

Daniel Miller 2/13/2018 11:11 AM
Deleted: (at 0.865 µm). For a complete description on how vertical weighting is accounted for in the calculation of r_e(2WT) and v_e(2WT), see section 2 of (Miller et al., 2016). The r_e(2WT) and v_e(2WT) take into account the first-order sensitivity of the retrieval techniques to the vertical profile of clouds.

Daniel Miller 2/13/2018 10:53 AM
Moved up [2]: section 2 of (Miller et al., 2 ... [4]

Daniel Miller 2/13/2018 1:11 PM
Deleted: . We note that the 2WT vertical weighting function provides a reasonable approximation when the signal is contributed mainly by single scattering (i.e., 3.7 µm or polarimetric reflectances) but becomes less accurate for spectral bands with more multiple scattering (Platnick ... [5]

microphysics, they are essentially equivalent for practical purposes. In this study, we simply aggregate r_e(VW) and v_e(VW) from the native LES resolution of 50 m to obtain average values at desired resolution (e.g., 800 m).

Three LES cases are the focus of this study. The first (referred to as "ATEX clean" hereafter) and second ("ATEX polluted") cases are based on an idealized case study from the Atlantic Trade Wind Experiment (ATEX), with different aerosol loadings (Stevens et al., 2001). The ATEX cases are representative of a trade wind cumulus regime in which scattered cumuli rise into a thin, broken stratocumulus layer. The third case (referred to as "DYCOMS-II" hereafter), originally presented in Stevens et al. (2005), is an idealized setup based on clouds observed during the second research flight (RF02) of the Second Dynamics and Chemistry of Marine Stratocumulus project (DYCOMS-II) (Stevens et al., 2003). This case is representative of nocturnal marine stratocumulus under a dry inversion. The DYCOMS-II case has a domain size of 6.4×6.4×1.5 km (128x128x96 grid points), while each of the ATEX simulations has a domain size of 7.2×7.2×3 km (144×144×200 grid points). The horizontal grid spacing of these LES cases is fixed at 50 m, while the vertical grid is stretched, with a minimum spacing of 5 m near the surface and the capping temperature inversion to better resolve small-scale turbulence there. Further details of the model setup for the DYCOMS-II case are provided in Ackerman et al. (2009). The ATEX cases are updated model runs with increased spatial resolution that are similar to the cases discussed in Fridlind and Ackerman (2011). For each LES scene a snapshot of cloud microphysical and optical properties is saved every half hour after the first hour of each simulation, resulting in numerous cloud fields. A single time step of each of the cases was selected to be the focus of this retrieval study, each occurring ~3 hours into the simulation.

The variability of cloud optical and microphysical properties in each of the LES cases is highlighted in Figure 2 and Table 1. Spatial inhomogeneity of both optical and microphysical properties of these scenes is evident, with the ATEX polluted and DYCOMS-II cases exhibiting lower spatial inhomogeneity and the ATEX clean case being more broken and inhomogeneous. One method for quantifying the optical inhomogeneity of a cloud scene is to use the sub-pixel inhomogeneity index,

$$H_\sigma(\text{resolution}) = \frac{\text{std}\left[R_i(0.865\ \mu\text{m}, 50\ \text{m})\right]}{\text{mean}\left[R_i(0.865\ \mu\text{m}, 50\ \text{m})\right]}, \tag{4}$$

where the numerator and denominator are the standard deviation and mean of the native LES resolution (50 m) reflectances within a coarser resolution pixel. Thus, the value of H_σ is computed for a coarser spatial resolution pixel (800 m in Table 1) using the highest-resolution nadir viewing reflectances (50 m). The value of H_σ increases with increasing sub-pixel inhomogeneity, making it a useful measure for unresolved cloud variability. In addition to optical inhomogeneity, each of the LES scenes also has characteristically different microphysical properties. The average value of r_e(VW) of each scene varies, in part because of the initial background CCN in each particular case but also cloud top height variability. In these LES cases v_e is spatially anti-correlated with τ and organized in a cellular structure — regions with higher τ tend to have smaller v_e(VW) and regions with lower τ tend to have large v_e(VW).

Daniel Miller 2/27/2018 9:45 AM
Deleted: (

Daniel Miller 2/27/2018 9:45 AM
Deleted: Shang et al. 2015),

Daniel Miller 2/13/2018 1:13 PM
Deleted: 2WT

Daniel Miller 2/13/2018 1:13 PM
Deleted: 2WT

Daniel Miller 3/4/2018 12:59 PM
Deleted: the

Daniel Miller 2/26/2018 1:23 PM
Deleted: Stevens et al. (2005)

Daniel Miller 2/26/2018 1:23 PM
Deleted: Ackerman et al. (2009)

Daniel Miller 2/26/2018 1:23 PM
Deleted: Fridlind and Ackerman (2011)

Daniel Miller 2/13/2018 9:35 AM
Deleted: at

Daniel Miller 2/13/2018 9:35 AM
Deleted: and

Daniel Miller 2/13/2018 1:15 PM
Deleted: 2WT

Daniel Miller 2/13/2018 1:15 PM
Deleted: 2WT

Daniel Miller 2/13/2018 1:15 PM
Deleted: 2WT

4 Results and Analysis

4.1 Retrieval and LES Property Comparison

Before comparing the retrieval results from the two techniques to one another, we must first carry out a comparison of LES and retrieval properties to assess and understand the differences between the retrieval results and the original LES cloud fields at the native 50 m spatial resolution. This is a necessary sanity check that will help understand the accuracy and uncertainty of our retrieval routines. More importantly, this study will help to interpret the retrievals based on homogeneous cloud assumption when the LES cloud fields have naturally inhomogeneous vertical profiles. Note that the retrievals compared throughout the following sections are compared for all combinations of viewing and solar geometries indicated in the section 3.

The bispectral retrieval comparison to LES properties in Figure 3 depicts joint histograms of r_e and τ retrievals using both the 2.13 and 3.75 µm bands against the reference values derived from the LES fields, r_e(VW), v_e(VW), and τ_{LES}. It is important to note that these joint histograms are presented as the logarithmic percent of the population, to emphasize deviations from the one-to-one line. Also, the mean regression biases reported throughout this study are stated relative to the plotted axes as, $\mu_{\mathrm{bias}}=<y-x>$ and $\mu_{|\mathrm{bias}|}=<|y-x|>$ (i.e., x and y denoting x and y axes). The two bispectral r_e retrievals, r_e(2.13 µm) and r_e(3.75 µm), are in agreement with the LES ground-truth (Figure 3(a) and (b)) with strong correlations, both exceeding 0.95. The biases between these two retrievals and the LES properties differ slightly. Compared to the LES, both r_e retrievals have relatively small sub-micron mean biases and the mean absolute biases are also sub-micron. Additionally, it is important to note a limitation of this population: none of the LES scenes in this study have a mean cloud top r_e near 10 µm. To examine the two bispectral τ retrievals, τ(2.13 µm) and τ(3.75 µm) in Figure 3(c) and (d), we compare them in terms of percent differences, because the regression is so highly correlated (R>0.99). A slight systematic high bias on the order of 2-5% exists. The origin of this high bias is likely associated with deviations of the droplet size distribution from the assumed gamma distribution form. The LES size distributions sometimes exhibit longer large-droplet tails than the assumed form. As explained earlier in Section 2.2, the bispectral method suffers from a reduction of retrieval sensitivity when clouds are optically thin. Therefore, if we sample only LES columns that are optically thick (τ>3) a substantial improvement in the regression correlations of the two r_e retrievals (Figure 3(e) and (f)) is achieved. However, some outlier points still remain. In particular, a small population of both r_e(2.13 µm) and r_e(3.75 µm) retrievals have biases exceeding r_e(VW) by as much as 20 µm. The cause of these outliers and some other differences between the retrievals and LES fields will be discussed in detail in section 4.3.

The polarimetric retrieval comparison to LES properties in Figure 4 depicts comparisons of the polarimetric retrievals, r_e(pol) v_e(pol), and τ(pol), against corresponding LES properties. The r_e(pol) retrieval compares very well to r_e(VW) (Figure 4(a)), with a regression correlation exceeding 0.98, a mean bias of less than 0.1 µm. The quality of this retrieval comparison to LES properties also further supports the single scattering definition of r_e(VW) for the polarimetric

Daniel Miller 2/13/2018 2:22 PM
Deleted: in this section …e must first carry ... [6]

Daniel Miller 3/4/2018 4:44 PM
Deleted: SWIR …ands against the referenc ... [7]

Daniel Miller 2/26/2018 10:09 AM
Deleted: The joint histograms …n Figure 4 ... [8]

retrieval. In contrast, the polarimetric retrieval of v_e(pol) reveals a regression against v_e(VW) (Figure 4(c)) that does not perform quite as well. In this case the regression correlation is much weaker (R=0.62) with a mean bias of −0.013. While the mean bias is on the order of the v_e LUT grid spacing, it is clear that the regression correlation is poor because of a systematic low bias for v_e(VW) larger than about 0.15. It should also be noted that the increased concentration of v_e(pol) retrievals at v_e=0.3 is a result of the boundaries of the retrieval space, v_e=[0.01, 0.3]. The upper limit of which is a consequence of the gamma distribution of Hansen and Travis (1974) becoming monotonic for $v_e \geq 0.3$. Comparing only the population with v_e(VW)≤0.15 (not shown here) results in an improved correlation of R=0.84 with negligible mean bias. The v_e retrieval quality also depends on the assumption that LES droplet size distributions are accurately described using a single-mode gamma distribution. The DSD's in the LES sometimes deviate significantly from this assumption. In the context of the parametric polarimetric retrieval used in this study this is difficult to remedy or address. However, a different polarimetric retrieval, the Rainbow Fourier Transform (RFT) introduced in Alexandrov et al. (2012a) offers the possibility of retrieving an arbitrary droplet size distribution shape. The final retrieval product, τ(pol) (Figure 4(e)), indicates that a more accurate a priori r_e and v_e estimate has little impact on the retrieval of τ. As explained earlier in Section 2.2, the polarimetric method suffers a reduction of sensitivity when the DSD is broad, a finding that is consistent with previous work (Alexandrov et al., 2012b). This explains, for the r_e(pol) retrieval, why limiting the regression population to LES columns with v_e(VW)≤0.15 in Figure 4(b) increases the correlation and decreases the absolute bias. This appears to be an indication of sensitivity to degradation of the supernumerary bow features for large v_e, features that are necessary for reliable r_e(pol) and v_e(pol) retrievals.

For v_e(pol) we find that by sampling LES columns that are optically thick (τ>3), there is moderate improvement in the correlation and reduced biases (Figure 4(d)). This improvement stems from the correlation between the population of optically thin clouds and high v_e(VW) (Figure 4(f)) that are found near cloud edges in the LES scenes. It should be noted that an increased τ does not implicitly lead to better polarimetric retrievals, but here it is observed to be a consequence of aforementioned correlated relationship between DSD and optical properties.

4.2 Sensitivity to Measurement Uncertainty

The measurement uncertainties of total and polarized reflectances differ, leading one to expect that bispectral and polarimetric retrievals may have different sensitivities to uncertainty. Their relationships to uncertainty are further complicated by differences in retrieval approaches; namely interpolating two independent uncertain observations in a LUT (bispectral) or curve fitting through numerous observations that are each independently uncertain (polarimetric). Targeted uncertainties for cloud and aerosol remote sensing are δDOLP=0.5% in degree of linear polarization and δI=3% in total reflectance (Knobelspiesse et al., 2012). A simple propagation of uncertainty analysis yields a polarized reflectance uncertainty of δQ=2.5% (in the principal plane). Using these uncertainties as a starting point, we can perturb the LES reflectances with uncorrelated random noise and perform retrievals that we can then compare to the original unperturbed

Daniel Miller 2/26/2018 10:13 AM
Deleted: retrieval

Daniel Miller 2/26/2018 10:12 AM
Deleted: is indeed well represented by the single-scattering "2WT" vertical weighting

Daniel Miller 2/13/2018 1:37 PM
Deleted: 2WT

Daniel Miller 3/4/2018 9:50 PM
Deleted: Figure 4

Daniel Miller 2/13/2018 1:37 PM
Deleted: 2WT

Daniel Miller 2/13/2018 9:46 AM
Deleted: (footnote 2).

Daniel Miller 2/13/2018 1:37 PM
Deleted: 2WT

Daniel Miller 2/27/2018 9:49 AM
Deleted: 0.86

Daniel Miller 3/4/2018 9:50 PM
Deleted: Figure 4

Daniel Miller 2/25/2018 10:10 AM
Deleted: s

Daniel Miller 2/25/2018 10:10 AM
Deleted: have

Daniel Miller 2/14/2018 10:27 AM
Deleted: ,

Daniel Miller 2/13/2018 1:37 PM
Deleted: 2WT

Daniel Miller 3/4/2018 9:50 PM
Deleted: Figure 4

Daniel Miller 3/4/2018 9:50 PM
Deleted: Figure 4

Daniel Miller 2/13/2018 1:37 PM
Deleted: 2WT

Daniel Miller 3/4/2018 9:50 PM
Deleted: Figure 4

retrievals. Note that while the focus here is on uncorrelated randomly distributed noise, other sources of observational uncertainty exist and would need to be accounted for in the context of a specific instruments' uncertainty model. As the properties of particular instruments are not the focus of this study, we will focus on this more general uncertainty analysis.

For the bispectral retrieval, a randomly distributed reflectance perturbation between +/-3% was added to each LES reflectance. A histogram of the percent bias of bispectral retrievals of r_e induced by the addition of the reflectance uncertainty is shown in Figure 5(a). The mean and standard deviation of these bias distributions are stated, allowing us to interpret the results. First, the introduction of uncertainty has very little impact on the mean bias of bispectral r_e retrievals (on the order of 0.1%). Second, the introduction of uncertainty results in a broad distribution of r_e retrieval biases with standard deviations of 5.44% and 4.02% for the 2.13µm and 3.75µm retrievals respectively. Together these two results indicate that biases associated with measurement uncertainty will not be systematic, with absolute variability on the order of 1 µm or less for droplet sizes below 20 µm (the most prevalent population in this LES study). The impact of observational uncertainty on all of the τ retrievals is the focus of Figure 5(b). The two bispectral retrievals, τ(2.13µm) and τ(3.75), each have very minimal mean biases of 0.1%. However, like the biases for the effective radius retrievals, the distribution of retrieval bias is broadened to standard deviations of 8.2% and 5.6% for τ(2.13µm) and τ(3.75) respectively. The polarimetric τ(pol) retrieval on the other hand, being methodically quite similar to the bispectral retrievals, exhibits a small systematic low bias of about -2.43% as shown in Figure 5(b). The origin of this systematic bias is a known characteristic of single-band optical thickness retrievals, and is clearly demonstrated in figure 1 of Marshak et al. (2006). The convexity of a single-band LUT curve produces low-biased retrievals for symmetrically distributed (or averaged) reflectances. The bias distribution also has a smaller variability (3.8%) than the two bispectral retrievals, likely because the uncertainty in the SWIR/MWIR band also (weakly) influences the bispectral τ bias distributions.

The consequences of measurement uncertainty are markedly different for the polarimetric retrieval. This is a result of the polarimetric retrieval being a search for a similar curve in the phase function library, making the deviations in the magnitude of observations in any one angle less important when searching for the optimal curve – and therefore discrete r_e and v_e combination. The discretely binned nature of the polarimetric retrieval makes description of bias distributions like the ones in Figure 5 problematic. One way to describe how uncertainty in polarized reflectances influences polarimetric retrievals is to describe the population of retrievals that are unchanged, and the population of retrievals that changed. After the introduction of random noise 88.1% of the polarimetric r_e(pol) retrievals were unbiased, with 9.1% biased high by one grid point (+0.25 µm) and 2.7% biased low by one grid point (-0.25 µm). All together, these three populations accounted for the vast majority (99.9%) of retrieval outcomes. The percent bias of the r_e(pol) retrieval had a mean of 0.06% and a standard deviation of 0.78%. These results agree with previous studies, for example the finding of Shang et al. (2015) indicating that the POLDER retrieval performed well as long as reflectance uncertainty was less than 10%. It should be noted however that the sensitivity to uncertainty is also tied to the number of angular measurements available, and the properties of the droplet size distribution. The polarimetric v_e(pol) retrievals behaved similarly, with 85.2% of all retrievals being unaffected, 12.7% were biased high by one grid point (+0.01) and 1.9% were biased low by one grid point (-0.01). Again, these three populations account for the vast majority of (99.9%) of retrieval outcomes. The percent bias of the ve pol retrieval had a mean of 1.14%, consistent with a 0.01 bias and a standard deviation of 22.6%. The greater tendency toward large biases for the effective variance is likely due to smoothing of polarized reflectance curves after the addition of uncertainty. The large majority of biases in the polarimetric retrieval of v_e are coming from the population of v_e near 0.1-0.15 where the supernumerary bow peaks are significantly eroded and small shifts in the magnitude of reflectances at angles near these peaks could easily shift the retrieval to the next grid point.

Overall, the lack of strong systematic biases associated with uncertainty in the case of either retrieval supports an approach of neglecting the measurement uncertainty in further analyses. Of course, this requires acknowledging that biases that are below δr_e=5%, δv_e=10%, or $\delta\tau$=7% in either retrieval are probably not as important because they likely are not detectable due to observational uncertainty.

Daniel Miller 3/4/2018 4:32 PM
Formatted: Indent: First line: 0.5"

4.3 Retrieval Comparison at High Resolution

Daniel Miller 2/13/2018 10:16 AM
Deleted: 2

In practice, most observational studies do not have access to the underlying cloud properties with which to compare, so instead different instruments and techniques are often compared to one another. At the native spatial resolution of the LES (50 m) a direct intercomparison of polarimetric and bispectral retrieval techniques is possible, providing an opportunity to diagnose different sources of bias. The joint histograms of r_e retrievals in Figure 6 compare the two bispectral retrievals, r_e(2.13 µm) and r_e(3.75 µm), to the polarimetric retrieval, r_e(pol), for all LES cases and observation geometries[3]. The regressions for the comparison of both r_e(2.13 µm) (Figure 6(a)) and r_e(3.75 µm) (panel b) indicate high correlation (R≈0.95) and have relatively small mean biases of less than a micron. A couple of notable features are evident in these regressions. **(1)** The sign of the mean bias appears to be sensitive to the SWIR/MWIR band selection due to vertical weighting differences, resulting in r_e(2.13µm)<r_e(pol)<r_e(3.75µm). **(2)** There are numerous statistical outliers with small r_e(pol)~5-9 µm but broadly distributed r_e(2.13 µm) or r_e(3.75 µm). One way to understand these features is to constrain the data set to LES columns where both retrieval techniques yield reliable results. As discussed previously, both the bispectral and polarimetric retrievals are sensitive to biases for thin clouds (τ<3) and the polarimetric retrieval is sensitive to biases for broad droplet size distributions (v_e>0.15). Based on these criteria (τ>3 and v_e≤0.15), the constrained joint histograms (Figure 6(c) and (d)) feature much tighter regression relationships (R≈0.99) and reduced mean absolute biases are observed. These filters indicate that the poorly correlated population corresponds to situations in which both retrievals are expected to suffer from significant biases. The retrieval regression can be further improved if the bispectral retrieval is artificially provided with more complete information about the shape of the droplet size distribution. Providing the v_e(pol) retrieval as an a priori assumption for the bispectral LUT can demonstrate the sensitivity of the bispectral r_e retrievals to the v_e=0.1 assumption. This serves as a test of

Daniel Miller 2/13/2018 2:40 PM
Deleted: s

Daniel Miller 3/4/2018 1:55 PM
Deleted: offer the possibility of diagnosing

Daniel Miller 2/24/2018 12:28 PM
Deleted: Figure 5

Daniel Miller 2/24/2018 12:28 PM
Deleted: Figure 5

Daniel Miller 2/26/2018 6:20 PM
Deleted: 4

Daniel Miller 2/24/2018 12:28 PM
Deleted: Figure 5

[3] Note that ~1% of pixels in the LES retrieval data correspond to a "failed" bispectral retrieval due to falling outside of the LUT space. These pixels are omitted from the intercomparison. Different reasons for bispectral retrieval failure are discussed in (Cho et al., 2015).

Daniel Miller 2/27/2018 2:24 AM
Deleted: .

how collocated bispectral and polarimetric retrievals might assist one another. To create these new retrieval results we coupled the selection of the bispectral retrieval LUT to the pixel-by-pixel value, thus making sure that the respective LUT had a matching v_e to the v_e(pol) retrieval. The new r_e(2.13 μm) retrievals (Figure 6(e)) are largely unchanged from the v_e=0.1 results, although a slight increase in the two biases indicates that v_e=0.1 was both an appropriate and sufficient assumption for the r_e(2.13 μm) retrieval. In contrast, the r_e(3.75 μm) retrieval (Figure 6(f)) is shown to benefit from this additional a priori information, improving the correlation and reducing the small systematic low bias (~0.25 μm). The differences between the two SWIR band retrievals can be explained in two ways. Firstly, the vertically weighted DSD of the 2.13 μm SWIR band might result in a broader DSD (i.e., a larger v_e) compared to the 3.75 μm SWIR band, due simply to deeper penetration into cloud. This could provide one explanation for why the r_e(2.13 μm) retrieval might improve with the v_e=0.1 assumption. Alternatively, the R(2.13 μm) reflectance might simply be less sensitive to the broader DSD shape than the R(3.75 μm) reflectance. Overall, these results demonstrate a feature well known to the remote sensing community; the bispectral retrieval of r_e is not particularly sensitive to v_e (Nakajima and King, 1990a). Indeed, comparison of the coupled bispectral retrieval of r_e to the polarimetric retrieval of r_e confirms that the advantage of retrieving v_e changes the bispectral retrieval of r_e by less than a micron, so it is appropriate to neglect this level of detail of the DSD for bispectral retrieval purposes. The slight improvement demonstrates that when the two retrievals are compared on equal information footing they are nearly equivalent.

The origin of the broadly distributed high-biased bispectral retrievals in the small droplet size regime (r_e(pol)~5 μm) stems from the ATEX polluted case, where such small droplets make up about 3.5% of the LES scene[4]. A close examination of this case reveals that there are no bispectral retrievals below 5 μm, despite approximately 5% of the cloudy pixels (as defined by τ_{LES}>0.1) in the scene being characterized by r_e(VW)<5μm. This feature is a consequence of the bispectral LUT state space[5], which covers a r_e range of 5-30 μm. In contrast, the polarimetric retrieval space covers 1-30 μm. The differences between these two LUT spaces is not so much a matter of decision-making, but is more reflective of complexities of the bispectral retrieval for small r_e. To demonstrate this point panels (a) and (b) of Figure 7 depict the cloud reflectances from the ATEX polluted case (colors) within the respective bispectral LUT. It is obvious that the black isolines for τ and r_e increasingly overlap with the standard LUT space as τ decreases. In this region of the state space, there are multiple solutions for a single reflectance pair; one solution is representative of a small r_e (<5 μm, extended LUT), while the other indicates a much larger r_e (≥5 μm, standard LUT). There is also a modest impact on τ, but due to the curvature of the LUT this impact is less severe. The overlapping region between the standard and extended LUT is referred to as the "multiple solution space" and the amount of LUT overlap is determined by both the observation geometry and the selected spectral bands. Depending on the optical thickness, the larger r_e retrieval may be significantly larger, because the extended LUT isolines cross numerous larger r_e isolines in the standard LUT. The associated bispectral retrieval bias, shown in Figure

4 Additionally, ~1.3% of the cloudy pixels in this scene exhibit values below 4 μm.
5 Note that the MODIS LUT extends its range down to 4 μm, and in situations with multiple solutions the larger retrieval value is selected.

Daniel Miller 2/24/2018 12:28 PM
Deleted: Figure 5

Daniel Miller 2/24/2018 12:28 PM
Deleted: Figure 5

Daniel Miller 2/25/2018 5:31 PM
Deleted: 5

Daniel Miller 2/13/2018 1:38 PM
Deleted: 2WT

Daniel Miller 2/24/2018 12:28 PM
Deleted: Figure 6

Daniel Miller 3/4/2018 4:45 PM
Deleted: r_e(SWIR)–r_e(2WT)

Daniel Miller 2/25/2018 5:30 PM
Deleted: 2.5

7(c) and (d), highlights the conclusion that for optically thick clouds the bispectral r_e retrievals exhibits only moderate retrieval biases on the order of ±1 µm. However, for very thin clouds (near cloud edge) the retrieval bias can increase significantly. For some of these thinner clouds the retrievals also fall within the multiple solution space, so it is possible to attribute the very large biases to the presence of ambiguous retrieval results. Furthermore, the multiple solution space also provides an additional explanation for why the removal of optically thin (τ<3) observations significantly improved the bispectral retrieval comparisons.

In contrast to the intercomparison of r_e retrievals, the τ retrieval intercomparison in Figure 8 reveals very few differences between the bispectral and polarimetric techniques. This is not surprising, because the τ(pol) retrieval is simply an implementation of the bispectral technique with additional constraints on r_e and v_e (as discussed in section 2.2).

4.4 Sensitivity to Unresolved Spatial Inhomogeneity

Unresolved spatial inhomogeneity influences the bispectral and polarimetric cloud retrievals in very different ways. Even for 100% cloudy pixels these retrievals can exhibit sensitivity to sub-pixel inhomogeneity. This section focuses on the ATEX cases because they exhibit a broader distribution of H_σ, allowing us to highlight the impact of spatial inhomogeneity on retrievals. Spatial resolution and sub-pixel inhomogeneity index (H_σ) are inherently intertwined with one another. This is demonstrated in Figure 9, where the broadening and shifting of the distribution of H_σ for increasingly coarsened spatial resolutions is clearly demonstrated using data from both the ATEX clean and polluted cases. In light of this relationship between resolution and inhomogeneity, the inclusion of data from all spatial resolutions together broadens our sampling of different inhomogeneity regimes. To that end, Figure 10 combines all of the coarse spatial resolution data from the two ATEX cases into a single retrieval bias histogram. Retrieval biases here are stated relative to their relevant vertically weighted LES property. For the bispectral retrievals in Figure 10 (a,b), these histograms clearly show that increasing sub-pixel inhomogeneity tends to result in larger biases. In contrast, the polarimetric r_e(pol) retrieval in Figure 10 (c) does not appear to have a clear systematic bias. The v_e(pol) retrieval in Figure 10 (d) tells a more complicated story, the median value of the bias is clearly close to zero, but there is a tendency toward low biased retrievals with increasing inhomogeneity. It should be noted that the v_e(VW) itself increases with increasing H_σ, which is presumably a consequence of the anticorrelation between τ and v_e(VW). This might explain why for large values of H_σ, where the v_e(VW)>0.15 population is more common, there are more negative biases.

To further emphasize how unresolved inhomogeneity can influence these two retrieval techniques, we will highlight a particularly inhomogeneous pixel from the ATEX clean case at the coarsest resolution (800m). Focusing first on the bispectral retrieval using the 2.13 µm SWIR band, the LUT scatterplot in Figure 11(a) reveals that there is significant variability in the sub-pixel (i.e., 50 m) VNIR reflectances, indicated by a large value of the sub-pixel inhomogeneity index (H_σ=0.5637). In contrast to the variability of VNIR reflectances, the microphysical properties are largely homogeneous in this 800 m pixel, indicated by the narrow distribution of sub-pixel $r_e(VW)_{50\,m}$ (color of the points). The sub-pixel mean of

Daniel Miller 2/24/2018 12:28 PM
Deleted: Figure 6

Daniel Miller 2/24/2018 12:28 PM
Deleted: Figure 7

Daniel Miller 2/13/2018 10:16 AM
Deleted: 3

Daniel Miller 2/14/2018 3:30 PM
Deleted: affects

Daniel Miller 2/14/2018 3:31 PM
Deleted: These

Daniel Miller 2/14/2018 3:31 PM
Deleted: different

Daniel Miller 2/14/2018 3:32 PM
Deleted: ies

Daniel Miller 2/14/2018 3:31 PM
Deleted: even for 100% cloudy pixels

Daniel Miller 2/14/2018 12:54 PM
Deleted: As coarsened s

Daniel Miller 2/14/2018 12:54 PM
Deleted: the

Daniel Miller 2/24/2018 8:25 PM
Deleted: correlated

Daniel Miller 2/14/2018 12:55 PM
Deleted: r, so our comparisons here address these two properties simultaneously. To that end,

Daniel Miller 2/14/2018 3:39 PM
Deleted: panels (a) and (b) of Figure 8 compare r_e(pol) to the r_e(2.13 µm) and r_e(3.75 µm) respectively at increasingly coarsened spatial resolutions (as indicated by the size of the circles). In addition to the spatial resolution, these plots a ... [9]

Daniel Miller 2/24/2018 8:34 PM
Deleted: probe how

Daniel Miller 2/26/2018 12:38 PM
Deleted: influences

Daniel Miller 2/24/2018 8:34 PM
Deleted: examine

Daniel Miller 2/14/2018 3:40 PM
Deleted: a very coarse resolution

Daniel Miller 2/24/2018 12:28 PM
Deleted: Figure 9

Daniel Miller 2/24/2018 12:10 PM
Deleted: of this

Daniel Miller 2/24/2018 12:10 PM
Deleted: are largely homogeneous

Daniel Miller 2/13/2018 1:38 PM
Deleted: 2WT

<r_e(VW)>$_{50\ m}$ =19.23 µm agrees well with the mean of both sub-pixel retrievals, <r_e(2.13 µm)>$_{50\ m}$=18.73 µm and <r_e(pol)>$_{50\ m}$=18.92 µm. This combination of optical inhomogeneity and microphysical homogeneity leads to an average reflectance (indicated by the black star) for the 800 m pixel that falls significantly below the r_e=20 µm isoline (i.e., the closest isoline to the mean sub-pixel retrievals). Thus, the coarse resolution 800 m reflectance results in an 800 m bispectral retrieval with r_e(2.13 µm)$_{800\ m}$=23.62 µm, which is biased high by ~4 µm. This effect is attributable to the well-documented PPH bias induced by the curvature of the bispectral LUT with respect to the optical thickness (Zhang and Platnick, 2011; Zhang et al., 2012; 2016). The PPH bias has a stronger influence on the 2.13 µm retrieval compared to the 3.75 µm retrieval (shown in Figure 11(b)) because the curvature of the LUT is more pronounced.

The polarimetric retrieval has a fundamentally different relationship to the unresolved sub-pixel inhomogeneity. This can be demonstrated with the sub-pixel polarized reflectance histogram in Figure 11(b). The reflectances in this figure have been binned by scattering angle to create a distribution of polarized reflectances for the 50 m sub-pixels within the selected 800 m pixel footprint. Within the plot there are also two curves, shifted in amplitude away from the histogram for clarity, that display the mean 800 m multi-angular polarized reflectance and corresponding 800 m retrieved polarized phase function (with appropriate fitting coefficients). Note that, while this histogram gives a sense of the variability of the magnitude and scale of the polarized reflectances, what ultimately matters for the coarse resolution polarimetric retrieval is the relative shape of the 800 m averaged polarized reflectance curve. It is evident from this histogram and these curves that the mean angular position of the supernumerary bow does not shift, indicating that there is no significant difference between r_e(pol)$_{800\ m}$, <r_e(pol)$_{50\ m}$>, and <r_e(VW)$_{50\ m}$>. This agrees with previous studies on the impact of unresolved inhomogeneity on polarimetric r_e retrievals (Shang et al., 2015). In contrast, there is clear variability in the amplitude of sub-pixel polarized reflectances. This variability owes itself to both optical (τ), and microphysical inhomogeneity (i.e., v_e(VW)>0.15) within the coarse resolution pixel. For thin clouds (τ<3) the supernumerary bow amplitude is dependent on both τ and v_e (Alexandrov et al., 2012b). With v_e fixed the polarized reflectance converges towards an asymptotic maximum for optically thick clouds (τ≥3), a consequence of increasing depolarization due to multiple scattering. Similarly, for a fixed τ, reflectances corresponding to v_e(VW)>0.15 also produce decreased polarization in the primary and supernumerary bow features, as discussed in section 2. Each of these effects reduces sensitivity to the cloudbow features; and thus unresolved variability in τ and v_e could influence coarse resolution retrievals. For example, Shang et al. (2015) found that unresolved spatial inhomogeneity of τ and v_e increased retrieval biases in v_e(pol), while they were not able to discern a trend in retrieval biases in their study. However, in our case study featured in Figure 11(b) we do not see a significant difference between coarse (v_e(pol)$_{800\ m}$) and fine scale (<v_e(pol)$_{50\ m}$>) retrievals, but both retrievals are low-biased relative to the mean LES property (<v_e(VW)$_{50\ m}$>). This result was surprising, because both fine and coarse resolution retrievals were biased similarly. It appears as though coarse resolution retrievals arrive at the same answer as the fine scale retrievals through different processes. The average of fine scale retrievals (that are systematically biased low) and the retrieval based on the average of fine scale reflectances (which are reduced for reasons discussed above) results in a similar retrieval outcome. Unlike the bispectral retrieval, where retrievals differ from one another at different resolutions, the polarimetric retrieval seems to

Daniel Miller 2/13/2018 1:38 PM
Deleted: 2WT

Daniel Miller 2/25/2018 8:47 PM
Deleted: Figure

Daniel Miller 2/16/2018 1:04 PM
Deleted: , as shown in

Daniel Miller 2/24/2018 12:28 PM
Deleted: Figure 9

Daniel Miller 2/26/2018 12:58 PM
Deleted: demonstrate

Daniel Miller 2/26/2018 12:58 PM
Deleted: the

Daniel Miller 2/26/2018 12:58 PM
Deleted: 50 m sub-pixel

Daniel Miller 2/16/2018 1:07 PM
Deleted: the

Daniel Miller 2/13/2018 1:38 PM
Deleted: 2WT

Daniel Miller 2/13/2018 1:38 PM
Deleted: 2WT

Daniel Miller 2/26/2018 7:22 PM
Deleted: a

Daniel Miller 2/26/2018 7:22 PM
Deleted: v_e and varying τ

Daniel Miller 2/13/2018 1:38 PM
Deleted: 2WT

Daniel Miller 3/4/2018 9:50 PM
Deleted: Figure

compare well to itself at both resolutions – even when it might be biased relative to the underlying microphysics of the physical scene. To examine this this further we performed polarimetric retrievals on subpopulations of the 50 m polarized reflectances within this 800 m pixel that omitted either the v_e(VW)>0.15 or τ<3 from the population. Removing these thin or broad droplet size distributions from the high resolution dataset had little to no impact on either the coarse resolution r_e(pol) or v_e(pol) retrieval. From these results and the histogram in Figure 10 (d) it appears that the impact of spatial resolution on v_e(pol) retrievals is largely a consequence of an unresolved anticorrelation between τ and v_e rather than a feature directly related to spatial resolution.

4.4 Sensitivity to Angular Resolution and Sampling

The polarimetric retrieval requires high-resolution multi-angular data to resolve the supernumerary bow features. To test how angular resolution influences polarimetric retrievals we examined coarse spatial resolution (800 m) r_e(pol) retrievals at different angular resolutions. Each angular resolution (i.e., changing angular step size) was also convoluted with shifting angular sampling (i.e., changing the initial angle). This convolution is necessary in order to account for all possible sets of scattering angle observations associated with each resolution. These coarse resolution retrievals were then compared to the original high angular resolution retrieval. The results of this experiment (**Figure 12**(a)) reveal that coarsening angular resolution does not systematically bias r_e(pol) retrievals, although angular resolutions exceeding 3° do result in a marked increase in retrieval variability (i.e., a constant mean bias, but increased absolute bias). In contrast, **Figure 12**(b) demonstrates that angular resolutions exceeding 3° lead to both high-biased v_e(pol) and increased retrieval variability. An explanation for the origin of the observed degradation in retrieval accuracy above 3° angular resolution is demonstrated in Figure 13(a). Two different polarized phase functions with r_e=15 µm and v_e=[0.03, 0.2] (solid and dashed-dotted, respectively) are sampled at an angular resolution of 3.5° (indicated by the gray vertical lines). This resolution is coarser than the spacing between the supernumerary bow features. As a consequence, this particular angular sampling intersects these curves at nearly the same amplitudes. This degeneracy yields a relatively low cost function during the best-fit optimization step of the polarimetric curve fitting retrieval algorithm, making it possible to obtain an inaccurate solution if this results in a cost-function minimum. The lack of observed differences between these two curves results in a lack of v_e information, which could be exacerbated by observational uncertainty. However, under different angular sampling conditions, e.g., shifting the initial angle by a few degrees to the right, the supernumerary bow peaks of the low v_e curve would be sampled and the similarity between the observations of these two curves would vanish. This example highlights an important feature of multi-angular polarimetry: observations at poor angular resolutions can suffer from increased biases depending on whether or not important angles are sampled. Generalizing this result requires determining the angular spacing of the supernumerary bow features for other r_e. Pursuing this, we find that decreasing cloud droplet size widens and dilates supernumerary bow features, making it easier to resolve supernumerary bow features at coarse angular resolution. The peak-to-peak distance of the supernumerary bow oscillations can be treated as the Nyquist frequency, or in this case Nyquist resolution. In signal

Daniel Miller 2/26/2018 2:00 PM
Deleted: we find that these features do not systematically bias the v_e(pol) retrieval in this case. In fact, rather surprisingly, we

Daniel Miller 3/4/2018 2:33 PM
Deleted: find that the most important bias for the coarse spatial resolution v_e(pol) retrieval is the lack of sensitivity on v_e(2WT)>0.15, a feature that was also present for the high spatial resolution retrievals. This finding is also supported for

Daniel Miller 3/4/2018 2:44 PM
Deleted:

Daniel Miller 3/4/2018 2:33 PM
Deleted: performed on

Daniel Miller 2/26/2018 8:54 PM
Deleted: samples

Daniel Miller 2/26/2018 8:54 PM
Deleted: of

Daniel Miller 2/13/2018 1:38 PM
Deleted: 2WT

Daniel Miller 3/4/2018 2:33 PM
Deleted: ; removing either of them had little

Daniel Miller 2/26/2018 4:31 PM
Deleted: .

Daniel Miller 2/26/2018 3:47 PM
Deleted: Possible explanations for this behavior will be discussed in section 5.

Daniel Miller 2/13/2018 10:16 AM
Deleted: 4

Daniel Miller 2/24/2018 12:28 PM
Deleted: Figure 10

Daniel Miller 2/24/2018 12:28 PM
Deleted: Figure 10

Daniel Miller 2/24/2018 12:28 PM
Deleted: Figure 11

analysis, a sampling resolution finer than the Nyquist frequency is required to appropriately resolve features of an oscillatory signal. The Nyquist angular resolution required for resolving the supernumerary bow oscillations changes with both r_e and λ according to the behavior illustrated in Figure 13(b). This analysis indicates that multi-angular observations in a shorter wavelength spectral band would require finer angular resolutions. The Nyquist angular resolution for λ=0.865 and r_e=15 µm is 3°, providing an explanation for the increased variability in r_e(pol) and v_e(pol) LES retrievals at angular resolutions coarser than the Nyquist limit.

Daniel Miller 2/24/2018 12:28 PM
Deleted: Figure 11

Daniel Miller 3/5/2018 10:43 AM
Deleted: uncertainty

5 Summary and Discussion

The analysis in this study, which features comparisons of fundamentally different passive cloud property retrieval techniques, is facilitated by comparisons to LES cloud fields used as input to the retrievals. At the native LES resolution (50 m) there are promising results for both the bispectral and polarimetric retrievals (with 1-D radiative transfer assumptions). For the bispectral retrieval, the LES comparison shows significant biases for retrievals of very thin clouds, as well as only small differences between the vertically weighted cloud properties in each of the two SWIR/MWIR bands (2.13 and 3.75 µm). Meanwhile, for the polarimetric retrieval, the comparison demonstrates that the r_e(pol) retrieval agrees well with the vertically weighted in situ properties of each LES scene. However, the v_e(pol) retrieval exhibits persistent low biases due to a lack of retrieval sensitivity to very broad droplet size distributions (i.e., v_e(VW)>0.15). The optical thickness retrievals from both methods are effectively the same, with the caveat that the polarimetric technique performs the r_e(pol) retrieval as an a priori constraint on the τ retrieval space. Regarding τ, both bispectral and polarimetric retrievals were found to have a small systematic high bias on the order of 2-5%.

Daniel Miller 3/4/2018 3:00 PM
Deleted: vastly

Daniel Miller 2/13/2018 1:38 PM
Deleted: 2WT

The uncertainty in observed total and polarized reflectances was found to introduce only weak systematic biases in bispectral or polarimetric r_e retrievals (0.1% or less). Similarly, the bispectral τ retrievals were also not systematically biased. In contrast, total reflectance uncertainty did produce a slight systematic bias of -2.43% in the polarimetric τ(pol) retrieval that can be linked to the convexity of the single-band LUT used to perform the retrieval. This sort of bias, could perhaps be accounted for by introducing a Taylor expansion correction similar to the one discussed in Zhang et al. (2016) in the context of unresolved inhomogeneity. Beyond these systematic biases, we found that the induced uncertainties in the bispectral retrievals were δr_e=5% or $\delta\tau$=7%. The influence of polarimetric retrieval is likely sensitive the polarimetric LUT grid spacing, but here we found uncertainties that were less than the bispectral retrieval of r_e, δr_e(pol)=1 to 4%, and δv_e(pol)=10 to 20%. In the context of the rest of our comparison studies, the lack of systematic biases and relatively small uncertainties allowed us to discuss retrieval behavior in the absence of uncertainty.

The retrieval intercomparison of polarimetric and bispectral retrievals in this study demonstrates that both techniques yield very similar results, especially when the most reliable populations of cloud properties are selected for each method (τ>3 and v_e around 0.1). While the physical principles and measurement requirements are vastly different, both retrieval techniques seem to be able to capture similar information about r_e and τ. These results agree with high-resolution airborne

Daniel Miller 3/4/2018 3:16 PM
Deleted:

observations obtained during the PODEX and ORACLES field campaigns, where RSP and AMS microphysical retrievals are compared (Alexandrov et al., 2015; Knobelspiesse et al., 2017). These high spatial resolution field campaign observations indicate that the two retrieval techniques agree well to within the tolerances also found in the present study. The bispectral r_e retrievals are found to be moderately sensitive to v_e in the 3.75 µm band, and less so in the less absorptive and more deeply penetrating 2.13 µm band. Coupling the retrieved v_e(pol) to the bispectral r_e(3.75 µm) retrieval led to slight improvements in the r_e(pol) and r_e(VW) comparison. It should be noted that for MODIS cloud products the bias due to the v_e=0.1 assumption does not substantially impact the r_e retrieval compared to other sources of bias (i.e., cloud inhomogeneity or 3-D radiative effects). In addition, the MODIS Collection 6 cloud product includes uncertainty estimates associated with the v_e assumption. The intercomparison of the bispectral and polarimetric τ retrievals indicates that the two produce very similar results. This was to be expected, as the polarimetric technique also uses a bispectral LUT approach to derive τ. When the results from the two methods diverge, the observations tend to be related to the thin cloud regimes.

The presence of a multiple solution space in the bispectral LUTs, where small droplet sizes (r_e<5) have the same reflectance as larger droplets, was shown to induce numerous outliers resulting in a significant high bias in the bispectral retrievals for both r_e and (to a lesser extent) τ. This multiple solution space likewise impacts the MODIS operational products, since the bispectral LUTs used in the MODIS collection 6 cloud products include theoretical r_e solutions as low as 4 µm. However, for retrievals with multiple LUT solutions the MODIS product only reports the larger r_e value, leading to a systematic bias if the observed cloud really includes a population of small droplets. As a consequence, for thin clouds with small droplet sizes one can expect the comparison of polarimetric and bispectral retrievals to disagree. This strong high-bias for small r_e retrievals provides a plausible explanation for the large discrepancies observed in the small droplet size regime in the intercomparison of MODIS and POLDER retrievals (Bréon and Doutriaux-Boucher, 2005). Absent a solution to this issue, future intercomparisons or combined climatological datasets should be limited to retrievals of r_e(pol) exceeding 5-7 µm (depending on the respective bispectral LUT multiple solution space properties).

At the coarse spatial resolutions of most satellite instruments, cloud inhomogeneity can significantly impact retrievals. In the context of this study we find that the influence of unresolved spatial inhomogeneity is a dominant source of bias between the polarimetric and bispectral r_e retrievals. In this study we found that even for 100% cloudy pixels (at a coarse 800 m horizontal resolution) the influence of the PPH bias is significant, with the average r_e bias exceeding 1 µm in the most inhomogeneous LES scene (ATEX clean). Based on these results we still expect that the overall systematic bias observed in the MODIS and POLDER intercomparison of moderate droplet size regimes is in large part attributable to the influence of this PPH bias (Bréon and Doutriaux-Boucher, 2005). Recently, great effort has been made to account for the influence of the PPH bias on bispectral MODIS retrievals. The 2-D Taylor expansion technique implemented by Zhang et al. (2016) offers the possibility of quantifying (and potentially correcting for) the impact of PPH bias on bispectral retrievals. This approach requires high spatial resolution measurements in at least one spectral band to obtain the sub-pixel reflectance variability, which is used to determine corrections for the bias of r_e and τ. In addition to PPH bias, 3-D radiative effects are also influenced by spatial resolution. The focus on 1-D radiative transfer in this study leaves questions for future studies

Daniel Miller 2/13/2018 1:38 PM
Deleted: 2WT

Daniel Miller 2/26/2018 2:57 PM
Deleted: may

Daniel Miller 2/26/2018 1:48 PM
Deleted: be

regarding the influence of these 3-D radiative effects. Future work will need to identify the relative differences between 3-D radiative effects on total and polarized reflectances and retrievals.

Sufficient angular resolution is one of the more important requirements of the polarimetric retrieval technique. We find that resolving the multi-angular polarized reflectance at a resolution coarser than the Nyquist angular resolution of the supernumerary bow results in greater uncertainty (r_e(pol) and v_e(pol)) and biased (v_e(pol)) polarimetric retrievals. The required angular resolution is dependent both on droplet size and wavelength. Future cloud polarimetric instrumentation should consider these angular resolution requirements. While we have not explicitly tested the so-called "super-pixel" approach implemented for POLDER retrievals, these coarse spatial and angular resolution studies lead to some anticipated biases induced by this technique. We would expect such an approach to further bias v_e(pol) retrievals low, due to the lack of sensitivity to unresolved high-v_e populations. In addition, this current study indicates that r_e(pol) retrieval variance might increase, but the mean bias might not increase significantly. However, if there is significant correlation between the unresolved r_e and v_e populations within an observation footprint, the mean r_e bias would be expected to suffer.

Ultimately, the utitlity of any optical property dataset depends on the science questions for which the dataset will be used. These questions may focus on the determination of domain-averaged water mass, radiative flux calculations, or microphysical process studies on a range of scales. The appropriate retrieval may differ for each of these science questions and as a consequence the comparison of the bispectral and polarimetric retrievals discussed here ought to be viewed through the lens of a particular application.

Acknowledgements

The hardware used in the computational studies is part of the UMBC High Performance Computing Facility (HPCF). The facility is supported by the U.S. National Science Foundation through the MRI program (grant nos. CNS-0821258 and CNS-1228778) and the SCREMS program (grant no. DMS-0821311), with additional substantial support from the University of Maryland, Baltimore County (UMBC). See www.umbc.edu/hpcf for more information on HPCF and the projects using its resources.

Appendix

We often treat the droplet size distribution observed by in-situ instruments (on the order of meters) as relatable to the inferred size distribution properties obtained by remote sensing retrievals (on the order of kilometers). This mathematical analysis addresses how resolution and scale influence the inferred cloud microphysical distribution. The modified gamma-distribution not only suits observations of in-situ cloud droplet size distributions, but it also exhibits several useful mathematical relationships:

$$\begin{aligned}\left\langle r^2\right\rangle &= r_e^2\left(v_e-1\right)\left(2v_e-1\right)\\ \left\langle r^3\right\rangle &= r_e^3\left(v_e-1\right)\left(2v_e-1\right)\\ \left\langle r^4\right\rangle &= r_e^4\left(v_e-1\right)\left(2v_e-1\right)\left(v_e+1\right)\end{aligned} \quad . \qquad (5)$$

From a retrieval perspective all droplet size distributions are treated as gamma-distributed. There is a potential disconnect here, from the perspective of scale analysis, when retrievals at a 50 m spatial resolution (our LES resolution) and retrievals at 1 km (MODIS retrieval resolution), or even 150 km (POLDER retrieval resolution) each are being treated as gamma-distributed. However, not all droplet microphysics information is created equal; the droplet size distributions at higher resolution (subscript, *i*) influence the low-resolution (subscript, *lr*) droplet size distributions. With high-resolution information the different moments of the coarser resolution droplet size distribution should be able to be constructed from the high-resolution microphysics. For a distribution made up of the summation of gamma size distributions the moments of the low-resolution distribution can be expressed by the following relationship, because summation and integration are each linear operators:

$$\begin{aligned}\left\langle r^n\right\rangle_{lr} &= \int_r r^n\left[\sum_i^k N_i\left(r, r_{e,i}, v_{e,i}\right)\right]\mathrm{d}r\\ \left\langle r^n\right\rangle_{lr} &= \sum_i^k\left[\int_r r^n N_i\left(r, r_{e,i}, v_{e,i}\right)\mathrm{d}r\right] = \sum_i^k\left[\left\langle r^n\right\rangle_i\right]\end{aligned} \quad . \qquad (6)$$

With this mathematical rule in mind, the values of r_e and v_e for the low-resolution droplet size distribution can be obtained by substitution into eq. (2) and eq. (3):

$$r_e{}' \equiv \frac{\left\langle r^3\right\rangle_{lr}}{\left\langle r^2\right\rangle_{lr}} = \frac{\sum_i^k\left\langle r^3\right\rangle_i}{\sum_i^k\left\langle r^2\right\rangle_i} \quad , \qquad (7)$$

Daniel Miller 3/5/2018 11:06 AM
Formatted: Font:Times, 10 pt

Daniel Miller 3/5/2018 11:06 AM
Formatted: Font:Times, 10 pt

$$v'_e \equiv \frac{\left\langle r^4 \right\rangle_{lr} \left\langle r^2 \right\rangle_{lr}}{\left(\left\langle r^3 \right\rangle_{lr}\right)^2} - 1 = \frac{\sum_i^k \left\langle r^4 \right\rangle_i \left\langle r^2 \right\rangle_i}{\left(\sum_i^k \left\langle r^3 \right\rangle_i\right)^{2x}} - 1 \ . \tag{8}$$

Henceforth, we will refer to the r'_e and v'_e relationships in eq. (7) and eq. (8) as microphysical "aggregation rules." It should be noted that these rules fundamentally treat the DSD as gamma-distributed at all scales.

The microphysical aggregation rules allow for the explanation of some features of the coarse polarimetric retrieval experiments displayed in Shang et al., (2015). Referring to the inhomogeneous polarimetric retrieval experiments in table 2 and figure 4 of their paper, we reproduced their results and calculated the corresponding r_e' and v_e' in our **Table 2**, which contains the same retrieval examples and corresponding r_e' and v_e' results for the cases examined in their study. There is a clear difference between the mean r_e or v_e and the polarimetric retrieval results. Using the microphysical aggregation rules defined above, we derived that the appropriate distribution properties, r_e' and v_e', are generally in closer agreement with the polarimetric retrievals of r_e(pol). These results offer a possible explanation as to why the polarimetric retrieval does not agree with the average of the sub-scale microphysics in Shang et al.'s study. A couple of things should be noted here: **1)** When there is little variability in the unresolved r_e (e.g., r_e=[15,20] μm) the mean, retrieval, and the estimated mixture are generally all in agreement (e.g., <r_e>=17.5, r_e(pol)=18, and r_e'=18.2 μm). **2)** When large variability in the unresolved r_e (e.g., r_e=[5,20]) is present, both the retrieved and estimated mixture strongly favor the larger droplet effective radius (e.g., r_e(pol)=19 and r_e'=19.12 μm). **3)** Large variability in unresolved r_e sometimes results in large differences between v_e(pol) and v_e'. The last two points are likely a consequence of the resulting coarse resolution (multi-modal) distribution differing significantly from the gamma-distribution assumption stated previously.

Applying this analysis to the aggregation of LES scene microphysics will allow for the determination of how accurate a spatial mean aggregation reflects the true coarse resolution microphysical parameters. We first assumed that all of the highest resolution vertically weighted size-distributions can be assumed to be appropriately characterized by a gamma distribution with r_e=r_e(VW) and v_e=v_e(VW). We then aggregated these LES microphysical properties at the 50 m native resolution to increasingly coarser resolutions (100, 200, 400, and 800 m), using both the mean and the aggregation rules. We found that the differences between the two techniques are negligible (Δr_e~0.01 μm and Δv_e~0.001) and do not significantly vary with final resolution. Apparently, the importance of the aggregation rules in the LES are far less important than what we had found in the multiple-moment cases tested in Shang, et al. (2015). One clear difference between the these multiple moment cases and the LES was that the toy models are reductive bimodal distributions, exhibiting very large sub-scale microphysical inhomogeneity in r_e. This non-physical variability is something that is not commonly observed in the LES or in observational studies. To address this, we performed a theoretical examination of how important the aggregation rules are for calculating the bias between simple average aggregation and mathematical rule aggregation. In this experiment we

Daniel Miller 3/2/2018 3:02 PM
Deleted: v_e'

Daniel Miller 2/13/2018 1:38 PM
Deleted: 2WT

Daniel Miller 2/13/2018 1:38 PM
Deleted: 2WT

established various distributions of unresolved DSD's with varying r_e and v_e populations. These joint distributions of r_e and v_e were used to test how the variance (i.e., the unresolved variability) would influence the average and mathematical rule aggregated results. This test confirmed, that large differences between the simple average and mathematical aggregation rules requires spatial inhomogeneity of microphysics that much larger than those observed in the LES or typical observational studies. Based on these results we recommend that future studies focusing on the effect of unresolved microphysical inhomogeneity on polarized retrievals should consider more realistic inhomogeneity conditions on both r_e and v_e.

References

Ackerman, A. S., Kirkpatrick, M. P., Stevens, D. E. and Toon, O. B.: The impact of humidity above stratiform clouds on indirect aerosol climate forcing, Nature, 432(7020), 1014–1017, 2004.

Ackerman, A. S., vanZanten, M. C., Stevens, B., Savic-Jovcic, V., Bretherton, C. S., Chlond, A., Golaz, J.-C., Jiang, H., Khairoutdinov, M., Krueger, S. K., Lewellen, D. C., Lock, A., Moeng, C.-H., Nakamura, K., Petters, M. D., Snider, J. R., Weinbrecht, S. and Zulauf, M.: Large-Eddy Simulations of a Drizzling, Stratocumulus-Topped Marine Boundary Layer, Mon. Wea. Rev., 137(3), 1083–1110, doi:10.1175/2008MWR2582.1, 2009.

Alexandrov, M. D., Cairns, B. and Mishchenko, M. I.: Rainbow Fourier transform, Journal of Quantitative Spectroscopy and Radiative Transfer, 113(18), 2521–2535, doi:10.1016/j.jqsrt.2012.03.025, 2012a.

Alexandrov, M. D., Cairns, B., Emde, C., Ackerman, A. S. and van Diedenhoven, B.: Accuracy assessments of cloud droplet size retrievals from polarized reflectance measurements by the research scanning polarimeter, Remote Sensing of Environment, 125, 92–111, doi:10.1016/j.rse.2012.07.012, 2012b.

Alexandrov, M. D., Cairns, B., Wasilewski, A. P., Ackerman, A. S., McGill, M. J., Yorks, J. E., Hlavka, D. L., Platnick, S. E., Thomas Arnold, G., van Diedenhoven, B., Chowdhary, J., Ottaviani, M. and Knobelspiesse, K. D.: Liquid water cloud properties during the Polarimeter Definition Experiment (PODEX), Remote Sensing of Environment, 169, 20–36, doi:10.1016/j.rse.2015.07.029, 2015.

Bréon, F. M. and Doutriaux-Boucher, M.: A comparison of cloud droplet radii measured from space, IEEE Trans. Geosci. Remote Sensing, 43(8), 1796–1805, doi:10.1109/TGRS.2005.852838, 2005.

Bréon, F. M. and Goloub, P.: Cloud droplet effective radius from spaceborne polarization measurements, Geophys. Res. Lett., 25(11), 1879–1882, 1998.

Cairns, B., Russell, E. E. and Travis, L. D.: Research Scanning Polarimeter: calibration and ground-based measurements, SPIE's Conference on Polarization: Measurement, Analysis, and Remote Sensing II, 186–196, doi:10.1117/12.366329, 1999.

Cho, H. M., Zhang, Z., Meyer, K., Lebsock, M., Platnick, S., Ackerman, A. S., Di Girolamo, L., C Labonnote, L., Cornet, C., Riedi, J. and Holz, R. E.: Frequency and causes of failed MODIS cloud property retrievals for liquid phase clouds over global oceans, J. Geophys. Res., 120(9), 4132–4154, doi:10.1002/2015JD023161, 2015.

De Haan, J. F., Bosma, P. B. and Hovenier, J. W.: The adding method for multiple scattering calculations of polarized light, Astronomy and Astrophysics, 183, 371–391, 1987.

Deirmendjian, D.: Scattering and polarization properties of water clouds and hazes in the visible and infrared, Appl. Opt., 3(2), 187–196, 1964.

Deschamps, P. Y., Breon, F. M., Leroy, M., Podaire, A., Bricaud, A., Buriez, J. C. and Seze, G.: The POLDER mission: instrument characteristics and scientific objectives, IEEE Trans. Geosci. Remote Sensing, 32(3), 598–615, doi:10.1109/36.297978, 1994.

Diner, D. J., Xu, F., Garay, M. J., Martonchik, J. V., Rheingans, B. E., Geier, S., Davis, A., Hancock, B. R., Jovanovic, V. M., Bull, M. A., Capraro, K., Chipman, R. A. and McClain, S. C.: The Airborne Multiangle SpectroPolarimetric Imager (AirMSPI): a new tool for aerosol and cloud remote sensing, Atmos. Meas. Tech., 6(8), 2007–2025, doi:10.5194/amt-6-

2007-2013, 2013.

Fridlind, A. M. and Ackerman, A. S.: Estimating the Sensitivity of Radiative Impacts of Shallow, Broken Marine Clouds to Boundary Layer Aerosol Size Distribution Parameter Uncertainties for Evaluation of Satellite Retrieval Requirements, J. Atmos. Oceanic Technol., 28(4), 530–538, doi:10.1175/2010JTECHA1520.1, 2011.

Hansen, J. E.: Circular Polarization of Sunlight Reflected by Clouds, http://dx.doi.org/10.1175/1520-0469(1971)028<1515:CPOSRB>2.0.CO;2, doi:10.1175/1520-0469(1971)028<1515:CPOSRB>2.0.CO;2, 2010.

Hansen, J. E. and Travis, L. D.: Light scattering in planetary atmospheres, Space Sci Rev, 16(4), 527–610, 1974.

King, M. D., Menzel, W. P., Kaufman, Y. J., Tanré, D., Bo-Cai Gao, Platnick, S., Ackerman, S. A., Remer, L. A., Pincus, R. and Hubanks, P. A.: Cloud and aerosol properties, precipitable water, and profiles of temperature and water vapor from MODIS, IEEE Trans. Geosci. Remote Sensing, 41(2), 442–458, doi:10.1109/TGRS.2002.808226, 2003.

Knobelspiesse, K., Cairns, B., Mishchenko, M., Chowdhary, J., Tsigaridis, K., van Diedenhoven, B., Martin, W., Ottaviani, M. and Alexandrov, M.: Analysis of fine-mode aerosol retrieval capabilities by different passive remote sensing instrument designs, Opt. Express, 20(19), 21457–21484, doi:10.1364/OE.20.021457, 2012.

Knobelspiesse, K., Segal-Rosenhaimer, M., Redemann, J., Cairns, B. and Alexandrov, M. D.: Multi-angle, polarimetric cloud observations using a radiative transfer model trained neural network, College Park, MD. 2017.

Liu, Y. and Diner, D. J.: Multi-Angle Imager for Aerosols, Public Health Reports, 132(1), 14–17, doi:10.1177/0033354916679983, 2017.

Lohmann, U., Stier, P., Hoose, C., Ferrachat, S., Kloster, S., Roeckner, E. and Zhang, J.: Cloud microphysics and aerosol indirect effects in the global climate model ECHAM5-HAM, Atmos. Chem. Phys., 7(13), 3425–3446, doi:10.5194/acp-7-3425-2007, 2007.

Marbach, T., Phillips, P., Lacan, A. and Schlussel, P.: The 3MI Mission: Multi-Viewing -Channel -Polarisation Imager of the EUMETSAT Polar System - Second Generation (EPS-SG) dedicated to aerosol and cloud monitoring, in Sensors, Systems, and Next-Generation Satellites XVII, vol. 8889, p. 88890I, International Society for Optics and Photonics. 2013.

Marshak, A., Platnick, S., Várnai, T., Wen, G. and Cahalan, R. F.: Impact of three-dimensional radiative effects on satellite retrievals of cloud droplet sizes, J. Geophys. Res., 111(D9), D09207, doi:10.1029/2005JD006686, 2006.

Martin, G. M., Johnson, D. W. and Spice, A.: The measurement and parameterization of effective radius of droplets in warm stratocumulus clouds, J. Atmos. Sci., 51(13), 1823–1842, 1994.

Martins, J. V., Fernandez-Borda, R., McBride, B., Espinosa, R. and Remer, L.: Combination between in-situ and remote sensing of tropospheric aerosols, College Park, MD. 2017.

Miles, N. L., Verlinde, J. and Clothiaux, E. E.: Cloud Droplet Size Distributions in Low-Level Stratiform Clouds, J. Atmos. Sci., 57(2), 295–311, doi:10.1175/1520-0469(2000)057<0295:CDSDIL>2.0.CO;2, 2000.

Miller, D. J., Zhang, Z., Ackerman, A. S., Platnick, S. and Baum, B. A.: The impact of cloud vertical profile on liquid water path retrieval based on the bispectral method: A theoretical study based on large-eddy simulations of shallow marine boundary layer clouds, J. Geophys. Res., 121(8), 4122–4141, doi:10.1002/2015JD024322, 2016.

Mishchenko, M. I., Cairns, B., Travis, L. D., Kopp, G., Schueler, C. F., Fafaul, B. A., Hooker, R. J., Maring, H. B., Itchkawich, T., Hansen, J. E., Kopp, G., Schueler, C. F., Fafaul, B. A., Hooker, R. J., Maring, H. B. and Itchkawich, T.: Accurate Monitoring of Terrestrial Aerosols and Total Solar Irradiance: Introducing the Glory Mission, http://dx.doi.org/10.1175/BAMS-88-5-677, 88(5), 677–691, doi:10.1175/BAMS-88-5-677, 2007.

Nakajima, T. and King, M. D.: Determination of the Optical Thickness and Effective Particle Radius of Clouds from Reflected Solar Radiation Measurements. Part I: Theory, J. Atmos. Sci., 47(15), 1878–1893, doi:10.1175/1520-0469(1990)047<1878:dotota>2.0.co;2, 1990a.

Nakajima, T. and King, M. D.: Determination of the optical thickness and effective particle radius of clouds from reflected solar radiation measurements. Part I: Theory, J. Atmos. Sci., 47(15), 1878–1893, 1990b.

Planck, M.: The theory of heat radiation, 2nd ed., P. Blakiston's Son & Co., Philadelphia, PA. [online] Available from: http://gutenberg.org/ebooks/40030, 1914.

Platnick, S.: Vertical photon transport in cloud remote sensing problems, J. Geophys. Res., 105(D18), 22919–22935, 2000.

Platnick, S., King, M. D., Ackerman, S. A., Menzel, W. P., Baum, B. A., Riedi, J. C. and Frey, R. A.: The MODIS cloud products: algorithms and examples from terra, IEEE Trans. Geosci. Remote Sensing, 41(2), 459–473, doi:10.1109/TGRS.2002.808301, 2003.

Platnick, S., Meyer, K. G., King, M. D., Wind, G., Amarasinghe, N., Marchant, B., Arnold, G. T., Zhang, Z., Hubanks, P. A., Holz, R. E., Yang, P., Ridgway, W. L. and Riedi, J.: The MODIS Cloud Optical and Microphysical Products: Collection 6 Updates and Examples From Terra and Aqua, IEEE Trans. Geosci. Remote Sensing, 55(1), 502–525, doi:10.1109/TGRS.2016.2610522, 2017.

Pruppacher, H. R. and Klett, J. D.: Diffusion Growth and Evaporation of Water Drops and Ice Crystals, in Microphysics of Clouds and Precipitation, pp. 412–463, Springer Netherlands, Dordrecht. 1978.

Roebeling, R. A., Feijt, A. J. and Stammes, P.: Cloud property retrievals for climate monitoring: Implications of differences between Spinning Enhanced Visible and Infrared Imager (SEVIRI) on METEOSAT-8 and Advanced Very High Resolution Radiometer (AVHRR) on NOAA-17, J. Geophys. Res., 111(D20), D20210, doi:10.1029/2005JD006990, 2006.

Rosenfeld, D., Liu, G., Yu, X., Zhu, Y., Dai, J., Xu, X. and Yue, Z.: High-resolution (375 m) cloud microstructure as seen from the NPP/VIIRS satellite imager, Atmos. Chem. Phys., 14(5), 2479–2496, doi:10.5194/acp-14-2479-2014, 2014.

Shang, H., Chen, L., Breon, F. M., Letu, H., Li, S., Wang, Z. and Su, L.: A better understanding of POLDER's cloud droplet size retrieval: impact of cloud horizontal inhomogeneity and directional sampling, Atmos. Meas. Tech. Discuss., 8(7), 6559–6597, doi:10.5194/amtd-8-6559-2015, 2015.

Stevens, B., Ackerman, A. S. and Albrecht, B. A.: Simulations of trade wind cumuli under a strong inversion, J. Atmos. Sci., 58(14), 1870–1891, doi:10.1175/1520-0469(2001)058<1870:sotwcu>2.0.co;2, 2001.

Stevens, B., Lenschow, D. H., Vali, G., Gerber, H., Bandy, A., Blomquist, B., Brenguier, J. L., Bretherton, C. S., Burnet, F., Campos, T., Chai, S., Faloona, I., Friesen, D., Haimov, S., Laursen, K., Lilly, D. K., Loehrer, S. M., Malinowski, S. P., Morley, B., Petters, M. D., Rogers, D. C., Russell, L., Savic-Jovcic, V., Snider, J. R., Straub, D., Szumowski, M. J., Takagi, H., Thornton, D. C., Tschudi, M., Twohy, C., Wetzel, M. and van Zanten, M. C.: Dynamics and chemistry of marine stratocumulus–DYCOMS-II, Bull. Amer. Meteor. Soc., 84(5), 579–593, doi:10.1175/BAMS-84-5-579, 2003.

Stevens, B., Moeng, C.-H., Ackerman, A. S., Bretherton, C. S., Chlond, A., de Roode, S., Edwards, J., Golaz, J.-C., Jiang, H., Khairoutdinov, M., Kirkpatrick, M. P., Lewellen, D. C., Lock, A., Müller, F., Stevens, D. E., Whelan, E. and Zhu, P.: Evaluation of Large-Eddy Simulations via Observations of Nocturnal Marine Stratocumulus, Mon. Wea. Rev., 133(6), 1443–, doi:10.1175/MWR2930.1, 2005.

Tampieri, F. and Tomasi, C.: Size distribution models of fog and cloud droplets in terms of the modified gamma function, Tellus, 28(4), 333–347, doi:10.1111/j.2153-3490.1976.tb00682.x, 1976.

Twomey, S.: The Influence of Pollution on the Shortwave Albedo of Clouds, J. Atmos. Sci., 34(7), 1149–1152, doi:10.1175/1520-0469(1977)034<1149:TIOPOT>2.0.CO;2, 1977.

Werner, F., Siebert, H., Pilewskie, P., Schmeissner, T., Shaw, R. A. and Wendisch, M.: New airborne retrieval approach for trade wind cumulus properties under overlying cirrus, J. Geophys. Res., 118(9), 3634–3649, doi:10.1002/jgrd.50334, 2013.

Wiscombe, W. J.: Mie scattering calculations: Advances in technique and fast, vector-speed computer codes, NCAR Tech, National Center for Atmospheric Research, Boulder, Colorado. 1979.

Zhang, Z. and Platnick, S.: An assessment of differences between cloud effective particle radius retrievals for marine water clouds from three MODIS spectral bands, J. Geophys. Res., 116(D20), D20215, doi:10.1029/2011JD016216, 2011.

Zhang, Z., Ackerman, A. S., Feingold, G., Platnick, S., Pincus, R. and Xue, H.: Effects of cloud horizontal inhomogeneity and drizzle on remote sensing of cloud droplet effective radius: Case studies based on large-eddy simulations, J. Geophys. Res., 117(D19), n/a–n/a, doi:10.1029/2012JD017655, 2012.

Zhang, Z., Dong, X., Xi, B., Song, H., Ma, P. L., Ghan, S. J., Platnick, S. and Minnis, P.: Intercomparisons of marine boundary layer cloud properties from the ARM CAP-MBL campaign and two MODIS cloud products, J. Geophys. Res., 122(4), 2351–2365, doi:10.1002/2016JD025763, 2017.

Zhang, Z., Platnick, S., Yang, P., Heidinger, A. K. and Comstock, J. M.: Effects of ice particle size vertical inhomogeneity on the passive remote sensing of ice clouds, J. Geophys. Res., 115(D17), doi:10.1029/2010JD013835, 2010.

Zhang, Z., Werner, F., Cho, H. M. and Wind, G.: A framework based on 2-D Taylor expansion for quantifying the impacts of subpixel reflectance variance and covariance on cloud optical thickness and effective …, Journal of …, doi:10.1063/1.4975502, 2016.

Zinner, T., Wind, G., Platnick, S. and Ackerman, A. S.: Testing remote sensing on artificial observations: impact of drizzle and 3-D cloud structure on effective radius retrievals, Atmos. Chem. Phys., 10(19), 9535–9549, doi:10.5194/acp-10-9535-2010, 2010.

Daniel Miller 2/26/2018 1:23 PM

Deleted: Ackerman, A. S., Kirkpatrick, M. P., Stevens, D. E. and Toon, O. B.: The impact of humidity above stratiform clouds on indirect aerosol climate forcing, Nature, 432(7020), 1014–1017, 2004. ... [10]

Table 1: Mean values (μ) and standard deviations (σ, in parenthesis) of various optical (τ and H_σ) and microphysical properties (r_e(VW) and v_e(VW)) of the LES scenes examined in this study. Note that vertically weighted properties are listed for the polarimetric vertical weighting function. Cloudy pixels is defined using a threshold of τ_{LES}>0.1.

LES Case	CCN Concentration [#/cm^3]	Scene Cloud Fraction	τ [unitless]	r_e(VW) [μm]	v_e(VW) [unitless]	H_σ(800 m) [unitless]
DYCOMS-II	60	0.998	17.95 (6.22)	15.52 (1.00)	0.071 (0.11)	0.13 (0.10)
ATEX Clean	40	0.941	7.90 (8.02)	16.93 (2.62)	0.16 (0.12)	0.42 (0.17)
ATEX Poll.	600	0.985	17.48 (14.71)	7.29 (0.91)	0.13 (0.068)	0.24 (0.13)

Daniel Miller 2/13/2018 1:38 PM
Deleted: 2WT

Daniel Miller 2/13/2018 1:38 PM
Deleted: 2WT

Daniel Miller 2/27/2018 2:24 AM
Deleted: .

Daniel Miller 2/13/2018 1:38 PM
Deleted: 2WT

Daniel Miller 2/13/2018 1:38 PM
Deleted: 2WT

Table 2: The influence of unresolved microphysical inhomogeneity on polarimetric retrievals is explored in Shang et al. (2015). There results are replicated here and compared to the arithmetic mean r_e ($<r_e>$), and the mathematical aggregation results (r_e' and v_e') defined in eq. (7) and eq. (8).

Sub-scale Size Distribution Mixture		Arithmetic Mean	Polarimetric Retrieval		Aggregation Rules	
r_e	v_e	$<r_e>$	r_e(pol)	v_e(pol)	r_e'	v_e'
[5, 10]	[0.01, 0.01]	7.5	8.0	0.10	9.00	0.060
[5, 15]	[0.01, 0.01]	10.0	14.5	0.01	14.00	0.056
[5, 20]	[0.01, 0.01]	12.5	19.0	0.01	19.12	0.044
[10, 15]	[0.01, 0.01]	12.5	13.0	0.05	13.46	0.040
[10, 20]	[0.01, 0.01]	15.0	16.5	0.10	18.00	0.060
[15, 20]	[0.01, 0.01]	17.5	18.0	0.01	18.20	0.028
[5, 10, 15]	[0.01, 0.01, 0.01]	10.0	12.0	0.10	12.85	0.069
[5, 10, 20]	[0.01, 0.01, 0.01]	11.7	14.0	0.10	17.38	0.087
[5, 15, 20]	[0.01, 0.01, 0.01]	13.3	17.5	0.02	17.69	0.049
[10, 15, 20]	[0.01, 0.01, 0.01]	15.0	16.0	0.10	17.07	0.055

Daniel Miller 3/5/2018 11:06 AM
Formatted: Font:9 pt, Not Bold
Daniel Miller 3/5/2018 11:06 AM
Formatted: Font:9 pt, Not Bold

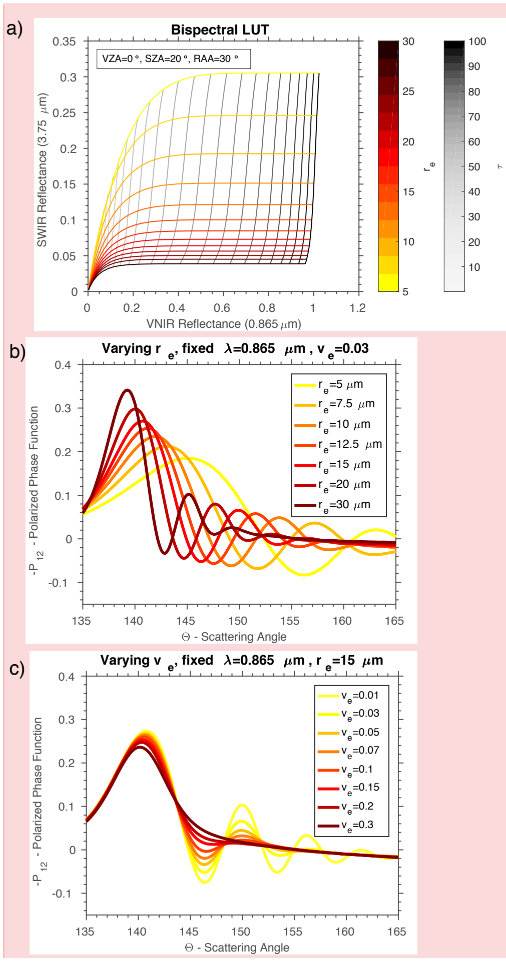

Figure 1: Demonstrations of the microphysical sensitivity of the bispectral and the polarimetric techniques. Panel (a) features the bispectral LUT exhibiting sensitivity to r_e (colored iso-lines), due to absorption in the SWIR/ reflectance. The VNIR reflectances provide sensitivity to optical thickness (gray iso-lines). Panels (b) and (c) demonstrate the sensitivity of polarimetric technique to r_e and v_e respectively. The supernumerary bow peaks of the polarized phase function ($-P_{12}$) shift and become narrower with increasing droplet size (r_e), whereas the peaks erode in magnitude for broadened droplet size distributions (v_e).

Daniel Miller 2/12/2018 11:29 AM
Comment [1]: Figure updated to correct error in original axes label of panel (a).

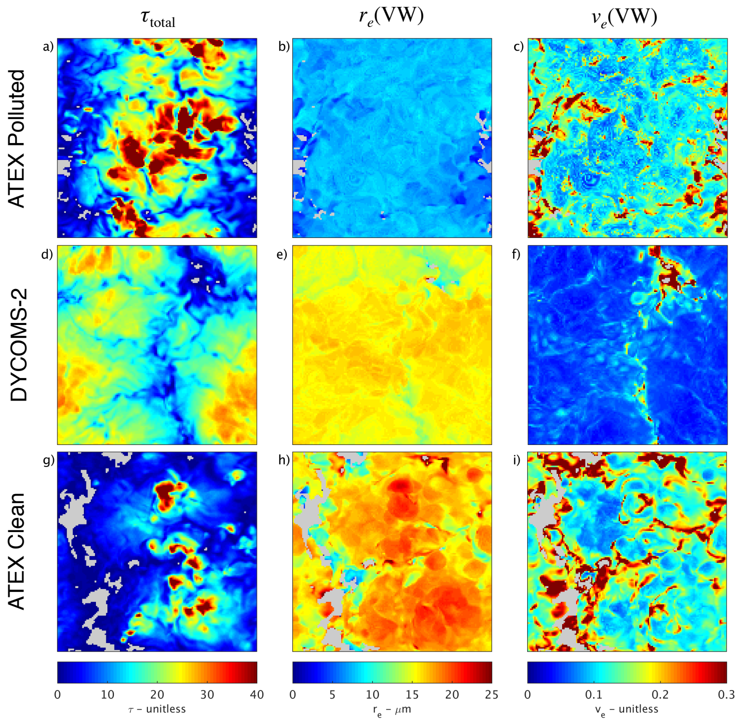

Figure 2: The optical and microphysical properties (τ, r_e, and v_e) of the LES cases examined in this study. The panels are arranged such that each LES case appears row-wise and the different properties are appear column-wise. Note that the vertically weighting functions used for the displayed re(VW) and ve(VW) correspond to single-scattering assumptions. Cloud-free masking in each of the images appears in gray. Refer to sections 2 and 3 for discussion and definition of each of these properties. Axes labels have been removed to enlarge each map, but the spatial dimensions of each scene are roughly 7 x 7 km (refer to section 3 for the specific resolutions of each LES case.)

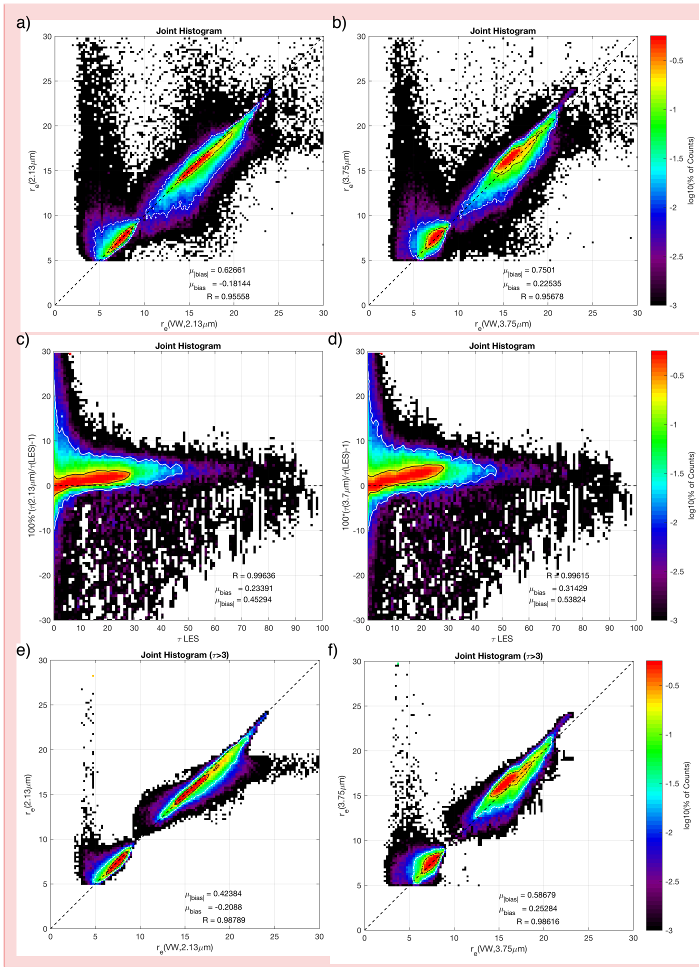

Figure 3: Joint histogram regressions of r_e and τ in all LES cases comparing the bispectral retrievals to the LES cloud microphysical properties. Panels (a) and (b) are regressions of the bispectral r_e(2.13 μm) and r_e(3.75 μm) retrievals against the physical analogue r_e(VW). Panels (c) and (d) are regressions of the bispectral τ(2.13 μm) and τ(3.75 μm) retrievals against the physical τ(LES). Panels (e) and (f) display the regression of the bispectral r_e(2.13 μm) and r_e(3.75 μm) retrievals for only optically thick pixels (τ>3). Note that in each panel the correlation is quantified with a linear correlation coefficient (R) and the black and white contours encompass 66% and 95% of the population, respectively.

Daniel Miller 2/25/2018 4:25 PM
Comment [2]: Figure updated to include data from the new vertical weighting defintions.

Daniel Miller 2/13/2018 2:35 PM
Deleted: or

Daniel Miller 2/13/2018 1:38 PM
Deleted: 2WT

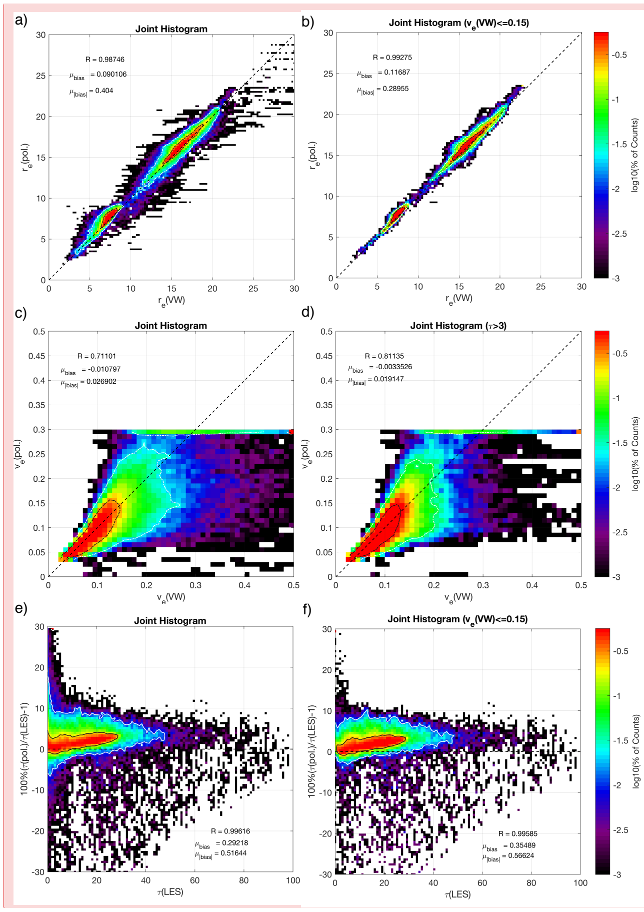

Figure 4: Joint histogram regressions of r_e, v_e, and τ in all LES cases comparing the polarimetric retrievals to the LES cloud microphysical properties. Panel (a) depicts the regression of the polarimetric r_e(pol) retrieval against the physical analogue r_e(VW), while panel (b) is sub-selection of the same regression for low v_e. Panel (c) depicts the regression of the polarimetric v_e(pol) retrieval against the physical analogue v_e(VW), while panel (d) is a sub-selection of the same regression for thick clouds (τ>3). Panel (e) depicts the regression of the polarimetric τ(pol) retrieval against the physical analogue τ(LES), while panel (f) is sub-selection of the same regression for low v_e. Note that in each panel the correlation is quantified with a linear correlation coefficient (R) and the black and white contours encompass 66% and 95% of the population, respectively.

Daniel Miller 3/2/2018 11:31 AM
Comment [3]: Figure updated to include data from the new vertical weighting defintions.

Daniel Miller 2/13/2018 1:38 PM
Deleted: 2WT

Daniel Miller 2/13/2018 1:38 PM
Deleted: 2WT

Daniel Miller 2/23/2018 4:08 PM
Formatted: Centered, Keep with next

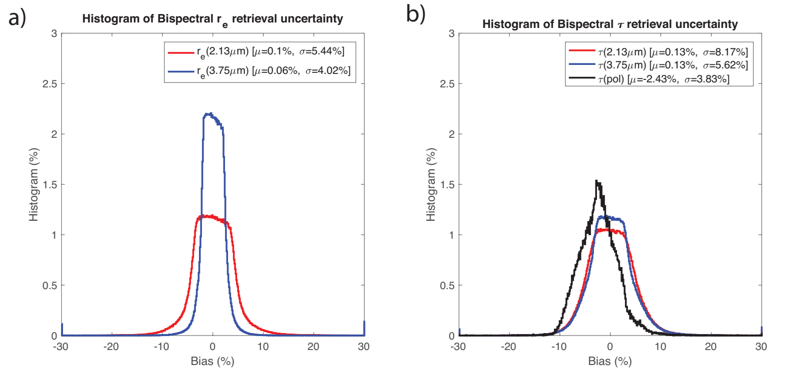

Figure 5: Histograms of the percent retrieval bias of retrievals based on perturbed reflectances stated relative to unperturbed retrievals. Panel (a) displays retrieval biases for the bispectral r_e retrieval. Panel (b) displays retrieval biases for the bispectral and polarimetric τ retrievals. Refer to the text for more information about the polarimetric r_e and v_e retrieval biases.

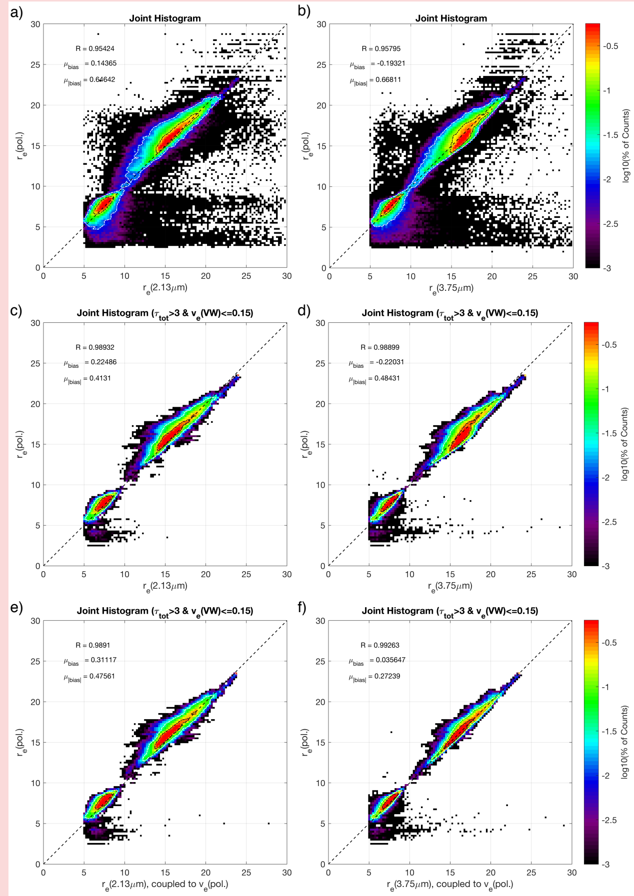

Figure 6: Joint histogram regressions of r_e retrievals for all LES cases comparing the bispectral and polarimetric techniques. Panels (a) and (b) display the unfiltered regressions of r_e(pol) at 0.865 μm wavelength against the r_e(2.13 μm) and r_e(3.75 μm) bispectral retrievals. After introducing filters to these regressions to remove thin clouds (τ<3) and broad droplet size distributions (v_e>0.15) panels (c) and (d) the retrieval intercomparison improves. Panels (e) and (f) each replicate the results from the previous selection criteria but additionally provide bispectral retrieval in this regression with v_e(pol) as an a priori for each retrieval. In each panel the quality of the correlation is quantified and a black iso-contour is drawn surrounding 75% data in the histogram. Note that in each panel the correlation is quantified with a linear correlation coefficient (R) and the black and white contours encompass 66% and 95% of the population, respectively.

Daniel Miller 3/2/2018 12:13 PM
Comment [4]: Figure updated to include data from the new vertical weighting defintions.

Daniel Miller 2/23/2018 4:08 PM
Deleted: 5

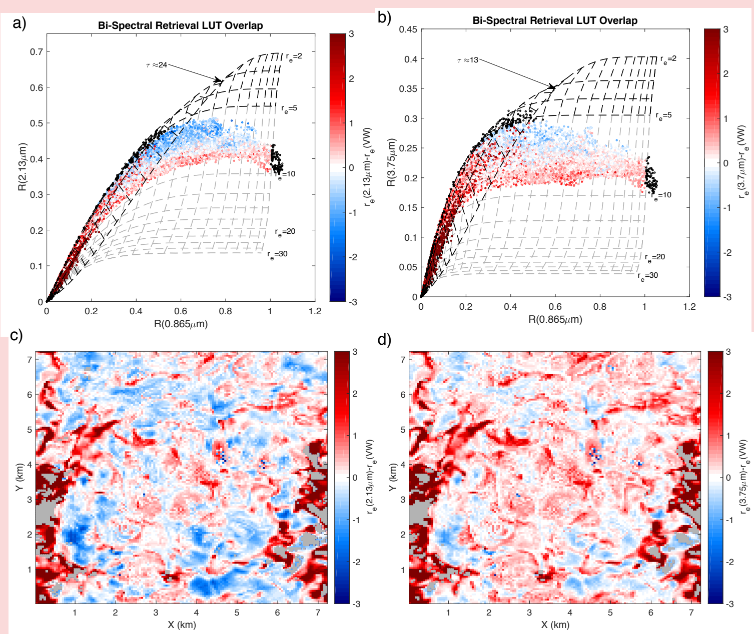

Figure 7: Panel (a) and (b) depict the standard bispectral LUT (light gray dashed lines) for both SWIR bands with the scattered reflectance points for the ATEX polluted LES case plotted overtop. The scatterplot is colored by the bias between the bispectral retrieval and the physical reference (r_e(bispectral)−r_e(VW)), which is also shown below as a spatial variability map. Note that some points are colored in black to indicate retrieval failure due to falling outside the LUT space. In addition to the standard LUT, an extended LUT including droplet sizes from 2-4μm is included (black dashed lines), revealing an overlapping region of the two LUT for smaller τ referred to as the "multiple solution space".

Daniel Miller 2/25/2018 6:07 PM
Comment [5]: Figure updated with new vertically weighted properties.

Daniel Miller 3/4/2018 4:47 PM
Deleted: (SWIR

Daniel Miller 2/13/2018 1:38 PM
Deleted: 2WT

Daniel Miller 2/13/2018 2:36 PM
Deleted: reflectance

Daniel Miller 2/13/2018 2:37 PM
Deleted: standard

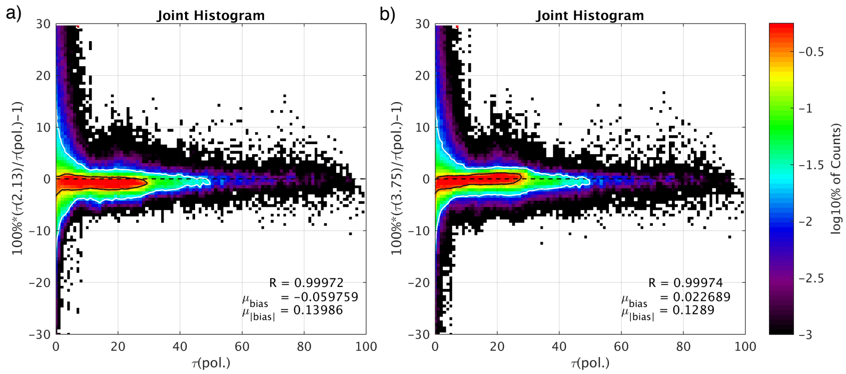

Figure 8: Joint histogram regressions of τ retrievals for all LES cases comparing the bispectral and polarimetric techniques. Panel (a) and (b) display the τ(2.13 µm) and τ(3.75 µm) retrievals respectively. In each panel the quality of the correlation is quantified and the black and white population density iso-contours are drawn surrounding 66% and 95% of the data respectively.

Daniel Miller 2/23/2018 4:08 PM
Deleted: 7

Daniel Miller 2/14/2018 11:45 AM
Formatted: Keep with next

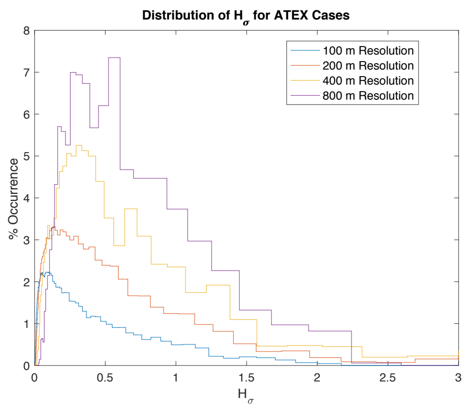

Figure 9: Probability distributions of H_σ for the combined ATEX polluted and clean datasets at all coarsened spatial resolution (100, 200, 300, 400, 800 m).

Daniel Miller 2/25/2018 9:45 AM

Deleted: 10

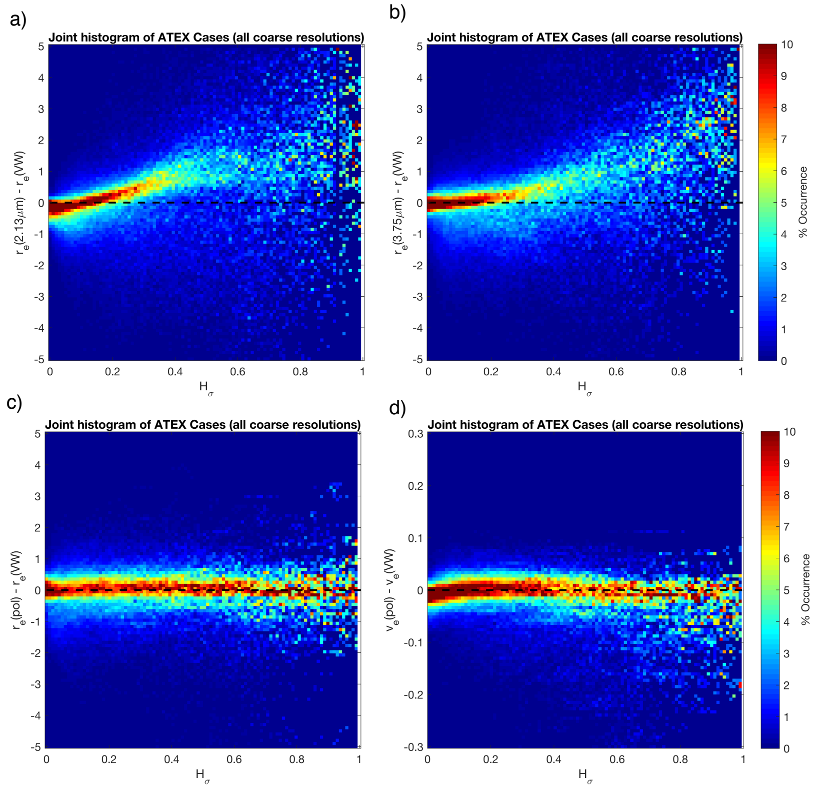

Figure 10: Joint histograms of retrieval biases (relative to each relevant vertically weighted LES property) with respect to H_σ for the combined ATEX clean and polluted datasets with all observation geometries and coarsened spatial resolution (100, 200, 300, 400, 800 m). The color bar indicates percent occurrence. Panels (a) and (b) depict biases for the two bispectral r_e retrievals, and panels (c) and (d) depict biases for the polarimetric r_e and v_e retrieval.

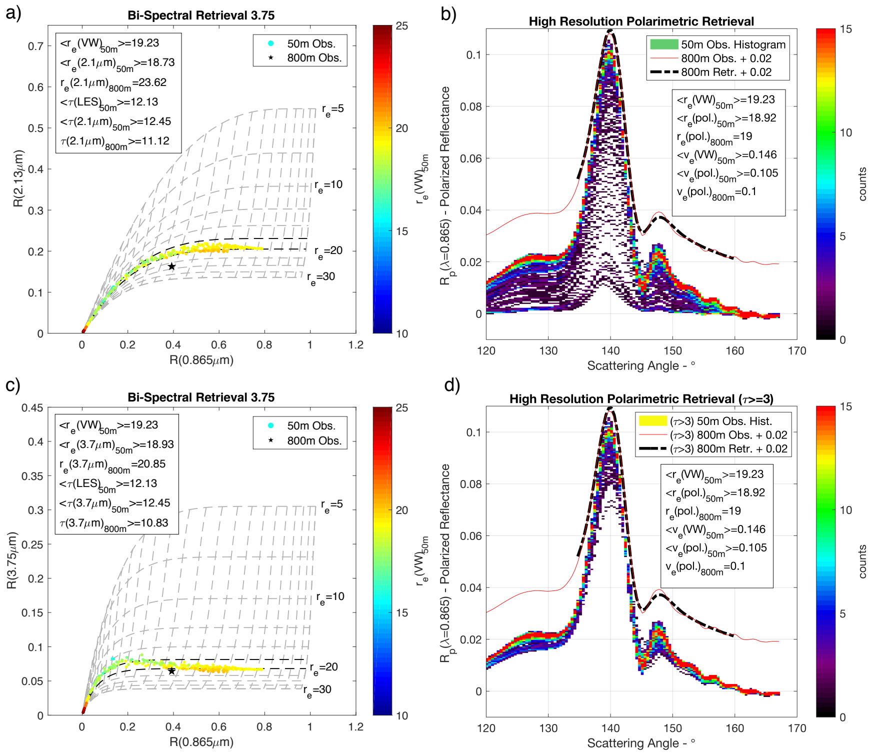

Figure 11: Panels (a) and (c) depict the bispectral LUT's and 50 m reflectances for the 2.13 and 3.75 μm bispectral retrievals respectively for a particularly inhomogeneous 800 m pixel. The scattered points correspond to 50 m reflectances with color corresponding to r_e(VW), while the black star corresponds to the 800 m reflectance pair (the average of the 50 m data). The polarimetric reflectance distribution histograms in panels (b) and (d) address how the high-resolution (50 m) reflectance distribution influences the polarimetric retrieval at coarse resolution (800m). The two curves (plotted with a 0.02 reflectance shift for clarity) are the 800 m observed reflectance (black dashed curve) and the 800 m retrieval (red solid curve). All of these figures include statistics on the high-resolution averages of physical properties and retrievals along with their coarse resolution counterparts for comparison.

Daniel Miller 2/14/2018 11:45 AM
Deleted: 9

Daniel Miller 3/4/2018 4:47 PM
Deleted: SWIR

Daniel Miller 2/13/2018 1:38 PM
Deleted: 2WT

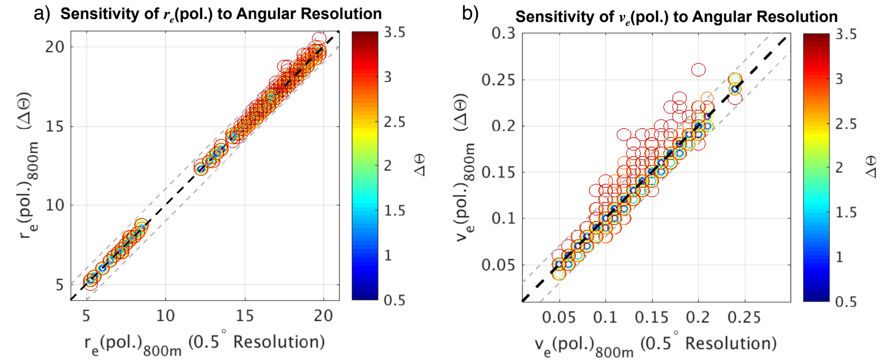

Figure 12: Angular resolution sensitivity experiments examining polarimetric retrievals of r_e (panel a) and v_e (panel b) for all LES scenes at the 800 m spatial resolution. The color and size of scattered points denote the angular resolution of each retrieval. The gray dashed lines denote the ±1 step in the LUT space of the polarimetric retrieval.

Daniel Miller 2/14/2018 11:45 AM
Deleted: 10

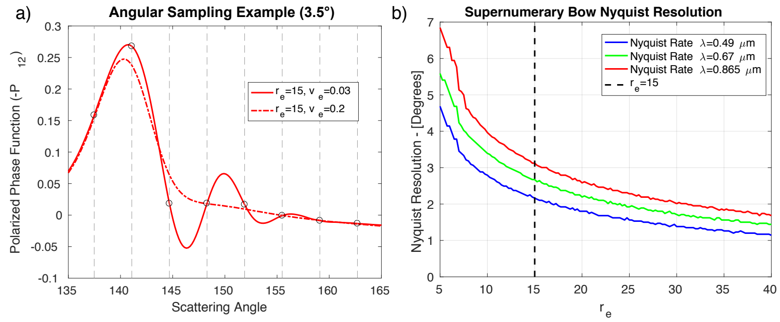

Figure 13: Panel (a) features the polarized phase functions r_e=15 (red) at v_e=0.03 (solid) and v_e=0.2 (dashed). Grey dashed lines and circles indicate a 3.4° observation sampling of the phase functions. The Nyquist resolution is obtained by measuring the peak-to-peak distance of the supernumerary bow oscillations and dividing that distance in half. The Nyquist resolution changes as a function of r_e and λ as shown in panel b, where the gray vertical line highlights the Nyquist resolutions required for the r_e=15 case.

Daniel Miller 2/14/2018 11:45 AM
Deleted: 11